

Application of functional near-infrared spectroscopy in the healthcare industry: A review

Keum-Shik Hong^{*,†,‡} and M. Atif Yaqub^{*}

**School of Mechanical Engineering
Pusan National University
Busan 46241, Republic of Korea*

*†Department of Cogno-Mechatronics Engineering
Pusan National University
Busan 46241, Republic of Korea
‡kshong@pusan.ac.kr*

Received 22 May 2019

Accepted 6 September 2019

Published 16 October 2019

Functional near-infrared spectroscopy (fNIRS), a growing neuroimaging modality, has been utilized over the past few decades to understand the neuronal behavior in the brain. The technique has been used to assess the brain hemodynamics of impaired cohorts as well as able-bodied. Neuroimaging is a critical technique for patients with impaired cognitive or motor behaviors. The portable nature of the fNIRS system is suitable for frequent monitoring of the patients who exhibit impaired brain activity. This study comprehensively reviews brain-impaired patients: The studies involving patient populations and the diseases discussed in more than 10 works are included. Eleven diseases examined in this paper include autism spectrum disorder, attention-deficit hyperactivity disorder, epilepsy, depressive disorders, anxiety and panic disorder, schizophrenia, mild cognitive impairment, Alzheimer's disease, Parkinson's disease, stroke, and traumatic brain injury. For each disease, the tasks used for examination, fNIRS variables, and significant findings on the impairment are discussed. The channel configurations and the regions of interest are also outlined. Detecting the occurrence of symptoms at an earlier stage is vital for better rehabilitation and faster recovery. This paper illustrates the usability of fNIRS for early detection of impairment and the usefulness in monitoring the rehabilitation process. Finally, the limitations of the current fNIRS systems (i.e., nonexistence of a standard method and the lack of well-established features for classification) and future research directions are discussed. The authors hope that the findings in this paper would lead to advanced breakthrough discoveries in the fNIRS field in the future.

Keywords: fNIRS; brain impairment; psychiatric disorder; degenerative brain disease; brain injury; patient.

[‡]Corresponding author.

Keum-Shik Hong and M. Atif Yaqub have contributed equally to this study.

This is an Open Access article published by The Author(s). It is distributed under the terms of the Creative Commons Attribution 4.0 (CC BY) License which permits use, distribution and reproduction in any medium, provided the original work is properly cited.

Abbreviations

AD:	Alzheimer's disease
ADHD:	Attention-deficit hyperactivity disorder
ASD:	Autism spectrum disorder
BA:	Brodmann area
BCI:	Brain-computer interface
BD:	Bipolar disorder
BPD:	Borderline personality disorder
CBF:	Cerebral blood flow
CBV:	Cerebral blood volume
CDT:	Clock drawing test
COMT:	Catechol-O-methyltransferase
CPS:	Complex partial seizures
DBS:	Deep brain stimulation
DST:	Digit span task
EEG:	Electroencephalography
fMRI:	Functional magnetic resonance imaging
fNIRS:	Functional near-infrared spectroscopy
FOF:	Fear of fall
FOG:	Freezing of gait
GPi:	<i>Globus pallidus internus</i>
HbO:	Oxygenated hemoglobin
HbR:	Deoxygenated hemoglobin
HbT:	Total hemoglobin
LDA:	Linear discriminant analysis
MCI:	Mild cognitive impairment
MD:	Mood disorder
MDD:	Major depressive disorder
MEG:	Magnetoencephalography
NPSR1:	Neuropeptide S receptor gene
PCA:	Principal component analysis
PD:	Parkinson's disease
PDD:	Pervasive development disorder
PET:	Positron emission tomography
PFC:	Prefrontal cortex
PLM:	Periodic limb movements
RSFC:	Resting state functional connectivity
rTMS:	Repetitive transcranial magnetic stimulation
SAD:	Social anxiety disorder
SMA:	Supplementary motor area
SPECT:	Single-photon emission computed tomography
SVM:	Support vector machine
SZ:	Schizophrenia
TBI:	Traumatic brain injury
tDCS:	Transcranial direct current stimulation
TOI:	Tissue oxygenation index
UD:	Unipolar disorder
VFT:	Verbal fluency task
VIM:	Ventralis intermedius

1. Introduction

The purpose of this paper is to review the applications of functional near-infrared spectroscopy (fNIRS) for diseased populations in the healthcare industry. The aging people of the world currently have various psychiatric and neurological

impairments. Further, the brain functions of these patients are profoundly impaired, thereby restricting their independence in daily life. The aggravated state of these patients results in the constant involvement of caregivers to live their lives. The fatality rate is very high in the case of brain diseases. The impairments affecting this population include various types of dementias that are associated with memory loss and impaired executive functioning. The common forms of dementia are Alzheimer's disease (AD), vascular dementia, Lewy body dementia, medication-induced dementia, and frontotemporal disorder. AD is the most widespread form of dementia, accounting for almost 60% of all dementia-related cases.¹ Stroke is a type of permanent impairments that are caused by either a blockage in a brain vessel or by its bursting; thereby resulting in the death of the brain cells that are associated with the distribution of blood oxygen through that vessel. Stroke is treated as a medical emergency and can be highly fatal. Parkinson's disease (PD) is the most common form of movement impairments that are known as Parkinsonian syndromes. PD is associated with trembling and experiencing hardship while walking and during movements and coordination. Epilepsy involves recurring, impulsive seizures, or disturbed brain activity that causes changes in the attention span or behavior of a patient. Psychiatric impairments muddle a patient's thoughts, perceptions, characteristics, and their ability to relate to others. Common psychiatric impairments include anxiety disorders, bipolar disorder (BD), depression, schizophrenia (SZ), eating disorders, impulse control and addiction disorders, and personality disorders. Impairments other than psychiatric ones are mostly irreversible and progressive. Several medications and rehabilitation techniques are utilized to reduce the gradual decline and to improve the quality of life of these patients. The degradation starts much earlier in the brain compared to when the symptoms first appear. Therefore, the early detection of these impairments is vital. The advancements made in various neuroimaging technologies and the researches that have used them have paved the way for studying as well as detecting brain impairments.

The neuroimaging modalities include event-related potentials measurement using electroencephalography (EEG), magnetic field measurement using magnetoencephalography (MEG), radioactive tracer-based positron emission tomography (PET),

gamma emission-based single-photon emission computed tomography (SPECT), and functional magnetic resonance imaging (fMRI). These modalities have allowed for valuable advancements made in the understanding of many of the neurological impairments. Examinations can only be conducted in restricted environments using fMRI, MEG, PET, and SPECT due to the large size of the machines involved and their lack of mobility, which limits the design of the study. Moreover, these systems are highly vulnerable to motion artifacts, costly, and invasive due to the insertion of radioactive tracers. They have low temporal resolution, which makes them inappropriate for conducting repeated measurements.² EEG has a high temporal resolution, but it lacks spatial resolution and is vulnerable to motion artifacts.³ The rehabilitation of patients with impaired brain functions is essential; however, these modalities cannot be used simultaneously with rehabilitating techniques, such as electric stimulation, as these techniques are affected by electric and magnetic fields.⁴

In contrast to established neuroimaging methods, fNIRS has proven its worthiness during the last decade. Most of the human tissues are comparatively more translucent than oxygenated (HbO) and deoxygenated hemoglobin (HbR) in a spectrum between 650 nm and 1000 nm. Therefore, optical wavelengths in this range are used to measure temporal transformations of HbO and HbR.⁵ The photons, emitted by the light sources attached to the head, moving through the different layers in the brain are either absorbed or scattered. Photodetectors are placed on the skin to receive these photons that travel in an expected banana-shaped photonic flow to reach the surface. Conventionally, fNIRS uses two wavelengths; however, introducing additional wavelengths also helps in achieving better neuronal activation.⁶ fNIRS has been utilized in studies to classify the sensory responses and motor cortex activation levels of different fingers.^{7,8} fNIRS can reveal the underlying neuronal networks and their complex connections in the form of functional connectivity.^{4,9} Various algorithms and techniques have been developed and explored using fNIRS to improve the brain-computer interfaces (BCIs) to help physically disabled persons.^{10–15}

This paper reviews the research works conducted to advance the understanding of the effects of various diseases on our brain using fNIRS. These studies mostly involve patients with degenerative brain or

psychiatric disorders. Each section of this paper is devoted to a single disease to summarize the associated research works and their findings. For every disease, we created different subsections based on the performed task during the fNIRS recording.

2. Autism Spectrum Disorder

Autism spectrum disorder (ASD), also known as pervasive development disorder (PDD) or Asperger's disease, is a mental disorder that affects communication. ASD is known as a developmental disorder, and it begins during childhood or even during infancy. Once an individual develops ASD, it usually remains throughout his/her life. However, several treatments and medications can improve the quality of life or even completely cure all the related symptoms. ASD patients may exhibit symptoms such as problems in talking and interacting with others, displaying repetitive behaviors, a lack of interest, or mismatched facial expressions. It is critical to diagnose ASD during early childhood because the treatment at a young age results in a much better outcome. Several studies have been conducted using fNIRS to elucidate the neuronal mechanism involved in ASD: The task-wise distribution of ASD papers is presented in Fig. 1, and all the studies are outlined in Table 1.

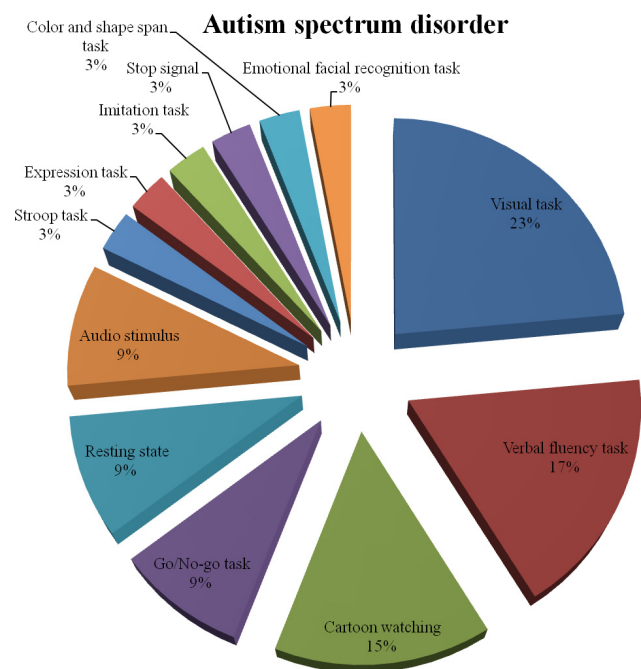


Fig. 1. Task-based distribution of studies on autism spectrum disorder (total studies: 34).

Table 1. Studies on autism spectrum disorder.

Work	Experimental population	Brain area under study	Instrument	No. of channels/ separation(s)	Analyzed parameters
Visual task Kita <i>et al.</i> ¹⁶ (2011)	11 Healthy adults (M), 21.9 ± 1.2 yrs; 13 Healthy children (M), 10.9 ± 1.0 yrs; 10 ASD patients (M), 10.2 ± 1.1 yrs	Prefrontal cortex	OEG-16	16/3 cm	HbO
Nakadoi <i>et al.</i> ¹⁷ (2012)	14 Healthy individuals (8 F and 6 M), 31.5 ± 4.8 yrs; 14 PDD patients (8 F and 6 M), 31.6 ± 5.0 yrs	Frontal region	ETG-4000	24/3 cm	HbO, HbR
Kajjume <i>et al.</i> ¹⁸ (2013)	6 Healthy individuals (M), 10.9 ± 1.6 yrs; 6 PDD patients (M), 10.7 ± 2.9 yrs	Bilateral middle temporal gyri	ETG-4000	24/3 cm	HbO
Ichikawa <i>et al.</i> ¹⁹ (2014)	9 ADHD patients (M), 9.8 ± 1.6 yrs; 8 ASD patients (M), 9.8 ± 1.4 yrs	Bilateral temporal region	ETG-4000	24/3 cm	HbO
Zhu <i>et al.</i> ²⁰ (2015)	20 Healthy individuals (6 F and 14 M), 8.09 ± 1.27 yrs; 20 ASD patients (4 F and 16 M), 8.75 ± 1.34 yrs	Prefrontal cortex	FOIRE-3000	22/3 cm	HbO
Jung <i>et al.</i> ²¹ (2016)	12 Healthy individuals (M), 14.5 ± 10.76 yrs; 8 ASD patients (M), 15.6 ± 9.55 yrs	Bilateral temporal areas	CW6	14/2.6 cm	HbO
Liu <i>et al.</i> ²² (2016)	2 Healthy individuals (F), 14 yrs and 16 yrs; 2 ASD patients (M), 11 yrs and 12 yrs	Bilateral temporal region	ETG-4000	24/3 cm	HbO
Lloyd-Fox <i>et al.</i> ²³ (2018)	16 Healthy infants with low-risk of ASD (6 F and 10 M), 153.81 ± 25.67 days 20 Healthy infants with high-risk of ASD (10 F and 10 M), 149.35 ± 27.28 days	Frontal and temporal areas	UCL-NIRS	26/2 cm	HbO, HbR

Table 1. (Continued)

Work	Experimental population	Brain area under study	Instrument	No. of channels/ separation(s)	Analyzed parameters
Verbal fluency task					
Kuwabara <i>et al.</i> ²⁴ (2006)	10 Healthy individuals (1 F and 9 M), 27.9 ± 4.1 yrs; 10 PDD patients (4 F and 6 M), 26.5 ± 7.1 yrs	Prefrontal cortex	ETG-100	24/3 cm	HbO, HbR
Kwakubo <i>et al.</i> ²⁵ (2009)	27 Healthy individuals (6 F and 21 M), 27 ASD patients (6 F and 21 M), 24 Healthy individuals with ASD siblings (13 F and 11 M)	Prefrontal region	NIRO-200	2/4 cm	HbO, HbR
Iwanami <i>et al.</i> ²⁶ (2011)	18 Healthy individuals (6 F and 12 M), 31.1 ± 4.7 yrs; 20 Asperger's patients (6 F and 14 M), 27.2 ± 8.5 yrs	Bilateral frontotemporal region	ETG-4000	24/3 cm	HbO
Ishii-Takahashi <i>et al.</i> ²⁷ (2014)	21 Healthy individuals (8 F and 13 M), 28.8 ± 5.5 yrs; 19 ADHD patients (8 F and 11 M), 30.6 ± 7.4 yrs; 21 ASD patients (13 F and 8 M), 30.8 ± 7.2 yrs	Bilateral frontotemporal region	ETG-4000	24/3 cm	HbO, HbR
Hirata <i>et al.</i> ²⁸ (2018)	18 Healthy individuals (5 F and 13 M), 28–38.5 yrs; 13 ASD patients (1 F and 12 M), 23.3–38.5 yrs; 15 Schizophrenia (3 F and 12 M), 29–47 yrs	Bilateral frontotemporal region	ETG-4000	24/3 cm	HbO
Yeung <i>et al.</i> ²⁹ (2019)	22 Healthy individuals (6 F and 16 M), 14.27 ± 1.75 yrs; 22 ASD patients (2 F and 20 M), 14.44 ± 2.23 yrs	Prefrontal region	OEG-SpO ₂ system	16/3 cm	HbO
Cartoon watching					
Li and Yu ³⁰ (2016)	12 Healthy individuals (3 F and 9 M), 6.1 ± 1.1 yrs; 12 ASD patients (3 F and 9 M), 6.1 ± 1.1 yrs	Bilateral frontal, temporal, and occipital regions	LABNIRS	44/3 cm	HbO, HbR, HbT

Table 1. (Continued)

Work	Experimental population	Brain area under study	Instrument	No. of channels/ separation(s)	Analyzed parameters
Li and Yu ³¹ (2018)	46 ASD patients (10 F and 36 M), 5.0 ± 1.7 yrs	Bilateral frontal, temporal, and occipital regions	LABNIRS	44/3 cm	HbO, HbR, HbT
Li <i>et al.</i> ³² (2018)	29 Healthy individuals (9 F and 20 M), 6.5 ± 1.2 yrs; 29 ASD patients (6 F and 23 M), 6.0 ± 1.2 yrs	Bilateral frontal, temporal, and occipital regions	LABNIRS	44/3 cm	HbO, HbR, HbT
Jia <i>et al.</i> ³³ (2018)	31 Healthy individuals (11 F and 20 M), 6.56 ± 1.2 yrs; 35 ASD patients (12 F and 23 M), 5.96 ± 1.22 yrs	Bilateral frontal, temporal, and occipital regions	LABNIRS	44/3 cm	HbO, HbR
Jia <i>et al.</i> ³⁴ (2018)	12 Healthy individuals, 6.1 ± 1.1 yrs; 12 ASD patients, 6.1 ± 1.1 yrs	Bilateral frontal, temporal, and occipital regions	LABNIRS	44/3 cm	HbO, HbR
Go/No-go task Xiao <i>et al.</i> ³⁵ (2012)	16 Healthy individuals (M), 9.69 ± 1.74 yrs; 16 ADHD patients (M), 9.75 ± 1.18 yrs; 19 ASD patients (M), 10.11 ± 2.08 yrs	Prefrontal region	JH-NIRS-BR-05	16	HbO
Ikeda <i>et al.</i> ³⁶ (2018)	24 Healthy individuals (6 F and 18 M), 9.6 ± 1.9 yrs; 24 ASD patients (7 F and 17 M), 10.0 ± 2.8 yrs	Bilateral frontotemporal region	ETG-4000	44/3 cm	HbO
Sutoko <i>et al.</i> ³⁷ (2019)	21 ADHD patients, 7.8 ± 1.7 yrs; 11 ADHD+ASD patients, 8.2 ± 2.1 yrs	Bilateral frontotemporal region	ETG-4000	44/3 cm	HbO, HbR
Resting state Kikuchi <i>et al.</i> ³⁸ (2013)	15 Healthy individuals (2 F and 13 M), 45–82 months; 15 ASD patients (2 F and 13 M), 47–86 months	Frontal region	FOIRE-3000	2/3 cm	HbO, HbR

Table 1. (Continued)

Work	Experimental population	Brain area under study	Instrument	No. of channels/ separation(s)	Analyzed parameters
Zhu <i>et al.</i> ³⁹ (2014)	10 Healthy individuals (M), 9.0 ± 1.3 yrs; 10 ASD patients (M), 8.9 ± 1.4 yrs	Bilateral inferior frontal and temporal cortices	FOIRE-3000	44/3 cm	HbO, HbR
Li <i>et al.</i> ⁴⁰ (2016)	22 Healthy (4 F and 18 M), 9.5 ± 1.6 yrs; 25 ASD (7 F and 18 M), 9.3 ± 1.4 yrs	Temporal cortex	FOIRE-3000	24/3 cm	HbO, HbR
Audio stimulus					
Minagawa-Kawai <i>et al.</i> ⁴¹ (2009)	9 Healthy individuals (2 F and 7 M), 7.3 ± 1.7 yrs; 9 ASD patients (2 F and 7 M), 9.2 ± 1.8 yrs	Bilateral auditory areas	ETG-7000	8/3 cm	HbO, HbR, HbT
Funabiki <i>et al.</i> ⁴² (2012)	12 Healthy individuals (2 F and 10 M), 14.2 ± 3.8 yrs; 11 ASD patients (1 F and 10 M), 16.8 ± 6.1 yrs	Prefrontal and temporal cortices	OMM-3000	32/2 cm	HbO, HbR
Lloyd-Fox <i>et al.</i> ²³ (2018)	16 Healthy infants with low-risk of ASD (6 F and 10 M), 153.81 ± 25.67 days; 20 Healthy infants with high-risk of ASD (10 F and 10 M), 149.35 ± 27.28 days;	Frontal and temporal areas	UCL-NIRS	26/2 cm	HbO, HbR
Stroop task					
Xiao <i>et al.</i> ³⁵ (2012)	16 Healthy individuals (M), 9.69 ± 1.74 yrs; 16 ADHD patients (M), 9.75 ± 1.18 yrs; 19 ASD patients (M), 10.11 ± 2.08 yrs	Prefrontal region	JH-NIRS-BR-05	16	HbO
Expression task					
Iwanaga <i>et al.</i> ⁴³ (2013)	16 Healthy individuals (4 F and 12 M), 11.4 ± 1.8 yrs; 16 ASD patients (2 F and 14 M), 11.5 ± 1.8 yrs	Frontal region	ETG-4000	22/3 cm	HbO

Table 1. (Continued)

Work	Experimental population	Brain area under study	Instrument	No. of channels/ separation(s)	Analyzed parameters
Imitation task					
Mori <i>et al.</i> ⁴⁴ (2015)	10 Healthy individuals (M), 9–14 yrs; 10 ASD patients (7 M), 9–14 yrs	Frontal region	OMM-3000	34/3 cm	HbO
Stop signal					
Ishii-Takahashi <i>et al.</i> ²⁷ (2014)	21 Healthy individuals (8 F and 13 M), 28.8 ± 5.5 yrs; 19 ADHD patients (8 F and 11 M), 30.6 ± 7.4 yrs; 21 ASD patients (13 F and 8 M), 30.8 ± 7.2 yrs	Bilateral frontotemporal region	ETG-4000	24/3 cm	HbO, HbR
Color and shape span task					
Yanagisawa <i>et al.</i> ⁴⁵ (2016)	22 Healthy individuals (16 F and 6 M), 19–51 yrs; 11 ASD patients (8 F and 3 M), 14–46 yrs	Frontal region	NIRO-200	2/3 cm	HbO, HbR
Emotional facial recognition task					
Hirata <i>et al.</i> ²⁸ (2018)	18 Healthy individuals (5 F and 13 M), 28–38.5 yrs; 13 ASD patients (1 F and 12 M), 23.3–38.5 yrs; 15 Schizophrenia patients (3 F and 12 M), 29–47 yrs	Bilateral frontotemporal region	ETG-4000	24/3 cm	HbO

2.1. Visual task

For ASD children, a lower level of activation in the right inferior frontal gyrus was related to the inability to recognize his/her face showing impairment in that region.¹⁶ The PDD patients showed a significantly lower HbO response in the prefrontal cortex (PFC) while watching fearful facial expressions when compared to healthy persons.¹⁷ The children with PDD showed a lower HbO response in the bilateral temporal regions and especially in the right hemisphere while watching and imitating tasks when compared to healthy persons.¹⁸ During the tasks showing familiar and unfamiliar faces, the children with ASD were differentiated from those with attention-deficit hyperactivity disorder (ADHD) using a support vector machine (SVM)-based classification.¹⁹ The children with ASD exhibited a lower HbO response and abnormal connections in the PFC during the joint attention situation in joint and nonjoint attention tasks.²⁰ While watching human faces, the ASD patients showed bilateral temporal-occipital activation as compared to healthy individuals having right hemisphere activation.²¹ The fNIRS-based neurofeedback was provided to the ASD patients during the facial identity recognition training to achieve better outcomes.²² The infants who exhibited lower activation in the inferior frontal and posterior temporal regions in response to the social video clips were diagnosed with ASD in their early childhood.²³

2.2. Verbal fluency task

The poor performance of PDD patients in this task was related to the low HbO level in the bilateral frontal region and specifically in the right hemisphere when compared to healthy persons.²⁴ The HbO levels of both ASD and healthy children were similar, but the adults with ASD showed lower cognitive activation as compared to healthy persons in the bilateral PFC.²⁵ The HbO levels of the patients with Asperger's disease in the PFC were significantly lower than those in healthy persons during the task period, thereby exhibiting the task-related impairment.²⁶ The HbO response in the left ventrolateral and dorsolateral PFCs of ASD patients was observed to be lower than that of healthy persons, but was not differentiable from that of ADHD patients.²⁷ Compared to healthy

persons, the patients with ASD showed decreased HbO activity in the bilateral frontotemporal region, which was also a different response from that of SZ patients.²⁸ In addition to the lateral frontopolar cortex activation that is observed in healthy persons, the medial frontopolar cortex of high-functioning ASD patients also exhibited activation, thereby demonstrating the compensation mechanism of an impaired brain.²⁹

2.3. Cartoon watching

A functional connectivity analysis of the young children with ASD, compared to typically developing children, revealed lower network efficiency in the prefrontal, temporal, and occipital regions.³⁰ The global and local network efficiencies, based on a functional connectivity measure using HbR and total hemoglobin (HbT) levels, decreased as the age of the ASD children increased: Their HbO-based network efficiency was reduced as well.³¹ The spatial complexity analysis of functional connectivity revealed impaired information exchange in the right hemisphere of the ASD children compared to that of healthy children.³² The long-range temporal correlation values measured using HbO levels were lower in the left temporal regions, and exponents obtained through the detrended fluctuation analysis were inversely linked with the severity of ASD.³³ The PFC of ASD children was largely responsible for the deteriorated functional connectivity.³⁴

2.4. Go/No-go task

When compared to healthy children, high-functioning children with ASD showed lower HbO activation levels in the right PFC during response inhibition tasks.³⁵ In a frontotemporal examination, the ASD patients showed impaired cortical activation in the inferior frontal gyrus and middle frontal gyrus.³⁶ The administration of methylphenidate in ASD-comorbid ADHD children was revealed to suppress the hemodynamic response.³⁷

2.5. Resting state

The resting state functional connectivity (RSFC) calculated based on low-frequency spontaneous fluctuations in the anterior PFC was higher in children with ASD than in healthy children, and it was associated with the Autism Diagnostic

Observation Schedule scores.³⁸ The children with ASD exhibited lower interhemispheric RSFC in the temporal cortex and altered local connections in both their temporal cortices.³⁹ The fluctuations of the HbO and HbR levels at a resting state were higher in children with ASD than in healthy children and were used in the SVM-based classification along with RSFC.⁴⁰

2.6. *Audio stimulus*

Compared to healthy children, the children with ASD exhibited weaker cortical activity in the left temporal cortex in response to phonemic words and the right temporal cortex in response to prosodic ones.⁴¹ The bilateral auditory cortex lesions in the ASD patients exhibited similar responses to those of healthy persons during attentive listening; however, this differed in the PFC that exhibited an attention impairment instead of an impaired auditory cortex.⁴² The infants who showed reduced and left-lateralized temporal cortical activation in response to vocal and nonvocal sounds were diagnosed with ASD a few years later when compared with infants who remained healthy.²³

2.7. *Stroop task*

The study that conducted a Stroop task did not reveal any differences in the hemodynamic responses among ASD, ADHD, and healthy children.³⁵

2.8. *Expression task*

The ASD children showed reduced PFC activation and were more expressive for nonemotional pictures as compared to healthy children while describing their mental state in response to viewing a black and white picture depicting human eyes.⁴³

2.9. *Imitation task*

The children with ASD showed enhanced neuronal activation while performing imitation tasks after undergoing imitation training when compared to the low activation levels before undergoing the training.⁴⁴

2.10. *Stop-signal*

Compared to healthy persons and ADHD patients, the ASD patients showed a reduced HbO response

in the ventrolateral PFC and, compared to ADHD patients, they exhibited impaired activation in the PFC during inhibitory control tasks.²⁷

2.11. *Color and shape span task*

A weighted separability index based on the HbO levels was utilized to reveal significant differences between the left dorsolateral PFCs of ASD patients and healthy persons during a working memory task.⁴⁵

2.12. *Emotional facial recognition task*

ASD patients in general and specifically those who paid a higher level of attention to details exhibited impaired cortical activity in the left frontotemporal region.²⁸

3. Attention-Deficit Hyperactivity Disorder

ADHD is a brain impairment that affects patients by causing lack of attention, excessive activity, and hastiness. This impairment is observed during childhood, and can remain throughout one's life. Most ADHD patients are diagnosed at an elementary school age when they are identified to be different from other children of the same age. A suffering child mostly overlooks details while working, makes careless mistakes, fidgets or squirms while sitting, talks without listening to others, or is unable to wait. The underlying reasons for ADHD are still unknown, and hence, it can neither be prevented nor fully cured. However, various therapies and medications can improve the quality of life of ADHD patients by reducing or managing the symptoms. Many research studies have been conducted using fNIRS to uncover the neuronal behavior that causes the symptoms. The task-wise distribution of ADHD papers is presented in Fig. 2, and the details are summarized in Table 2.

3.1. *Go/No-go tasks*

The children with ADHD showed little cortical activation in the right PFC during the inhibitory control in a no-go situation when compared to the higher activation observed in healthy children.^{35,46} The administration of methylphenidate to children with ADHD resulted in an improved HbO response

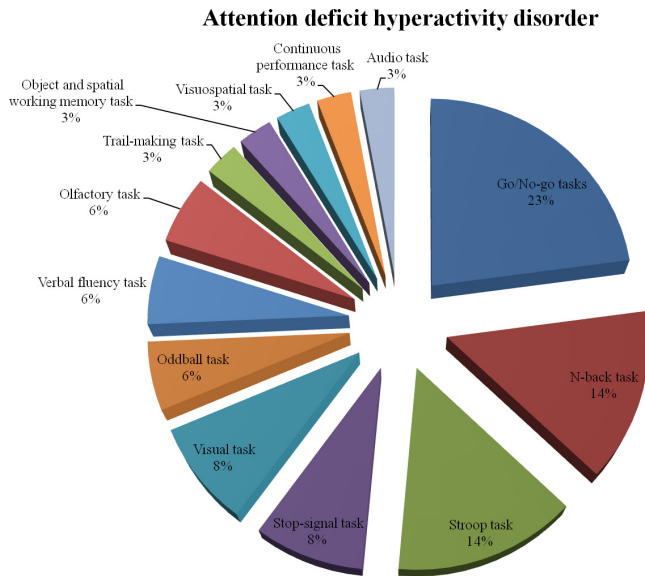


Fig. 2. Task-based distribution of studies on attention-deficit hyperactivity disorder (total studies: 35).

in the right lateral PFC that was related to a better performance during inhibitory response.⁴⁷ The reduced inferior and middle frontal gyri showed better hemodynamic activation due to methylphenidate administration, but this effect was not witnessed during the placebo-based activation.⁴⁸ The atomoxetine-administered children with ADHD exhibited similar improvements in cortical activation to those administered with methylphenidate during inhibitory control.⁴⁹ In a classification study, the reduced activation patterns in the region of the right PFC were useful for better distinguishing between children with ADHD and the healthy ones by resulting in high area-under-the-curve values and sensitivity levels.⁵⁰ The children with ADHD showed an overall reduced left frontopolar cortex activation, especially during response inhibition.⁵¹ Methylphenidate improved activation levels in children with ADHD, and this medicated response has been utilized efficiently for differentiating between ASD and ADHD.³⁷

3.2. N-back task

Compared to healthy individuals, the ADHD patients showed a decreased activation in the ventrolateral PFC during working memory tasks, especially in the case of high load conditions, such as a two-back task.⁵² A reduced HbO response was witnessed in ADHD patients during a working memory two-back task, which was unrelated to the

reduced HbO response due to response inhibition in the stop-signal task.⁵³ A complexity analysis via the permutation entropy value revealed its inverse correlation with hemodynamic activation in the PFC whereas its values of the right dorsolateral PFC of children with ADHD were higher than those of healthy children, and the entropy value was correlated with disease severity.⁵⁴ A machine learning-based classification study using multi-domain measures including blood fatty acid profiles, psychological parameters, and fNIRS performed efficiently in differentiating children with ADHD from healthy children, and utilization of HbR levels generated better results than HbO levels.⁵⁵ A multivariate pattern analysis-based classification showed 86% accuracy in differentiating between healthy and ADHD children and identified highly useful brain regions.⁵⁶

3.3. Stroop task

The boys with ADHD showed impaired dorsolateral PFC activation and higher brain activity in the right side as a compensation mechanism when compared to the activation in healthy boys.⁵⁷ The HbO responses were significantly increased in the bilateral inferior-PFC and especially in the inferior lateral region of healthy individuals as compared to those of ADHD patients during a Stroop color-word task.⁵⁸ The polymorphism of synaptosomal-associated protein 25 gene was associated with methylphenidate-related HbO and HbR changes in ADHD patients.⁵⁹ The go/no-go task produced significant differentiable changes between the HbO levels in the PFCs of healthy and ADHD patients while the Stroop task did not.³⁵ Compared to the Stroop task, the reverse Stroop task showed significant differentiable HbO responses among healthy, ASD, and ADHD children in the right lateral PFC.⁶⁰

3.4. Stop-signal task

Compared to those of healthy persons, the HbO and HbR responses in ADHD patients were weakened during the inhibitory process.⁵³ Further, during response inhibition, the cortical activity in the left ventrolateral PFC significantly differed in ADHD patients when compared to ASD patients and healthy persons.²⁷ A longitudinal study showed that ADHD patients exhibited improved prefrontal responses after a single dose of methylphenidate,

Table 2. Studies on attention-deficit hyperactivity disorder.

Work	Experimental population	Brain area under study	Instrument	No. of channels/ separation(s)	Analyzed parameters
Go/No-go tasks Xiao <i>et al.</i> ³⁵ (2012)	16 Healthy individuals (M), 9.69 ± 1.74 yrs; 16 ADHD patients (M), 9.75 ± 1.18 yrs; 19 ASD patients (M), 10.11 ± 2.08 yrs	Prefrontal region	JH-NIRS-BR-05	16	HbO
Inoue <i>et al.</i> ⁴⁶ (2012)	20 Healthy individuals (6 F and 14 M), 6–14 yrs; 20 ADHD patients (6 F and 14 M), 6–14 yrs	Prefrontal cortex	Cognoscope	16/2.5 cm	HbO, HbR
Monden <i>et al.</i> ⁴⁷ (2012)	12 ADHD patients (1 F and 11 M), 9.7 ± 2.4 yrs	Lateral prefrontal cortices	ETG-4000	44/3 cm	HbO, HbR
Monden <i>et al.</i> ⁴⁸ (2012)	16 Healthy individuals (6 F and 10 M), 8.9 ± 2.4 yrs; 16 ADHD patients (4 F and 12 M), 8.8 ± 2.2 yrs	Lateral prefrontal cortices	ETG-4000	44/3 cm	HbO, HbR
Nagashima <i>et al.</i> ⁴⁹ (2014)	16 Healthy individuals (2 F and 14 M), 8.9 ± 2.2 yrs; 16 ADHD patients (2 F and 14 M), 8.8 ± 2.2 yrs	Lateral prefrontal cortices	ETG-4000	44/3 cm	HbO, HbR
Monden <i>et al.</i> ⁵⁰ (2015)	30 Healthy individuals (5 F and 25 M), 9.7 ± 2.3 yrs; 30 ADHD patients (10 F and 20 M), 9.1 ± 2.6 yrs	Lateral prefrontal cortices	ETG-4000	44/3 cm	HbO
Miao <i>et al.</i> ⁵¹ (2017)	15 Healthy individuals (4 F and 11 M), 7.67 ± 1.05 yrs; 14 ADHD patients (4 F and 10 M), 7.71 ± 0.99 yrs	Bilateral frontotemporal region	ETG-4000	52/3 cm	HbO, HbR
Sutoko <i>et al.</i> ³⁷ (2019)	21 ADHD patients, 7.8 ± 1.7 yrs; 11 ADHD+ASD patients, 8.2 ± 2.1 yrs	Bilateral frontotemporal region	ETG-4000	44/3 cm	HbO, HbR
N-back task Ehls <i>et al.</i> ⁵² (2008)	13 Healthy individuals (5 F and 8 M), 26.8 ± 3.6 yrs; 13 ADHD patients (4 F and 9 M), 29.8 ± 8.0 yrs	Lateral prefrontal areas	ETG-100	24/3 cm	HbO, HbR

Table 2. (Continued)

Work	Experimental population	Brain area under study	Instrument	No. of channels/ separation(s)	Analyzed parameters
Schecklmann <i>et al.</i> ⁵³ (2013)	41 Healthy individuals (21 F and 20 M), 36.1 ± 10.1 yrs; 45 ADHD patients (21 F and 24 M), 36.4 ± 9.9 yrs	Bilateral frontotemporal region	ETG-4000	52/3 cm	HbO, HbR
Gu <i>et al.</i> ⁵⁴ (2017)	16 Healthy individuals (6 F and 10 M), 7.3 ± 1.3 yrs; 15 ADHD patients (5 F and 10 M), 7.6 ± 1.4 yrs	Bilateral frontotemporal region	ETG-4000	52/3 cm	HbO
Crippa <i>et al.</i> ⁵⁵ (2017)	22 Healthy individuals (1 F and 21 M), 11.4 ± 1.9 yrs; 22 ADHD patients (M), 11.5 ± 1.5 yrs	Bilateral frontotemporal region	DYNOT	32/2.7 cm	HbO, HbR
Gu <i>et al.</i> ⁵⁶ (2018)	25 Healthy individuals (9 F and 16 M), 7.4 ± 1.1 yrs; 25 ADHD patients (9 F and 16 M), 7.5 ± 1.2 yrs	Bilateral frontotemporal region	ETG-4000	52/3 cm	HbO
Stroop task					
Moser <i>et al.</i> ⁵⁷ (2009)	12 Healthy individuals (M), 10.6 ± 1.6 yrs; 12 ADHD patients (M), 10.1 ± 1.9 yrs	Lateral prefrontal cortex	NIRO-300	2/4 cm and 5 cm	HbO, HbR
Negoro <i>et al.</i> ⁵⁸ (2010)	20 Healthy individuals (3 F and 17 M), 9.35 ± 2.13 yrs; 20 ADHD patients (2 F and 18 M), 9.55 ± 1.93 yrs	Frontal regions	ETG-100	24/3 cm	HbO
Oner <i>et al.</i> ⁵⁹ (2011)	15 ADHD adults, 16 ADHD children	Prefrontal cortex	NIROSCOPE 301	16/2.5 cm	HbO, HbR
Xiao <i>et al.</i> ³⁵ (2012)	16 Healthy individuals (M), 9.69 ± 1.74 yrs; 16 ADHD patients (M), 9.75 ± 1.18 yrs; 19 ASD patients (M), 10.11 ± 2.08 yrs	Prefrontal region	JH-NIRS-BR-05	16	HbO

Table 2. (Continued)

Work	Experimental population	Brain area under study	Instrument	No. of channels/ separation(s)	Analyzed parameters
Yasumura <i>et al.</i> ⁶⁰ (2014)	15 Healthy individuals (9 F and 6 M), 9.56 ± 1.51 yrs; 10 ADHD patients (2 F and 8 M), 11.18 ± 2.23 yrs; 11 ASD patients (4 F and 7 M), 10.51 ± 2.30 yrs	Prefrontal cortex	OEG-16	16/3 cm	HbO, HbR
Stop-signal task					
Schecklmann <i>et al.</i> ⁵³ (2013)	41 Healthy individuals (21 F and 20 M), 36.1 ± 10.1 yrs; 45 ADHD patients (21 F and 24 M), 36.4 ± 9.9 yrs	Bilateral frontotemporal region	ETG-4000	52/3 cm	HbO, HbR
Ishii-Takahashi <i>et al.</i> ²⁷ (2014)	21 Healthy individuals (8 F and 13 M), 28.8 ± 5.5 yrs; 19 ADHD patients (8 F and 11 M), 30.6 ± 7.4 yrs; 21 ASD patients (13 F and 8 M), 30.8 ± 7.2 yrs	Bilateral frontotemporal region	ETG-4000	24/3 cm	HbO, HbR
Ishii-Takahashi <i>et al.</i> ⁶¹ (2015)	20 Healthy individuals (6 F and 14 M), 8.1 ± 1.6 yrs; 30 ADHD patients (4 F and 26 M), 8.6 ± 1.4 yrs	Bilateral frontotemporal region	ETG-4000	24/3 cm	HbO, HbR
Visual task					
Ichikawa <i>et al.</i> ⁶² (2014b)	13 Healthy individuals (M), 9.7 ± 1.3 yrs; 13 ADHD patients (M), 10.0 ± 1.3 yrs	Bilateral temporal region	ETG-4000	24/3 cm	HbO, HbR
Ichikawa <i>et al.</i> ¹⁹ (2014a)	9 ADHD patients (M), 9.8 ± 1.6 yrs; 8 ASD patients (M), 9.8 ± 1.4 yrs	Bilateral temporal region	ETG-4000	24/3 cm	HbO
Marx <i>et al.</i> ⁶³ (2015)	9 ADHD patients (3 F and 6 M), 9.9 ± 2.1 yrs	Bilateral frontal and temporal regions	ETG-4000	44/3 cm	HbO

Table 2. (Continued)

Work	Experimental population	Brain area under study	Instrument	No. of channels/ separation(s)	Analyzed parameters
Oddball task					
Nagashima <i>et al.</i> ⁶⁴ (2014)	15 Healthy individuals (3 F and 12 M), 10.1 ± 1.7 yrs; 15 ADHD patients (3 F and 12 M), 9.8 ± 1.26 yrs	Bilateral frontal and temporal regions	ETG-4000	44/3 cm	HbO
Nagashima <i>et al.</i> ⁶⁵ (2014)	22 Healthy individuals (5 F and 17 M), 9.8 ± 2.0 yrs; 22 ADHD patients (6 F and 16 M), 9.5 ± 2.0 yrs	Bilateral frontal and temporal regions	ETG-4000	44/3 cm	HbO
Verbal fluency task					
Schecklmann <i>et al.</i> ⁶⁶ (2008)	14 Healthy individuals (5 F and 9 M), 40.6 ± 8.9 yrs; 14 ADHD patients (6 F and 8 M), 40.4 ± 10.7 yrs	Bilateral frontal and temporal regions	ETG-4000	44/3 cm	HbO, HbR
Ishii-Takahashi <i>et al.</i> ²⁷ (2014)	21 Healthy individuals (8 F and 13 M), 28.8 ± 5.5 yrs; 19 ADHD patients (8 F and 11 M), 30.6 ± 7.4 yrs; 21 ASD patients (13 F and 8 M), 30.8 ± 7.2 yrs	Bilateral frontotemporal region	ETG-4000	24/3 cm	HbO, HbR
Olfactory task					
Schecklmann <i>et al.</i> ⁶⁷ (2011)	29 Healthy individuals (14 F and 15 M), 27.8 ± 4.1 yrs; 29 ADHD patients (14 F and 15 M), 28.2 ± 4.5 yrs	Bilateral frontal and temporal regions	ETG-4000	44/3 cm	HbO
Schecklmann <i>et al.</i> ⁶⁸ (2011)	22 Healthy individuals (14 F and 8 M), 149 ± 19 months; 27 ADHD patients (7 F and 20 M), 152 ± 17 months	Bilateral frontal and temporal regions	ETG-4000	44/3 cm	HbO
Trail-making task					
Weber <i>et al.</i> ⁶⁹ (2005)	9 Healthy individuals (M), 11.3 ± 1.3 yrs; 11 ADHD patients (M), 10.4 ± 1.2 yrs	Frontal region	NIRO-300	2/4.6 cm	HbO, HbR, CBV, Cyttox, TOI

Table 2. (Continued)

Work	Experimental population	Brain area under study	Instrument	No. of channels/ separation(s)	Analyzed parameters
Object and spatial working memory task					
Schecklmann <i>et al.</i> ⁷⁰ (2010)	19 Healthy individuals (4 F and 15 M), 138.6 ± 16.5 months; 19 ADHD patients (2 F and 17 M), 139.5 ± 17.3 months	Frontal cortex	ETG-4000	52/3 cm	HbO
Visuospatial task					
Tsujimoto <i>et al.</i> ⁷¹ (2013)	10 Healthy individuals (M), 10.1 ± 1.8 yrs; 16 ADHD patients (M), 10.9 ± 2.0 yrs	Lateral prefrontal cortex	OEG-16	16/3 cm	HbO
Continuous performance task					
Araki <i>et al.</i> ⁷² (2015)	12 ADHD patients (6 F and 6 M), 9.8 ± 2.3 yrs	Bilateral prefrontal cortex	ETG-100	24/3 cm	HbO, HbR
Audio task					
Kochel <i>et al.</i> ⁷³ (2015)	14 Healthy individuals (M), 121.93 ± 11.29 months; 14 ADHD patients (M), 123.43 ± 17.41 months	Bilateral temporal and parietal cortices	ETG-4000	48/3 cm	HbO, HbR

and its long-term use yielded an activation equivalent to that of a healthy person.⁶¹

3.5. Visual task

The children with ADHD did not exhibit cortical activity while watching angry faces, which illustrates the impairment of ADHD children to recognize an angry face.⁶² Using a five-fold cross-validation in an SVM-based classification of 24 channels of fNIRS data proved to be fruitful in achieving a maximum accuracy of 84% in differentiating between patients with ADHD and those with ASD.¹⁹ Neurofeedback training using a visual display yielded good results as it reportedly reduced the ADHD symptoms in children.⁶³

3.6. Oddball task

Compared to healthy children, the ADHD children exhibited a lack of activation in the right prefrontal and inferior parietal cortices, which was normalized after atomoxetine administration.⁶⁴ Administration of methylphenidate to ADHD children resulted in a normalization of activity in the right PFC but not in the inferior parietal lobe.⁶⁵

3.7. Verbal fluency task

The patients with ADHD showed a lower cortical activation in the inferior frontal region compared to healthy persons, and the activation was inversely related to task performance.⁶⁶ The hemodynamic responses of ADHD patients were differentiable from those of healthy persons but were similar to those of ASD patients, thereby restricting the use of verbal fluency tasks (VFTs) in the multicategory classification.²⁷

3.8. Olfactory task

In the temporal, somatosensory, and inferior frontal cortices, the cortical activation of ADHD patients was reduced compared to that of healthy persons.⁶⁷ Administering methylphenidate to ADHD children improved the HbO responses in the temporal cortex while the cessation of the medication resulted in the recurrence of diminished activation.⁶⁸

3.9. Trail-making task

The children with ADHD showed an increase in HbO and cerebral blood volume (CBV) levels during

short-attention tasks, while healthy children only showed increased activity during long-attention tasks.⁶⁹

3.10. Object and spatial working memory task

The cortical activations during object working memory tasks were higher than those during spatial working memory tasks for ADHD and healthy children, which showed no significantly different patterns.⁷⁰

3.11. Visuospatial task

Compared to healthy children, the ADHD children showed higher activation in the PFC in response to distraction during the task owing to the impairment in inhibition control.⁷¹

3.12. Continuous performance task

The long-term usage of atomoxetine medicine significantly improved the HbO and HbR responses in the right dorsolateral PFC of children with ADHD.⁷²

3.13. Audio task

Compared to healthy individuals, the ADHD patients exhibited lower activation levels in the superior temporal gyrus in response to angry prosody and supramarginal gyrus activation due to the compensatory mechanism.⁷³

4. Epilepsy

Epilepsy is a disease owing to which a patient suffers from seizures. The seizures can affect patients in many ways and can range from simply staring into space to experiencing their full-body shaking or even falling on the ground. In some cases, the symptoms are visible in the whole body, yet the cause of epilepsy is from brain impairment. To study epilepsy, various studies were conducted in different environments using fNIRS. The task-wise distribution is shown in Fig. 3, and the details are outlined in Table 3.

4.1. Ictal or seizure recording

In this type of video-EEG experiment, the patient is continuously monitored using video recording, and

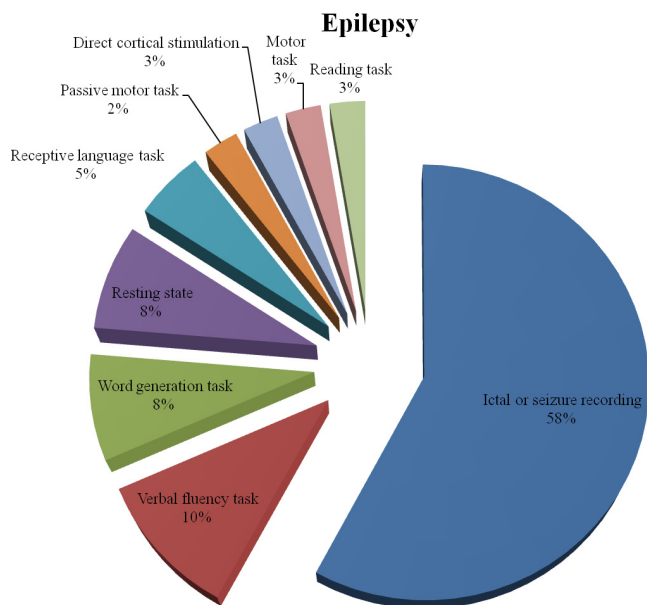


Fig. 3. Task-based distribution of studies on epilepsy (total studies: 38).

the exact timing of each seizure is matched with that of the recording. While this is happening, the subject can be in a resting or moving state. Initially, the onset of seizure was related to an increase in CBV.⁷⁴ In a study performed after this, a contradictory result showing a decrease in CBV at the time of seizure onset appeared.⁷⁵ It was later revealed that the increase or decrease in HbO levels in patients is associated with the type of seizure.⁷⁶ Cerebral oxygenation was utilized to distinguish between complex partial seizures (CPS) and rapidly secondarily generalized CPS.⁷⁷ The regional CBV was increased via some channels, thereby facilitating the identification of the focal aspect of seizures.^{78,79} Another study on children yielded similar results showing different CBV changes in different seizure types.⁸⁰ In a detailed study on absence seizures, the HbO level decreased while the HbR level increased.⁸¹ Further, another study proved fNIRS to be effective in drug management as an anticonvulsant medication administered to an infant resulted in a reduction in seizure frequency.⁸² Generalized spike-and-wave discharges are associated with absence epilepsy and exhibit oxygenation before the onset followed by deoxygenation, which is again followed by oxygenation and then returning to the baseline level in the frontal cortex.⁸³ An initial decrease in HbO level, known as the initial dip, that precedes the increase in HbO and HbT levels

was found at the onset of ictal seizures.⁸⁴ In a study focusing on temporal lobe seizures, the HbO and HbR changes were seen in the focal point (i.e., temporal region) as well as in the remote areas such as in the frontal or parietal cortices.⁸⁵ A recording of supplementary motor area (SMA) seizures in a nine-year-old girl revealed an increase in cerebral blood flow (CBF), which started in the SMA and extended to the premotor and sensorimotor cortices.⁸⁶

fNIRS was found to be helpful and, in some cases, it performed better than EEG in detecting frontal lobe seizures that show increased HbO and HbT levels and variable HbR responses in the focal as well as in the contralateral regions.⁸⁷ The sensitivity and specificity estimates resulting from a decrease in the HbR were higher than those resulting from an increase in HbO and HbT levels.⁸⁸ In the preictal and postictal periods, the regional cerebral oxygenation was increased while it was decreased near the onset time of ictal seizures, as shown in previous studies.⁸⁹ These seizure studies on epilepsy are largely affected by the issue of motion artifacts, which was resolved by using collodion-fixed prism-based optical fibers.⁹⁰ The decrease in HbR was more significant than the increase in HbO and HbT levels in a study on posterior epilepsies.⁹¹ The increase in oxygen saturation was associated not only with ictal but also with epileptiform discharges without seizures.⁹² The HbO values were observed to increase in both hemispheres, but the increase was more pronounced in one hemisphere, which allows for the localization of the epilepsy-affected region using fNIRS.⁹³ Utilizing a wireless fNIRS device to detect a seizure achieved a very low accuracy in seizure detection and contradicting results when utilized with a generic algorithm.⁹⁴ Among epilepsy studies, an EEG-fNIRS study provided better results in detecting interictal epileptic discharges than an EEG-fMRI one.⁹⁵

4.2. Verbal fluency task

The determination of language lateralization was achieved with a higher accuracy by displaying clear activation in the language areas of the brain in children as well as in adults.⁹⁶ The activation in the left Broca's area was higher than that in the right hemisphere, thereby showing the left-hemisphere dominance in children.^{84,97} The damage in the brain results in a reorganization, as shown in a six-year-old child, that the left-hemisphere dominance was

Table 3. Studies on epilepsy.

Work	Experimental population	Brain area under study	Instrument	No. of channels/ separation(s)	Analyzed parameters
Ictal or Seizure Recording Villringer <i>et al.</i> ⁷⁴ (1994)	17 Epilepsy patients, 23–75 yrs	Frontal and occipital regions	NIRO-500	2/3.5–7 cm	HbO, HbR
Steinhoff <i>et al.</i> ⁷⁵ (1996)	2 Epilepsy patients, 51 yrs and 36 yrs	Frontal cortex	INVOS-3100	32/2.5 cm and 3.5 cm	TOI
Adelson <i>et al.</i> ⁷⁶ (1999)	3 Epilepsy patients (2 F and 1 M), 4-month-old male and 45 yrs and 16 yrs females	Frontal region	INVOS-3100A, NIRO-500	1/3 cm and 4 cm, 1/4 cm	HbO, HbR, HbT, Cyttox SaO ₂
Sokol <i>et al.</i> ⁷⁷ (2000)	8 Epilepsy patients (4 F and 4 M), 26–47 yrs	Frontotemporal region	INVOS-3100A	1/3 cm and 4 cm	SaO ₂
Watanabe <i>et al.</i> ⁷⁸ (2000)	12 Epilepsy patients (7 F and 5 M), 8–45 yrs	Temporal and parietal regions		8 and 24/3 cm	CBV
Watanabe <i>et al.</i> ⁷⁹ (2002)	32 Epilepsy patients, 4–40 yrs	Temporal, frontal, and parietal regions	NIRS-1010	24/3 cm	CBV
Haginoya <i>et al.</i> ⁸⁰ (2002)	15 Epilepsy patients (6 F and 9 M), 1.5 months–16 yrs	Frontal cortex	NIRO-300	1/4 cm	HbO, HbR, HbT
Buchheim <i>et al.</i> ⁸¹ (2004)	3 Epilepsy patients (1 F and 2 M), 21, 28, and 46 yrs	Frontal cortex	NIRO-500	4 cm	HbO, HbR
Diaz <i>et al.</i> ⁸² (2006)	78-Day-old epileptic male	Frontal region	INVOS-300	2	SO ₂
Roche-Labarbe <i>et al.</i> ⁸³ (2008)	6 Epilepsy patients (2 F and 4 M), 1–16 yrs	Left frontal cortex	Imagent	1/3.5 cm	HbO, HbR, HbT
Gallagher <i>et al.</i> ⁸⁴ (2008)	10-Year-old epileptic boy	Right frontal, bilateral parasagittal, and bilateral rolandic regions	Imagent	128	HbO, HbR, HbT
Nguyen <i>et al.</i> ⁸⁵ (2012)	9 Epilepsy patients (4 F and 5 M), 11–56 yrs	Full head	Imagent	120/3 cm and 5 cm	HbO, HbR, HbT
Sato <i>et al.</i> ⁸⁶ (2013)	9-Year-old epileptic female	Bilateral motor- associated areas	ETG-7100	48/3 cm	HbT
Nguyen <i>et al.</i> ⁸⁷ (2013)	18 Epilepsy patients (11 F and 7 M), 13–46 yrs	Bilateral frontal, temporal, and parietal regions	Imagent	44–203/3 cm and 5 cm	HbO, HbR, HbT

Table 3. (Continued)

Work	Experimental population	Brain area under study	Instrument	No. of channels/ separation(s)	Analyzed parameters
Peng <i>et al.</i> ⁸⁸ (2014)	40 Epilepsy patients (14 F and 26 M), 10–62 yrs	Bilateral frontal, temporal, and central regions	Imagent	76–154/3–5 cm	HbO, HbR, HbT
Seval ⁸⁹ (2014)	6 Epilepsy patients (3 F and 3 M), 34–49 yrs	Frontal cortex	Nonin EQUANOX Model 7600	2/2 cm and 4 cm	HbO, HbR, HbT
Yücel <i>et al.</i> ⁹⁰ (2014)	2 Epilepsy patients (1 F and 1 M), 59 yrs and 36 yrs	Frontal and temporal regions	CW6	8	HbO, HbR, HbT, CMRO ₂ , CBF
Pouliot <i>et al.</i> ⁹¹ (2014)	9 Epilepsy patients (4 F and 5 M), 18–64 yrs	Full head	Imagent	Over 100/3–5 cm	HbO, HbR, HbT
Monrad <i>et al.</i> ⁹² (2015)	4 Epilepsy patients, 5–17 yrs	Frontal region	INVOS-5100C	44	SO ₂
Rizki <i>et al.</i> ⁹³ (2015)	6 Epilepsy patients (4 F and 2 M), 20–55 yrs	Temporal region	ETG-4000	44	HbO
Jeppesen <i>et al.</i> ⁹⁴ (2015)	15 Epilepsy patients, 20–58 yrs	Frontal region	PortaLite	2/3, 3.5, and 4 cm	HbO, HbR, HbT
Pellegrino <i>et al.</i> ⁹⁵ (2016)	9 Epilepsy patients (6 F and 3 M), 21–53 yrs	Frontal and temporal regions	Brainsight		HbO, HbR
Verbal fluency task					
Gallagher <i>et al.</i> ⁹⁶ (2007)	3 Healthy individuals (1 F and 2 M), 25–28 yrs; 6 Epilepsy patients (1 F and 5 M), 9–29 yrs	Broca's area, Wernicke's area, and same area in right hemisphere	Imagent	128/2–5 cm	HbO, HbR
Gallagher <i>et al.</i> ⁸⁴ (2008)	9-Year-old epileptic male	Broca's area, Wernicke's area, and same area in right hemisphere	Imagent	128/2–5 cm	HbO, HbR
Gallagher <i>et al.</i> ⁹⁷ (2008)	10-Year-old epileptic male	Right frontal, bilateral parasagittal, and bilateral rolandic regions	Imagent	128	HbO, HbR, HbT
Vannasing <i>et al.</i> ⁹⁸ (2016)	10-Year-old epileptic male	Broca's area, Wernicke's area, and same area in right hemisphere	Imagent		HbO, HbR

Table 3. (Continued)

Work	Experimental population	Brain area under study	Instrument	No. of channels/ separation(s)	Analyzed parameters
Word generation task Watanabe <i>et al.</i> ⁹⁹ (1998)	11 Healthy individuals, 25–47 yrs; 6 Epilepsy patients, 25–47 yrs	Frontotemporal area		24/3 cm	HbO, HbR, HbT
Watson <i>et al.</i> ¹⁰⁰ (2004)	8 Healthy individuals (3 F and 5 M), 24–49 yrs; 16 Epilepsy patients (8 F and 8 M), 20–58 yrs	Frontal cortex	ETG-100	24	HbT
Ota <i>et al.</i> ¹⁰¹ (2010)	28 Epilepsy patients (16 F and 12 M), 14–74 yrs	Frontotemporal area	ETG-4000	24	HbO
Resting state Machado <i>et al.</i> ¹⁰² (2011)	10-Year-old epileptic male	Right frontal, bilateral parasagittal, and bilateral rolandic regions	Imagent	128	HbO, HbR
Pouliot <i>et al.</i> ¹⁰³ (2012)	9-Year-old epileptic male	Broca's area, Wernicke's area, and same area in right hemisphere	Imagent	128/2–5 cm	HbO, HbR
Sirpal <i>et al.</i> ¹⁰⁴ (2019)	40 Epilepsy patients (13 F and 27 M), 11–62 yrs	Full head	Imagent	3–4 cm	HbO, HbR
Receptive language task Gallagher <i>et al.</i> ⁹⁷ (2008)	9-Year-old epileptic male	Broca's area, Wernicke's area, and same area in right hemisphere	Imagent	128/2–5 cm	HbO, HbR

Table 3. (Continued)

Work	Experimental population	Brain area under study	Instrument	No. of channels/ separation(s)	Analyzed parameters
Vannasing <i>et al.</i> ⁹⁸ (2016)	10-Year-old epileptic male	Broca's area, Wernicke's area, and same area in right hemisphere	Imagent		HbO, HbR
Passive motor task					
Honda <i>et al.</i> ¹⁰⁵ (2009)	6-Month-old epileptic male	Bilateral sensorimotor cortices	ETG-7100	24/3 cm	HbO
Direct cortical stimulation					
Sato <i>et al.</i> ¹⁰⁶ (2012)	18-Year-old epileptic male	Frontotemporal areas	ETG-4100	48	HbO, HbR
Motor task					
Visani <i>et al.</i> ¹⁰⁷ (2014)	12 Healthy individuals (4 F and 8 M), 32.2 ± 10 yrs; 10 Epilepsy patients (3 F and 7 M), 36 ± 10.2 yrs	Bilateral motor cortex	Class-I medical device by the Physics Department of the Politecnico of Milan	30	HbO, HbR
Reading task					
Safi <i>et al.</i> ¹⁰⁸ (2016)	42-Year-old epileptic male	Full head	Imagent		HbO, HbR

changed to the right-hemisphere dominance when the child became 10 years old.⁹⁸

4.3. *Word generation task*

One of the earliest researches on epilepsy using fNIRS noninvasively accessed the language dominance areas in the brain by showing activations on the same side as determined by the Wada test.⁹⁹ Patients exhibited better language lateralization results before surgery than after surgery.¹⁰⁰ The fNIRS was used in combination with fMRI and MEG to improve the detection of language lateralization.¹⁰¹

4.4. *Resting state*

When comparing methods to detect seizure activity efficiently, the Bayesian general linear model was more accurate and reliable than the wavelet generalized least-square algorithm.¹⁰² In terms of estimating the hemodynamic response, the Volterra kernel expansion method showed better results in the cases where the conventional methods failed.¹⁰³ A model based on long short-term memory in the recurrent neural networks demonstrated an efficient performance in seizure detection in a hybrid EEG–fNIRS study.¹⁰⁴

4.5. *Receptive language task*

While listening to storytelling, the Wernicke's and Broca's areas in both hemispheres were activated in a nine-year-old Yiddish boy.⁹⁷ The left hemisphere was dominant at first in an epilepsy patient who was six-year-old while the right hemisphere was dominant when the patient turned 10-year-old owing to the functional brain reorganization due to the damage caused by epilepsy.⁹⁸

4.6. *Passive motor task*

Once a portion of the brain is surgically removed to treat epilepsy, the functional loss is recovered by the healthy portion of the brain via reorganization. The movement of right arm was impaired due to a surgery performed in the left hemisphere, but rehabilitation through passive movement therapy showed activation in the right hemisphere.¹⁰⁵

4.7. *Direct cortical stimulation*

The cortical stimulation of the left temporal region resulted in a rise in the HbO and HbR levels in the

temporal as well as in the frontal regions, thereby displaying the possible functional connectivity of the language area.¹⁰⁶

4.8. *Motor task*

The epileptic patients showed an activation of a comparably smaller amplitude than the activation exhibited by healthy persons while gripping a soft item using their right hand.¹⁰⁷

4.9. *Reading task*

In a patient with reading epilepsy, the seizure activity was located in the left precentral gyrus covering the motor, premotor, and supplementary motor cortex areas while reading aloud or silently.¹⁰⁸

5. *Depressive Disorders*

Patients affected by various types of depressive disorders suffer from feelings of sorrow and hollowness. This condition intensely affects their thinking ability, emotions, and personality inclination. The patients can suffer from a lack of appetite, tiredness, loss of motivation in their daily life, frustration, or anger. The underlying reasons for depression can be a single factor or a combination of various factors like losing someone, trauma, or social, hormonal, or genetic issues. The symptoms can occur at any age, yet in most of the known cases, they developed in adults. The fNIRS has been used by several researchers to study depressive states. The task-wise distribution is presented in Fig. 4, and all studies are outlined in Table 4.

5.1. *Verbal fluency task*

This task has been widely used to test depressed populations. In the earliest studies conducted to discover the neuronal activation in patients with major depressive disorder (MDD) and BD, while monitoring only the left PFC, the increase in HbO levels was significantly lower in patients than in healthy individuals.¹⁰⁹ This result was also observed while monitoring the bilateral PFC in a study on BD patients.¹¹⁰ In a study on late-onset MDD patients, a smaller area in the PFC of the MDD patients was activated when compared to the healthy persons.¹¹¹ The patients with late-onset

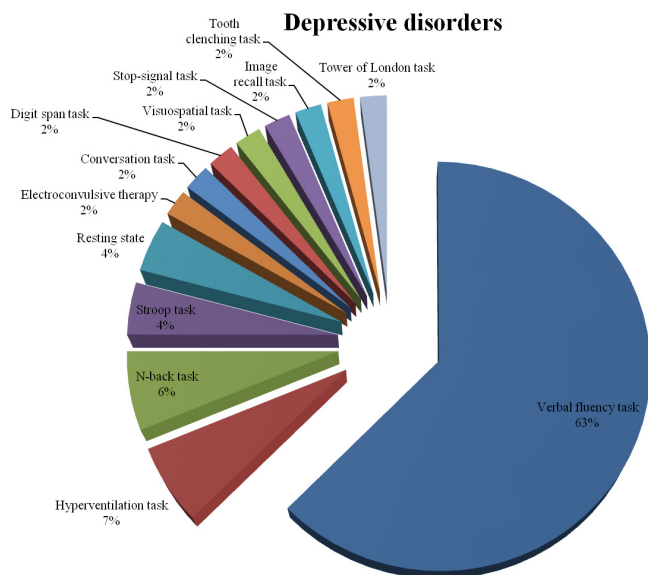


Fig. 4. Task-based distribution of studies on depressive disorders (total studies: 48).

depression exhibited impaired community interaction that was positively correlated with a reduced frontopolar HbO response.¹¹² Compared to healthy persons, the MDD patients showed a lower level of activation in the PFC as well as in the temporal regions.^{113,114} The area-under-the-curve and weighted-center values extracted from the time-series signal associated with the HbO responses showed significant differences between patients with unipolar disorder (UD) and those with BD.¹¹⁵ The changes in HbO levels in the right dorsolateral PFC were inversely linked with the severity of the disease in MDD patients.¹¹⁶

Rehabilitating patients with mood disorder (MD) using animal-assisted therapy resulted in significant improvements in cognitive activation in the PFC.¹¹⁷ The HbO changes, in general, were steeper in MDD patients than SZ patients, and in the dorsolateral and ventrolateral PFCs were correlated with the Global Assessment of Functioning scores of MDD patients.¹¹⁸ A higher ratio of positive thoughts versus negative thoughts in MDD patients was related to a higher HbO response in the left dorsolateral PFC and a lower HbO response in the right superior temporal gyrus.¹¹⁹ Children with depressive disorder showed improved frontopolar activation after receiving psychodynamic therapy for six months.¹²⁰ Patients with late-life depression showed a reduced and yet statistically non-significant activation when compared to AD patients.¹²¹ The increase in

depression in MDD patients was associated with increased HbO levels during cognitive activation in the frontopolar PFC and right dorsolateral PFC.¹²² A cognitive analysis of BD patients revealed that better social performance was linked with higher activation in the right PFC.¹²³ The HbO variations of hypomanic BD patients were significantly higher than those of depressed BD patients in the left dorsolateral PFC.¹²⁴ The depressive and euthymic states in BD patients were differentiated based on HbO levels in the left temporal region, whereas the intensity of the HbO change revealed the severity of the symptoms.¹²⁵ The social functioning of patients with depression during later stages in their lives was correlated with the activation levels in the frontopolar and dorsolateral PFCs while the right ventrolateral PFC predicted the effect of rehabilitation.¹²⁶ In a detailed study on MDD, patients with melancholic depression exhibited a significantly lower HbO response in the frontotemporal region when compared to the patients with nonmelancholic depression.¹²⁷ Depressed patients who exhibited non-suppressive effects in response to the administration of dexamethasone and corticotropin-releasing hormone showed significant differences in fNIRS responses when compared to the patients who exhibited suppressive behavior.¹²⁸

BD and MDD patients with family histories of psychiatric diseases showed highly impaired activation in the PFC compared to those without family histories of psychiatric diseases.¹²⁹ MDD patients with positive responsiveness to selective serotonin reuptake inhibitors showed a significantly higher HbO response compared to nonresponsive MDD patients.¹³⁰ Patients with menopausal depression and those with MDD showed lower activations in the right and left dorsolateral PFCs, which differentiated them from each other as well as from healthy persons.¹³¹ MDD patients who attempted suicide showed a smaller HbO response in the left precentral gyrus compared to those who did not attempt suicide and to healthy persons, and the HbO response was negatively correlated with impulsivity, hopelessness, and aggression levels.¹³² The dorsolateral PFC in BD patients showed higher activation than in SZ patients, demonstrating the less severe verbal memory impairment associated with BD compared to SZ.¹³³ The HbO response in the right dorsolateral PFC in BD patients with psychotic symptoms was negatively associated with the extent of disease and was lower compared to

Table 4. Studies on depressive disorders.

Work	Experimental population	Brain area under study	Instrument	No. of channels/ separation(s)	Analyzed parameters
Verbal fluency task Matsuo <i>et al.</i> ¹⁰⁹ (2002)	21 Healthy individuals (18 F and 3 M), 50.3 ± 12.6 yrs; 14 MDD patients (10 F and 4 M), 56.1 ± 17.3 yrs; 11 BD patients (8 F and 3 M), 47.9 ± 12.9 yrs	Left frontal region	HEO-200	1/4 cm	HbO, HbR
Matsuo <i>et al.</i> ¹¹⁰ (2004)	9 Healthy individuals (3 F and 6 M), 47.3 ± 14.6 yrs; 9 BD patients (5 F and 4 M), 47.4 ± 9.87 yrs	Frontal region	ETG-100	24/3 cm	HbO, HbR
Matsuo <i>et al.</i> ¹¹¹ (2005)	10 Healthy individuals (4 F and 6 M), 58.7 ± 5.8 yrs; 10 MDD patients (5 F and 5 M), 62.2 ± 4.8 yrs	Frontal region	ETG-100	24/3 cm	HbO, HbR
Pu <i>et al.</i> ¹¹² (2008)	30 Healthy individuals (16 F and 14 M), 72.0 ± 4.7 yrs; 24 MDD patients (18 F and 6 M), 72.3 ± 5.5 yrs	Bilateral prefrontal and superior temporal regions	ETG-4000	52/3 cm	HbO
Suto <i>et al.</i> ¹¹³ (2004)	16 Healthy individuals (4 F and 12 M), 42.9 ± 4.6 yrs; 10 MDD patients (1 F and 9 M), 47.9 ± 12.8 yrs; 13 Schizophrenia patients (4 F and 9 M), 37.9 ± 12 yrs	Bilateral prefrontal and temporal regions	ETG-100	48/3 cm	HbO, HbR, HbT
Pu <i>et al.</i> ¹¹⁴ (2012)	30 Healthy individuals (18 F and 12 M), 50.5 ± 19.2 yrs; 26 MDD patients (15 F and 11 M), 47.9 ± 19.2 yrs	Bilateral prefrontal and superior temporal regions	ETG-4000	52/3 cm	HbO
Shimodera <i>et al.</i> ¹¹⁵ (2012)	24 Healthy individuals (11 F and 13 M), 40.9 ± 10.6 yrs; 39 MDD patients (20 F and 19 M), 56.9 ± 12.6 yrs; 14 BD patients (7 F and 7 M), 51.4 ± 14.0 yrs	Bilateral prefrontal cortex	OMM-3000/16	42/3 cm	HbO
Noda <i>et al.</i> ¹¹⁶ (2012)	30 Healthy individuals (16 F and 14 M), 35.1 ± 9.4 yrs; 30 MDD patients (16 F and 14 M), 36.7 ± 11.6 yrs	Bilateral frontotemporal regions	ETG-4000	52/3 cm	HbO

Table 4. (Continued)

Work	Experimental population	Brain area under study	Instrument	No. of channels/ separation(s)	Analyzed parameters
Aoki <i>et al.</i> ¹¹⁷ (2012)	1 Healthy individual (M), 48 yrs; 2 MD patients (1 F and 1 M), 22 yrs and 26 yrs	Bilateral prefrontal cortex	FOIRE-300	42/3 cm	HbO
Kinou <i>et al.</i> ¹¹⁸ (2013)	32 Healthy individuals (17 F and 15 M), 45.7 ± 13.5 yrs; 32 MDD patients (17 F and 15 M), 44.8 ± 9.8 yrs; 32 Schizophrenia patients (17 F and 15 M), 41.7 ± 10.1 yrs	Bilateral prefrontal and superior temporal regions	ETG-4000	52/3 cm	HbO, HbR
Koseki <i>et al.</i> ¹¹⁹ (2013)	75 MDD patients (36 F and 39 M), 39.23 ± 12.49 yrs	Bilateral prefrontal and superior temporal regions	ETG-4000	52/3 cm	HbO, HbR
Usami <i>et al.</i> ¹²⁰ (2014)	10 MDD patients (9 F and 1 M), 12.9 ± 0.9 yrs	Prefrontal cortex	Spectrattech spectroscope	2/3 cm	HbO
Kito <i>et al.</i> ¹²¹ (2014)	33 Healthy individuals (22 F and 11 M), 69.6 ± 5.5 yrs; 30 MDD patients (21 F and 9 M), 71.1 ± 6.8 yrs; 28 AD patients (18 F and 10 M), 76.6 ± 6.9 yrs	Frontal and parietal cortices	FOIRE-3000	44/3 cm	HbO
Liu <i>et al.</i> ¹²² (2014)	30 Healthy individuals (14 F and 16 M), 33.2 ± 10.5 yrs; 30 MDD patients (18 F and 12 M), 38.38 ± 12.8 yrs	Prefrontal cortex	FOIRE-3000	45/3 cm	HbO, HbR, HbT
Nishimura <i>et al.</i> ¹²³ (2015)	65 Healthy individuals (35 F and 30 M), 36.1 ± 11.9 yrs; 33 BD patients (18 F and 15 M), 37.8 ± 10.7 yrs	Frontotemporal region	ETG-4000	52/3 cm	HbO, HbR
Nishimura <i>et al.</i> ¹²⁴ (2015)	12 Healthy individuals (8 F and 4 M), 46.4 ± 6.6 yrs; 27 BD patients (9 F and 18 M), 37.8 ± 10.7 yrs	Frontotemporal region	ETG-4000	52/3 cm	HbO
Mikawa <i>et al.</i> ¹²⁵ (2015)	28 Healthy individuals (17 F and 11 M), 37.0 ± 9.5 yrs; 55 BD patients (27 F and 28 M), 40.67 ± 13.6 yrs, 41.97 ± 11.3 yrs	Bilateral prefrontal and temporal regions	ETG-4000	52/3 cm	HbO

Table 4. (Continued)

Work	Experimental population	Brain area under study	Instrument	No. of channels/ separation(s)	Analyzed parameters
Pu <i>et al.</i> ¹²⁶ (2015)	29 Healthy individuals (22 F and 7 M), 71.6 ± 5.57 yrs; 29 MDD patients (22 F and 7 M), 72.4 ± 5.71 yrs	Frontotemporal region	ETG-4000	52/3 cm	HbO
Tsuji <i>et al.</i> ¹²⁷ (2016)	68 Healthy individuals (36 F and 32 M), 20–65 yrs; 82 MDD patients (49 F and 33 M), 20–73 yrs	Bilateral prefrontal and temporal regions	ETG-4000	52/3 cm	HbO
Kinoshita <i>et al.</i> ¹²⁸ (2016)	31 Depressive patients (16 F and 15 M), 44.2 ± 12.2 yrs	Frontal region	ETG-4000	22/3 cm	HbO, HbR
Ohi <i>et al.</i> ¹²⁹ (2017)	51 Healthy individuals (18 F and 33 M), 35.7 ± 11.9 yrs; 26 MDD patients (9 F and 17 M), 41.1 ± 12.7 yrs; 22 BD patients (9 F and 13 M), 39.9 ± 12.5 yrs; 45 Schizophrenia patients (29 F and 16 M), 35.4 ± 9.1 yrs	Bilateral prefrontal and temporal regions	ETG-4000	52/3 cm	HbO, HbR
Masuda <i>et al.</i> ¹³⁰ (2017)	63 Healthy individuals (28 F and 35 M), 41.7 ± 1.4 yrs; 47 MDD patients (26 F and 21 M), 48.6 ± 15.0 yrs	Bilateral prefrontal and temporal regions	ETG-7100	47/3 cm	HbO, HbR
Ma <i>et al.</i> ¹³¹ (2017)	30 Healthy individuals (F), 34.83 ± 8.77 yrs; 30 MDD patients (F), 37.50 ± 10.60 yrs; 30 MD patients (F), 51.17 ± 6.06 yrs	Prefrontal cortex	FOIRE-3000	45/3 cm	HbO, HbR, HbT
Tsuji <i>et al.</i> ¹³² (2017)	40 Healthy individuals (25 F and 15 M), 38.2 ± 10.5 yrs; 68 MDD patients (44 F and 24 M), 37.6 ± 10.0 yrs, 38.8 ± 9.7 yrs	Bilateral prefrontal and temporal regions	ETG-4000	52/3 cm	HbO
Yamamuro <i>et al.</i> ¹³³ (2018)	26 Healthy individuals (19 F and 7 M), 48.73 ± 8.40 yrs; 33 BD patients (22 F and 11 M), 50.03 ± 10.49 yrs; 38 Schizophrenia patients (26 F and 12 M), 45.58 ± 8.21 yrs	Prefrontal cortex	ETG-4000	48/3 cm	HbO

Table 4. (Continued)

Work	Experimental population	Brain area under study	Instrument	No. of channels/ separation(s)	Analyzed parameters
Sun <i>et al.</i> ¹³⁴ (2018)	23 Healthy individuals (11 F and 12 M), 32.91 ± 10.18 yrs; 29 BD psychotic patients (14 F and 15 M), 28.38 ± 6.83 yrs; 31 BD patients (17 F and 14 M), 30.93 ± 8.98 yrs	Frontal region	FOIRE-3000	45/3 cm	HbO
Akiyama <i>et al.</i> ¹³⁵ (2018)	50 Healthy individuals (40 F and 10 M), 32.7 ± 7.5 yrs; 177 MDD patients (104 F and 73 M), 47.2 ± 15.1 yrs	Bilateral prefrontal and temporal regions	ETG-4000	52/3 cm	HbO
Fujiwara <i>et al.</i> ¹³⁶ (2018)	17 Healthy individuals (4 F and 13 M), 22–65 yrs; 36 Ulcerative colitis patients (17 F and 19 M), 14–77 yrs, 32 Crohn's disease patients (6 F and 26 M), 15–52 yrs	Bilateral prefrontal and temporal regions	ETG-4000	52/3 cm	HbO
Yan <i>et al.</i> ¹³⁷ (2018)	32 Healthy individuals (17 F and 15 M), 24.7 ± 2.4 yrs; 43 BD patients (26 F and 17 M), 26.7 ± 7.0 yrs	Bilateral prefrontal regions	ETG-4000	41/3 cm	HbO
Satomura <i>et al.</i> ¹³⁸ (2019)	45 MDD patients (32 F and 13 M), 39.8 ± 11.8 yrs	Bilateral prefrontal and temporal regions	ETG-4000	52/3 cm	HbO
Hyperventilation task					
Matsuo <i>et al.</i> ¹⁰⁹ (2002)	21 Healthy individuals (18 F and 3 M), 50.3 ± 12.6 yrs; 14 MDD patients (10 F and 4 M), 56.1 ± 17.3 yrs; 11 BD patients (8 F and 3 M), 47.9 ± 12.9 yrs	Left frontal region	HFO-200	1/4 cm	HbO, HbR
Matsuo <i>et al.</i> ¹¹⁰ (2004)	9 Healthy individuals (3 F and 6 M), 47.3 ± 14.6 yrs; 9 BD patients (5 F and 4 M), 47.4 ± 9.87 yrs	Frontal region	ETG-100	24/3 cm	HbO, HbR

Table 4. (Continued)

Work	Experimental population	Brain area under study	Instrument	No. of channels/ separation(s)	Analyzed parameters
Matsuo <i>et al.</i> ¹¹¹ (2005)	10 Healthy individuals (4 F and 6 M), 58.7 ± 5.8 yrs; 10 MDD patients (5 F and 5 M), 62.2 ± 4.8 yrs	Frontal region	ETG-100	24/3 cm	HbO, HbR
<i>N</i> -back task					
Pu <i>et al.</i> ¹³⁹ (2011)	26 Healthy individuals (18 F and 8 M), 42.4 ± 9.3 yrs; 24 MDD (12 F and 12 M), 47.9 ± 13.9 yrs	Bilateral prefrontal and superior temporal regions	ETG-4000	52/3 cm	HbO
Pu <i>et al.</i> ¹⁴⁰ (2012)	35 Healthy individuals (24 F and 11 M), 70.9 ± 4.3 yrs; 36 MDD patients (27 F and 9 M), 71.8 ± 5.1 yrs	Bilateral prefrontal and superior temporal regions	ETG-4000	52/3 cm	HbO
Zhu <i>et al.</i> ¹⁴¹ (2018)	36 Healthy individuals (18 F and 18 M), 33.6 ± 10.3 yrs; 35 UD patients (24 F and 11 M), 35.9 ± 13.2 yrs; 39 BD patients (20 F and 19 M), 37.0 ± 12.9 yrs	Frontotemporal region	ETG-4000	52/3 cm	HbO, HbR
Stroop tasks					
Matsubara <i>et al.</i> ¹⁴² (2014)	20 Healthy individuals (10 F and 10 M), 41.4 ± 8.5 yrs; 16 MDD patients (8 F and 8 M), 45.4 ± 12.2 yrs; 16 BD patients (8 F and 8 M), 44.1 ± 17.5 yrs	Frontotemporal region	ETG-4000	52/3 cm	HbO, HbR
Yamamuro <i>et al.</i> ¹³³ (2018)	26 Healthy individuals (19 F and 7 M), 48.73 ± 8.40 yrs; 33 BD patients (22 F and 11 M), 50.03 ± 10.49 yrs; 38 Schizophrenia patients (26 F and 12 M), 45.58 ± 8.21 yrs	Prefrontal cortex	ETG-4000	48/3 cm	HbO
Resting state					
Zhu <i>et al.</i> ¹⁴³ (2017)	30 Healthy individuals (9 F and 21 M), 23.60 ± 2.03 yrs; 28 MD patients (20 F and 8 M), 23.32 ± 5.01 yrs	Prefrontal cortex	FOIRE-3000	42/3 cm	HbO

Table 4. (Continued)

Work	Experimental population	Brain area under study	Instrument	No. of channels/ separation(s)	Analyzed parameters
Wu <i>et al.</i> ¹⁴⁴ (2018)	62 Healthy individuals (30 F and 32 M), 24.6 ± 0.9 yrs; 15 Sleep disorder patients (8 F and 7 M), 26.2 ± 4.68 yrs	Prefrontal cortex	FOIRE-3000	42/3 cm	HbO, HbR
Electroconvulsive therapy					
Fujita <i>et al.</i> ¹⁴⁵ (2011)	10 MD patients (6 F and 4 M), 64.5 ± 10.1 yrs; 11 Schizophrenia patients (9 F and 2 M), 45.8 ± 13.6 yrs	Frontal region	NIRO-200	2/3 cm	HbO, HbR
Conversation task					
Takei <i>et al.</i> ¹⁴⁶ (2014)	31 Healthy individuals (20 F and 11 M), 33.6 ± 10.0 yrs; 29 MDD patients (15 F and 14 M), 34.5 ± 9.0 yrs; 31 BD patients (17 F and 14 M), 34.9 ± 6.6 yrs	Frontotemporal region	ETG-4000	52/3 cm	HbO
Digit span task					
Tian <i>et al.</i> ¹⁴⁷ (2014)	16 Healthy individuals (M), 29.4 ± 9.6 yrs; 16 PTSD patients (M), 29.4 ± 9.6 yrs	Prefrontal region	Cephalogics system	36/2.8 cm	HbO, HbR
Visuospatial task					
Kito <i>et al.</i> ¹²¹ (2014)	33 Healthy individuals (22 F and 11 M), 69.6 ± 5.5 yrs; 30 MDD patients (21 F and 9 M), 71.1 ± 6.8 yrs; 28 AD patients (18 F and 10 M), 76.6 ± 6.9 yrs	Frontal and parietal cortices	FOIRE-3000	44/3 cm	HbO
Stop-signal task					
Tsuji <i>et al.</i> ¹⁴⁸ (2018)	18 Healthy individuals (10 F and 8 M), 36.6 ± 10.7 yrs; 21 BD patients (12 F and 9 M), 36.9 ± 10.2 yrs; 20 Schizophrenia patients (11 F and 9 M), 33.6 ± 8.7 yrs	Frontotemporal region	ETG-4000	52/3 cm	HbO

Table 4. (Continued)

Work	Experimental population	Brain area under study	Instrument	No. of channels/ separation(s)	Analyzed parameters
Image recall task Kondo <i>et al.</i> ¹⁴⁹ (2018)	25 Healthy individuals (7 F and 18 M), 34.1 ± 10.1 yrs; 25 MDD patients (8 F and 17 M), 36 ± 8.91 yrs	Frontotemporal region	ETG-4000	44/3 cm	HbO, HbR
Tooth clenching task Zaproudina <i>et al.</i> ¹⁵⁰ (2018)	14 Healthy individuals (10 F and 4 M), 38.6 ± 10.0 yrs 12 Migraineurs (10 F and 2 M), 37.8 ± 11.3 yrs	Frontal region	OxyMon MkIII	2/3.5–4 cm	HbO, HbR, HbT
Tower of London task Yan <i>et al.</i> ¹³⁷ (2018)	32 Healthy individuals (17 F and 15 M), 24.7 ± 2.4 yrs; 43 BD patients (26 F and 17 M), 26.7 ± 7.0 yrs	Prefrontal cortex	ETG-4000	41/3 cm	HbO

that of BD patients without psychotic symptoms.¹³⁴ The depressive patients with the mandatory symptoms showed significantly lower activation in the left dorsolateral PFC compared to depressive patients without mandatory symptoms, which illustrated that a higher level of impairment in the left dorsolateral PFC is associated with mandatory symptoms.¹³⁵ Inflammatory bowel disease is linked with depression, and the patients with the disease also showed reduced cognitive activation in the PFC as observed via various studies on depressive disease.¹³⁶ BD patients showed lower activations in the right ventrolateral and dorsolateral PFCs and the bilateral PFC when compared to healthy persons.¹³⁷ The changes in HbO activation in MDD patients in the right inferior frontal gyrus and bilateral middle frontal gyri were associated with the extent of the disease and can be observed to distinguish different impairments.¹³⁸

5.2. *Hyperventilation task*

The patients with MDD and BD showed a significantly small reduction in HbO levels during hyperventilation as compared to healthy persons.^{109–111}

5.3. *N-back task*

The patients with MDD showed a lower level of activation in the lateral PFC and superior temporal region during a two-back task.¹³⁹ The late-onset disorder patients also showed reduced activation in the prefrontal and temporal regions during a two-back task, which was significantly related to lower scores on the Social Adaptation Self-Evaluation Scale.¹⁴⁰ Observing the reduced HbO response in the left frontopolar region and Broca's area was conclusive in differentiating between UD and BD patients.¹⁴¹

5.4. *Stroop task*

During an emotional Stroop task, the patients with BD exhibited similar HbO and HbR responses in the frontal regions to those of MDD patients in response to sad stimuli and different responses in response to happy stimuli.¹⁴² During a Stroop color-word task to measure inhibitory control, the BD patients exhibited lower activation in the frontopolar PFC.¹³³

5.5. *Resting state*

The RSFC in medicated patients with affective disorders was reduced compared to healthy persons in terms of the intrahemispheric, interhemispheric, and intraregional connections but was higher when compared to patients who were not medicated.¹⁴³ Thresholding the regional functional connectivity in a resting state facilitated the differentiation of patients from healthy persons.¹⁴⁴

5.6. *Electroconvulsive therapy*

Bilateral electroconvulsive therapy administered to MD patients resulted in reduced regional CBF in the frontal region that increased during the ictal onset and was maintained at that level during the postictal period.¹⁴⁵

5.7. *Conversation task*

PFC activation was reduced in MDD and BD patients, but the continuous activation and brisk fluctuations could differentiate the impairment characteristics.¹⁴⁶

5.8. *Digit span task*

A study on posttraumatic stress disorder patients revealed activations during the retention phase and deactivations during the forward or backward recall phases, thereby illustrating the inhibition in the PFC.¹⁴⁷

5.9. *Visuospatial task*

In a comparative study on AD and late-life depression patients, the AD patients showed higher activation in the parietal cortex during the Benton Judgment of Line Orientation task.¹²¹

5.10. *Stop-signal task*

The reaction time in BD patients was inversely associated with their HbO responses in the right inferior frontal gyrus.¹⁴⁸

5.11. *Image recall task*

Compared to healthy persons, the patients with MDD showed lower HbO responses in the bilateral

PFC during unpleasant image recalls, and the HbO response in the left PFC was inversely associated with the depression score.¹⁴⁹

5.12. *Tooth clenching task*

Migraine patients exhibited higher HbR and HbT values in the right PFC compared to healthy individuals, thereby displaying a microvascular oxygen delivery and utilization impairment.¹⁵⁰

5.13. *Tower of London task*

The BD patients revealed significantly smaller changes in the bilateral dorsolateral PFC compared to healthy persons, indicating impaired planning and problem-solving capabilities.¹³⁷

6. Anxiety and Panic Disorder

Anxiety is often perceived as a healthy emotion and is considered normal unless a person regularly feels inconsistent levels of this emotion, following which it may transform into a medical disorder. This disorder may lead to feelings of fear, worry, and uneasiness. Another associated state of this condition is called panic disorder that is characterized by sudden panic attacks accompanied by perspiration, wobbling, and dyspnea.¹⁵¹ Due to the portability of the fNIRS system, extensive research on patients with anxiety, panic disorder, stress, and many other types of mental health disorders has been performed and is currently underway. Here, we briefly review the fNIRS studies on patients with anxiety and panic disorders. Figure 5 shows the task-wise distribution of the studies, and Table 5 summarizes all fNIRS studies on patients with anxiety/fear and panic disorders.

6.1. *Verbal fluency task*

In a study involving a word-fluency cognitive task, the left inferior frontal lobe was significantly less activated (HbO) in patients with panic disorder when compared to healthy persons.¹⁵² This pilot study suggests that there is a dysfunction in the left frontal lobe of patients with panic disorder. Another subsequent study on these patients reported that the occurrence of panic attacks was significantly

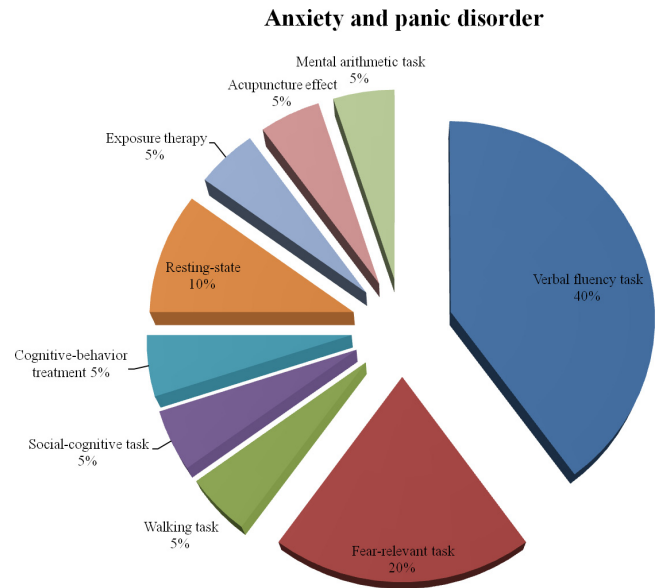


Fig. 5. Task-based distribution of studies on anxiety/fear and panic disorders (total studies: 19).

related to HbO changes in the left inferior PFC while the severity of symptoms was associated with the HbR changes in the right PFC.¹⁵³ A later study conducted with the same protocol outlines the relationship between frontal lobe function and the catechol-O-methyltransferase (COMT) genotype.¹⁵⁴ This study reported that the increase in HbO levels in the right lateral PFC is associated with the COMT gene of patients with panic disorder. Two studies were conducted using repetitive transcranial magnetic stimulation (rTMS) along with cognitive and additional emotional Stroop tasks, and the results associated with PFC activations/deactivations were compared with those of healthy persons.^{155,156} At the baseline (without rTMS), the fNIRS measurements associated with the VFT revealed hypofrontality in the dorsolateral PFC, in panic disorder patients, which significantly differed from the activations observed in healthy persons. However, after sham rTMS, a significant increase in activation was reported in the left inferior frontal gyrus. While performing the VFT, patients with social anxiety disorder (SAD) showed smaller changes in their HbO responses in the ventrolateral PFC as compared to healthy persons.¹⁵⁷ In another fNIRS study, hyperactivity was also reported in the left frontal area of SAD patients compared to healthy persons.¹⁵⁸

Table 5. Studies on anxiety disorders.

Work	Experimental population	Brain area under study	Instrument	No. of channels/ separation(s)	Analyzed parameters
Verbal fluency task Nishimura <i>et al.</i> ¹⁵¹ (2007)	33 Healthy individuals, 26.09 ± 4.30 yrs; 5 Panic disorder patients, 27.0 ± 6.04 yrs	Bilateral prefrontal and superior temporal regions	ETG-4000	52/3 cm	HbO, HbR
Nishimura <i>et al.</i> ¹⁵³ (2009)	109 Panic disorder patients (75 F and 34 M), 56.1 ± 17.3 yrs	Bilateral prefrontal and superior temporal regions	ETG-4000	52/3 cm	HbO, HbR
Tanii <i>et al.</i> ¹⁵⁴ (2009)	Panic disorder patients, 8 Met/Met (7 F and 1 M), 34.88 ± 10.47 yrs; 29 Val/Met (24 F and 5 M), 39.0 ± 9.11 yrs; 34 Val/Val (20 F and 14 M), 37.24 ± 9.49 yrs	Bilateral prefrontal and superior temporal regions	ETG-4000	52/3 cm	HbO, HbR
Deppermann <i>et al.</i> ¹⁵⁵ (2014)	23 Healthy individuals (14 F and 9 M), 19-64 yrs; 22 Panic disorder patients (14 F and 8 M), 22-56 yrs; 22 Panic disorder patients (13 F and 9 M), 19-63 yrs	Bilateral prefrontal and superior temporal regions	ETG-4000	52/3 cm	HbO, HbR
Deppermann <i>et al.</i> ¹⁵⁶ (2017)	23 Healthy individuals (14 F and 9 M), 19-64 yrs; 22 Panic disorder patients (14 F and 8 M), 22-56 yrs; 22 Panic disorder patients (13 F and 9 M), 19-63 yrs	Bilateral prefrontal and superior temporal regions	ETG-4000	52/3 cm	HbO, HbR
Yokoyama <i>et al.</i> ¹⁵⁷ (2015)	35 Healthy individuals (18 F and 17 M), 37.3 ± 10.9 yrs; 24 Anxiety disorder patients (12 F and 12 M), 36.3 ± 12.8 yrs	Bilateral prefrontal and superior temporal regions	ETG-4000	52/3 cm	HbO
Kawashima <i>et al.</i> ¹⁵⁸ (2016)	152 Healthy individuals (53 F and 99 M), 26.0 ± 6.3 yrs; 145 Anxiety disorder patients (61 F and 84 M), 26.5 ± 7.7 yrs	Bilateral prefrontal and superior temporal regions	ETG-7100	47	HbO

Table 5. (Continued)

Work	Experimental population	Brain area under study	Instrument	No. of channels/ separation(s)	Analyzed parameters
Visual task					
Marumo <i>et al.</i> ¹⁵⁹ (2009)	Anxiety study: 10 M, 33.5 ± 9.0 yrs; 10 F, 31.8 ± 9.0 yrs	Bilateral prefrontal and superior temporal regions	ETG-4000	52/3 cm	HbO, HbR, HbT
Roos <i>et al.</i> ¹⁶⁰ (2011)	Anxiety study: 32 Pregnant women, 24.8 ± 5.6 yrs; 32 Nonpregnant women, 25.3 ± 5.7 yrs	PFC	DYNOT		HbO
Kochel <i>et al.</i> ¹⁶¹ (2011)	24 Healthy individuals (F), 36.4 ± 14.9 yrs; 25 Phobic patients (F), 39.0 ± 11.3 yrs	Frontoparietal regions	ETG-4000	22	HbO
Tupak <i>et al.</i> ¹⁶² (2013)	Phobic genetic study: 92 Participants (61 F and 31 M), 24.38 ± 3.46 yrs	Bilateral prefrontal and superior temporal regions	ETG-4000	52/3 cm	HbO, HbR
Walking task					
Holtzer <i>et al.</i> ¹⁶³ (2019)	Phobic elderly study: 75 Participants (38 F and 37 M), 77.52 ± 6.41 yrs	Bilateral prefrontal and superior temporal regions	fNIRS Imager 1100	16/2.5 cm	HbO
Social-cognitive task					
Ruocco <i>et al.</i> ¹⁶⁴ (2010)	10 Healthy individuals (F), 19.0 ± 1.1 yrs; 10 Borderline personality disorder patients (F), 22.1 ± 7.3 yrs	PFC	Lab developed system	16	HbO
Cognitive-behavior treatment					
Glassman <i>et al.</i> ¹⁶⁵ (2016)	21 Public speaking anxiety patients (16 F and 5 M), 28.10 ± 9.30 yrs	PFC	ETG-4000	16	HbO, HbR

Table 5. (Continued)

Work	Experimental population	Brain area under study	Instrument	No. of channels/ separation(s)	Analyzed parameters
Resting state Fekete <i>et al.</i> ¹⁶⁷ (2014)	35 Healthy individuals (17 F and 18 M), Mean of 4.5 yrs	PFC	ETG-4000	24/2 cm	HbO, HbR, HbT
Jeong and Yuan ¹⁶⁶ (2017)	Anxiety study: 7 Healthy individuals 45.7 ± 6.8 yrs; 8 Heroin-dependent users 47.6 ± 6.1 yrs	PFC	CW6	12/3 cm	HbO, HbR
Exposure therapy Landowska <i>et al.</i> ¹⁶⁸ (2018)	14 Acrophobic patients (12 F and 2 M), 42.30 ± 16.57 yrs	PFC	NIRSport	20/3 cm	HbO, HbR
Acupuncture therapy Sakatani <i>et al.</i> ¹⁶⁹ (2016)	10 Anxiety patients (9 F and 1 M), 41.8 ± 6.8 yrs	PFC	PNIRS-10	2/3 cm	HbO
Mental arithmetic task Brugnera <i>et al.</i> ¹⁷⁰ (2017)	12 Anxiety patients (6 F and 6 M), 24.5 ± 4.6 yrs	PFC	PocketNIRS Duo	2/3 cm	HbO

6.2. Visual task

When emotional or fearful facial expressions were displayed as stimuli, women exhibited increased HbO responses in the right ventrolateral PFC compared to men.¹⁵⁹ Fearful stimuli were presented to healthy persons and pregnant women in another fNIRS study that revealed significant activation relative to the resting state in both groups.¹⁶⁰ However, in the group consisting of pregnant women, greater PFC activation was reported during the second trimester compared to during the third trimester, which was related to anxiety. Another interesting fNIRS study was conducted on patients with dental phobia and healthy persons.¹⁶¹ Compared to the healthy persons, the patients showed an increased HbO response in the supplementary motor cortex while listening to the sound of dental drilling; however, comparable activation was exhibited in a neutral condition. The effects of a genetic variant of the neuropeptide S receptor gene (NPSR1) combined with fear-relevant stimuli were assessed using fNIRS.¹⁶² Activations in the dorsolateral and medial PFCs were increased in response to the NPSR1 gene accompanied by fear-specific stimuli.

6.3. Walking task

Relative to healthy persons, participants with fear of fall (FOF) exhibited reduced HbO activation in the PFC from the first to the second trial while performing a dual-task walk.¹⁶³ No significant differences in PFC activation were reported in both the FOF patients and healthy persons while performing repeated single-task walks.

6.4. Social-cognitive task

The patients with borderline personality disorder (BPD) were compared with healthy persons in an fNIRS study during a social-cognitive task (playing of cards) in the presence of two associates.¹⁶⁴ During the task, BPD patients displayed left medial PFC hyperactivation that most likely resulted from an abnormality in the frontolimbic circuitry.

6.5. Cognitive-behavior treatment

In an fNIRS study, interventions, including cognitive-behavioral treatment and acceptance-based

behavioral treatment, were administered to the participants with public-speaking anxiety.¹⁶⁵ Individuals treated with the latter treatment showed a decrease in the blood volume in the left dorsolateral PFC in comparison to those treated with the former treatment.

6.6. Resting state

Strong RSFC and interhemispheric correlation were observed in the orbitofrontal cortex of heroin users relative to healthy persons.¹⁶⁶ Small-world network properties, which correlate with the predictors of the risk of developing psychopathology in young children, were also calculated in this study.¹⁶⁷

6.7. Exposure therapy

In an fNIRS study conducted on patients with acrophobia, during the first exposure therapy, the decreased HbO concentration changes were observed in the dorsolateral and medial PFCs; however, this activation improved towards normal levels over two more sessions.¹⁶⁸

6.8. Acupuncture therapy

The altered PFC HbO changes suggested a positive effect of acupuncture on decreasing the anxiety levels of anxiety patients.¹⁶⁹

6.9. Mental arithmetic task

Arithmetic tasks were performed by participants with low and high levels of anxiety traits in stress and experimental conditions.¹⁷⁰ Overall, while performing the stress arithmetic task, reduced PFC activity was reported in participants with high levels of anxiety traits compared to those with low anxiety levels.

7. Schizophrenia

SZ is a disease due to which patients appear to stray from reality. It has effects on the thinking, feeling, and behavior of the patient. SZ patients usually create supernatural beliefs, suffer from hallucinations, live in delusions, report hearing nonexistent sounds, have cognitive impairment, and/or experience limited motivation. The symptoms of this

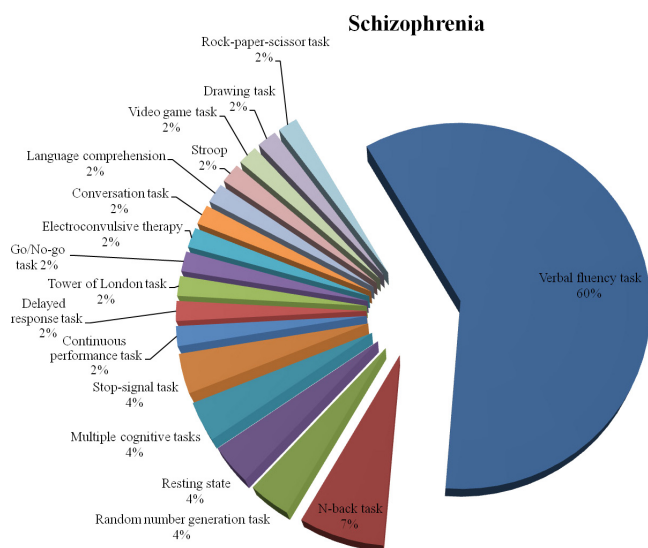


Fig. 6. Task-based distribution of studies on schizophrenia (total studies: 57).

disease typically start occurring at a young age and do not often develop in children. The causes of SZ are still not clear; however, it is linked with genetic factors, an imbalance in neurotransmitter levels, or tense relationships. Therefore, to treat SZ patients, symptom management is employed via medication or psychiatric counseling. The fNIRS has been used in various settings to reveal the impairing processes in an SZ brain. The task-wise distribution of SZ papers is shown in Fig. 6, and the corresponding studies are outlined in Table 6.

7.1. Verbal fluency task

In the earliest findings on SZ via fNIRS, HbO activation was reduced in patients compared to that in healthy individuals. Among patients, typically medicated persons exhibited even lower excitation levels compared to atypically medicated patients.¹⁷¹ In healthy individuals, the HbO response was higher during letter VFTs compared to semantic VFTs, whereas in SZ patients, higher activation in the PFC was observed during semantic VFTs compared to letter VFTs.¹⁷² The patients with SZ showed lower activations in the frontopolar regions compared to healthy persons, which was associated with poor scores in psychiatric and social evaluations.¹⁷³ Genetic polymorphisms were explored in SZ patients, and genotypes associated with poor cortical activations were identified in several studies.^{174–177} Impaired social functioning due to

divergent thinking was linked with the ventral region of the frontopolar area in these patients.¹⁷⁸ Further, SZ patients exhibited a decrease in activation in line with an increase in disease severity.¹⁷⁹ The reduced HbO activation response had lower variations compared to those of healthy individuals.¹⁸⁰ In multiple studies conducted on SZ patients along with other depressive patients, the hemodynamic responses differed, thereby allowing for the differentiation of SZ patients and their levels of depression.^{28,113,118,133,181–183} Clinically stable SZ patients exhibited a correlation between the activation in the right ventrolateral prefrontal and temporal areas and the cognitive insight, and that between the activation in the frontopolar, left ventrolateral, and bilateral dorsolateral prefrontal areas and their subjective well-being.^{184,185} Studying SZ patients revealed that their impaired thinking was associated with abnormal activation patterns in the left ventrolateral prefrontal area.¹⁸⁶ The early detection and treatment of symptoms are critical as patients with SZ who were untreated for psychosis for more than six months exhibited worse cortical activations in the frontotemporal regions compared to patients who were untreated for less than six months.^{187,188} The Chinese speaking SZ patients also showed lower hemodynamic responses in the PFC and superior temporal regions compared to healthy individuals.¹⁸⁹ SZ patients showed lower activation as well as lower functional connectivity in the prefrontal and temporal regions compared to healthy individuals, thereby revealing impaired neural connections.¹⁹⁰ Via a principal component analysis (PCA)-based feature selection and SVM-based classification, the HbO signal was utilized to differentiate the SZ patients from healthy individuals.¹⁹¹ Older SZ patients showed lower cortical activation compared to younger patients, which is similar in the case of healthy individuals.¹⁹² The reduced HbO response in SZ patients compared to healthy individuals was associated with their self-reported social abilities.¹⁹³ In a multimodal study that utilized fNIRS and fMRI, the association between hemodynamic activation and gray matter volume in the left pars triangularis was linked with the onset of SZ.¹⁹⁴ Using positive and negative syndrome scales, the level of impaired activation in the frontotemporal region of SZ patients was associated with their level of depression.¹⁹⁵ In SZ patients, the cognitive ability involved in performing routine tasks was linked with activation in the

Table 6. Studies on schizophrenia.

Work	Experimental population	Brain area under study	Instrument	No. of channels/ separation(s)	Analyzed parameters
Verbal fluency task Watanabe and Kato ¹⁷¹ (2004)	31 Healthy individuals (15 F and 16 M), 36.1 ± 11.6 yrs; 62 Schizophrenia patients (32 F and 30 M), 40.1 ± 12.3 yrs	Dorsolateral PFC	HEO-200	2/3 cm	HbO, HbR
Kubota <i>et al.</i> ¹⁷² (2005)	19 Healthy individuals (10 F and 9 M), 36.9 ± 14.3 yrs; 16 Schizophrenia patients (8 F and 8 M), 37.5 ± 13.0 yrs	PFC	NIRO-300	2/4 cm	HbO, HbR
Takizawa <i>et al.</i> ¹⁷³ (2008)	70 Healthy individuals (34 F and 36 M), 37.4 ± 13.6 yrs; 55 Schizophrenia patients (26 F and 29 M), 40.1 ± 11.1 yrs	Bilateral prefrontal and temporal regions	ETG-4000	52/3 cm	HbO
Takizawa <i>et al.</i> ¹⁷⁴ (2009)	30 Healthy individuals (Val) (14 F and 16 M), 37.7 ± 13.6 yrs; 30 Healthy individuals (Met) (12 F and 18 M), 37.2 ± 12.6 yrs; 20 Schizophrenia patients (Val) (12 F and 8 M), 41.5 ± 11.9 yrs; 25 Schizophrenia patients (Met) (13 F and 12 M), 41.0 ± 9.5 yrs	Bilateral prefrontal and temporal regions	ETG-4000	52/3 cm	HbO
Takizawa <i>et al.</i> ¹⁷⁵ (2009)	30 Healthy individual (Gln) (13 F and 17 M), 31.0 ± 6.6 yrs; 30 Healthy individual (Pro) (10 F and 20 M), 31.5 ± 5.8 yrs; 20 Schizophrenia patients (Gln) (10 F and 10 M), 40.7 ± 11.3 yrs; 20 Schizophrenia patients (Pro) (12 F and 8 M), 38.1 ± 8.1 yrs	Bilateral prefrontal and temporal regions	ETG-4000	52/3 cm	HbO
Ohi <i>et al.</i> ¹⁷⁶ (2011)	101 Healthy individuals (Gln) (56 F and 45 M), 35.8 ± 10.9 yrs; 115 Healthy individuals (Pro) (64 F and 51 M), 37.7 ± 12.2 yrs; 57 Schizophrenia patients (Gln) (25 F and 32 M), 37.2 ± 13.4 yrs; 70 Schizophrenia patients (Pro) (32 F and 38 M), 36.6 ± 11.5 yrs	PFC	NIRO-200	2	HbO, HbR

Table 6. (Continued)

Work	Experimental population	Brain area under study	Instrument	No. of channels/ separation(s)	Analyzed parameters
Nishimura <i>et al.</i> ¹⁷⁷ (2014)	38 Healthy individuals (GG) (20 F and 18 M), 38.9 ± 17.1 yrs; 28 Healthy individuals (GA) (16 F and 12 M), 37.6 ± 14.5 yrs; 7 Healthy individuals (AA) (3 F and 4 M), 41.4 ± 16.1 yrs; 38 Schizophrenia patients (GG) (20 F and 18 M), 38.3 ± 11.4 yrs; 28 Schizophrenia patients (GA) (16 F and 12 M), 36.1 ± 13.7 yrs; 7 Schizophrenia patients (AA) (3 F and 4 M), 38.3 ± 13.6 yrs	Bilateral prefrontal and temporal regions	ETG-4000	52/3 cm	HbO
Takeshi <i>et al.</i> ¹⁷⁸ (2010)	16 Healthy individuals (8 F and 8 M), 24.5 ± 3.4 yrs; 18 Schizophrenia patients (11 F and 7 M), 25.4 ± 5.8 yrs	Bilateral PFC	OMM-3000	24/3 cm	HbO, HbR
Koike <i>et al.</i> ¹⁷⁹ (2011)	30 Healthy individuals (13 F and 17 M), 24.3 ± 4.8 yrs; 38 Schizophrenia patients (16 F and 22 M), 31.3 ± 6.1 yrs; 22 Ultra-high-risk patients (9 F and 13 M), 21.6 ± 3.7 yrs; 27 First episode psychosis patients (9 F and 18 M), 25.2 ± 7.0 yrs	Bilateral prefrontal and temporal regions	ETG-4000	52/3 cm	HbO
Shimodera <i>et al.</i> ¹⁸⁰ (2012)	26 Healthy individuals (13 F and 13 M), 41.4 ± 10.4 yrs; 31 Schizophrenia patients (19 F and 12 M), 42.4 ± 15.7 yrs	Frontal regions	MM-3000/16	42/3 cm	HbO, HbR
Suto <i>et al.</i> ¹¹³ (2004)	16 Healthy individuals (4 F and 12 M), 42.9 ± 4.6 yrs; 13 Schizophrenia patients (4 F and 9 M), 37.9 ± 12 yrs; 10 MDD patients (1 F and 9 M), 47.9 ± 12.8 yrs	Bilateral prefrontal and temporal regions	ETG-100	48/3 cm	HbO, HbR, HbT

Table 6. (Continued)

Work	Experimental population	Brain area under study	Instrument	No. of channels/ separation(s)	Analyzed parameters
Kinou <i>et al.</i> ¹¹⁸ (2013)	32 Healthy individuals (17 F and 15 M), 45.7 ± 13.5 yrs; 32 Schizophrenia patients (17 F and 15 M), 41.7 ± 10.1 yrs; 32 MDD patients (17 F and 15 M), 44.8 ± 9.8 yrs	Bilateral prefrontal and superior temporal regions	ETG-4000	52/3 cm	HbO, HbR
Takizawa <i>et al.</i> ¹⁸¹ (2014)	590 Healthy individuals (314 F and 276 M), 43.9 ± 15.7 yrs; 136 Schizophrenia patients (67 F and 69 M), 43.7 ± 12.1 yrs; 153 MDD patients (77 F and 76 M), 43.8 ± 12.7 yrs; 134 BD patients (69 F and 65 M), 44.0 ± 14.9 yrs	Bilateral prefrontal and temporal regions	ETG-4000	52/3 cm	HbO, HbR
Yanamuro <i>et al.</i> ¹³³ (2018)	15 Psychosis patients (6 F and 9 M), 39.87 ± 11.20 yrs; 19 Schizophrenia patients (10 F and 9 M), 39.11 ± 7.01 yrs	Bilateral prefrontal regions	ETG-100	24/3 cm	HbO
Kawano <i>et al.</i> ¹⁸³ (2016)	25 MDD patients, 44.1 ± 9.3 yrs; 3 Schizophrenia patients; 5 BD patients; 2 Panic disorder patients; 3 Psychotic disorder patients; 3 Dysthymic disorder patients; 2 Obsessive Compulsive Disorder patients	Bilateral prefrontal and temporal regions	ETG-4000	22/3 cm	HbO
Hirata <i>et al.</i> ²⁸ (2018)	18 Healthy individuals (5 F and 13 M), 28–38.5 yrs; 13 ASD patients (1 F and 12 M), 23.3–38.5 yrs; 15 Schizophrenia patients (3 F and 12 M), 29–47 yrs	Bilateral frontotemporal region	ETG-4000	24/3 cm	HbO
Yanamuro <i>et al.</i> ¹³³ (2018)	26 Healthy individuals (19 F and 7 M), 48.73 ± 8.40 yrs; 33 BD patients (22 F and 11 M), 50.03 ± 10.49 yrs; 38 Schizophrenia patients (26 F and 12 M), 45.58 ± 8.21 yrs	Prefrontal cortex	ETG-4000	48/3 cm	HbO

Table 6. (Continued)

Work	Experimental population	Brain area under study	Instrument	No. of channels/ separation(s)	Analyzed parameters
Pu <i>et al.</i> ¹⁸⁴ (2013)	30 Healthy individuals (19 F and 11 M), 32.4 ± 11.1 yrs; 30 Schizophrenia patients (21 F and 9 M), 32.1 ± 10.47 yrs	Bilateral prefrontal and temporal regions	ETG-4000	52/3 cm	HbO
Pu <i>et al.</i> ¹⁸⁵ (2013)	24 Schizophrenia patients (16 F and 8 M), 33.6 ± 9.72 yrs	Bilateral prefrontal and temporal regions	ETG-4000	52/3 cm	HbO
Marumo <i>et al.</i> ¹⁸⁶ (2014)	56 Healthy individuals (29 F and 27 M), 40.9 ± 11.5 yrs; 56 Schizophrenia patients (29 F and 27 M), 40.0 ± 11.0 yrs	Bilateral prefrontal and temporal regions	ETG-4000	52/3 cm	HbO, HbR
Chou <i>et al.</i> ¹⁸⁷ (2014)	62 Schizophrenia patients: 33 Short duration of treatment patients (14 F and 19 M), 26.3 ± 9.0 yrs; 29 Long duration of treatment patients (16 F and 13 M), 31.3 ± 8.6 yrs	Bilateral prefrontal and temporal regions	ETG-4000	52/3 cm	HbO
Chou <i>et al.</i> ¹⁸⁸ (2015)	29 Healthy individuals (19 F and 10 M), 30.3 ± 10.6 yrs; 28 Schizophrenia patients (13 F and 15 M), 30.8 ± 6.1 yrs	Bilateral prefrontal and temporal regions	ETG-4000	52/3 cm	HbO
Quan <i>et al.</i> ¹⁸⁹ (2015)	100 Healthy individuals (35 F and 65 M), 34.43 ± 12.36 yrs; 140 Schizophrenia patients (60 F and 80 M), 33.81 ± 11.52 yrs	Bilateral prefrontal and temporal regions	ETG-4000	52/3 cm	HbO, HbR
Holper <i>et al.</i> ¹⁹⁰ (2015)	28 Healthy individuals (17 F and 11 M), 30 ± 5.952 yrs; 66 Paranoia patients (22 F and 44 M), 31 ± 6.985 yrs; 39 Psychoticism patients (23 F and 16 M), 31 ± 6.243 yrs; 55 Paranoia-Psychoticism patients (29 F and 26 M), 31 ± 6.757 yrs	Bilateral prefrontal and temporal regions	ETG-4000	52/3 cm	HbO, HbR
Li <i>et al.</i> ¹⁹¹ (2015)	120 Healthy individuals (53 F and 67 M), 32.8 ± 10.7 yrs; 120 Schizophrenia patients (57 F and 63 M), 31.5 ± 11.5 yrs	Bilateral prefrontal and temporal regions	ETG-4000	52/3 cm	HbO, HbR, HbT

Table 6. (Continued)

Work	Experimental population	Brain area under study	Instrument	No. of channels/ separation(s)	Analyzed parameters
Chou <i>et al.</i> ¹⁹² (2015)	106 Healthy individuals (53 F and 53 M), 31.9 ± 7.2 yrs; 109 Schizophrenia patients (54 F and 55 M), 33.0 ± 10.4 yrs	Bilateral prefrontal and temporal regions	ETG-4000	52/3 cm	HbO
Pu <i>et al.</i> ¹⁹³ (2015)	30 Healthy individuals (19 F and 11 M), 32.4 ± 11.1 yrs; 33 Schizophrenia patients (21 F and 12 M), 32.8 ± 8.5 yrs	Bilateral prefrontal and temporal regions	ETG-4000	52/3 cm	HbO
Iwashiro <i>et al.</i> ¹⁹⁴ (2016)	16 Healthy individuals (6 F and 10 M), 16–36 yrs; 18 First episode Schizophrenia patients (6 F and 12 M), 17–35 yrs; 23 Ultra-high-risk patients (10 F and 13 M), 16–29 yrs	Bilateral prefrontal and temporal regions	ETG-4000	52/3 cm	Brain activity
Pu <i>et al.</i> ¹⁹⁵ (2016)	41 Schizophrenia patients (23 F and 18 M), 33.6 ± 11.2 yrs	Bilateral prefrontal and temporal regions	ETG-4000	52/3 cm	HbO, HbR
Itakura <i>et al.</i> ¹⁹⁶ (2017)	22 Healthy individuals (11 F and 11 M), 35.8 ± 11.0 yrs; 23 Schizophrenia patients (11 F and 12 M), 42.1 ± 13.0 yrs	Bilateral prefrontal and temporal regions	ETG-4000	52/3 cm	HbO
Ohji <i>et al.</i> ¹²⁹ (2017)	51 Healthy individuals (18 F and 33 M), 35.7 ± 11.9 yrs; 26 MDD patients (9 F and 17 M), 41.1 ± 12.7 yrs; 22 BD patients (9 F and 13 M), 39.9 ± 12.5 yrs; 45 Schizophrenia patients (29 F and 16 M), 35.4 ± 9.1 yrs	Bilateral prefrontal and temporal regions	ETG-4000	52/3 cm	HbO, HbR
Noda <i>et al.</i> ¹⁹⁷ (2017)	30 Healthy individuals (16 F and 14 M), 32.5 ± 8.0 yrs; 30 Schizophrenia patients (14 F and 16 M), 31.7 ± 9.0 yrs	Bilateral prefrontal and temporal regions	ETG-4000	52/3 cm	HbO, HbR
Luo <i>et al.</i> ¹⁹⁸ (2018)	17 Healthy individuals (9 F and 8 M), 26.2 ± 6.3 yrs; 16 Schizophrenia patients (9 F and 7 M), 28.6 ± 7.8 yrs	PFC	CW5	32/3 cm	HbO

Table 6. (Continued)

Work	Experimental population	Brain area under study	Instrument	No. of channels/ separation(s)	Analyzed parameters
Narita <i>et al.</i> ¹⁹⁹ (2018)	26 Schizophrenia patients (11 F and 15 M), 40.5 ± 10.0 yrs	Bilateral prefrontal and temporal regions	ETG-4000	52/3 cm	HbO
N-back task					
Koike <i>et al.</i> ²⁰⁰ (2013)	26 Healthy individuals (13 F and 13 M), 33.4 ± 13.9 yrs; 26 Schizophrenia patients (13 F and 13 M), 30.9 ± 12.1 yrs	Bilateral prefrontal and temporal regions	ETG-4000	52/3 cm	HbO, HbR
Pu <i>et al.</i> ²⁰¹ (2014)	12 Healthy individuals (9 F and 3 M), 31.4 ± 9.60 yrs; 19 Schizophrenia patients (11 F and 8 M), 28.5 ± 7.60 yrs	Bilateral prefrontal and temporal regions	ETG-4000	52/3 cm	HbO
Pu <i>et al.</i> ²⁰² (2016)	50 Healthy individuals (30 F and 20 M), 34.4 ± 10.8 yrs; Schizophrenia patients: 49 Lower cognition patients (24 F and 25 M), 33.1 ± 11.0 yrs; 38 Higher cognition patients (26 F and 12 M), 34.1 ± 8.7 yrs	Bilateral prefrontal and temporal regions	ETG-4000	52/3 cm	HbO
Pu <i>et al.</i> ²⁰³ (2016)	26 Healthy individuals (18 F and 8 M), 31.2 ± 6.9 yrs; 26 Schizophrenia patients (18 F and 8 M), 31.6 ± 8.7 yrs	Bilateral prefrontal and temporal regions	ETG-4000	52/3 cm	HbO
Random number generation task					
Shimba <i>et al.</i> ²⁰⁴ (2004)	10 Healthy individuals (2 F and 8 M), 40.7 ± 9.8 yrs; 13 Schizophrenia patients (3 F and 10 M), 36.9 ± 12.3 yrs	Bilateral frontal regions	NIRO-300	2/5 cm	HbO, HbR, HbT
Koike <i>et al.</i> ²⁰⁵ (2011)	40 Healthy individuals (20 F and 20 M), 36.8 ± 15.3 yrs; 22 Schizophrenia patients (11 F and 11 M), 41.0 ± 11.6 yrs	Bilateral prefrontal and temporal regions	ETG-4000	52/3 cm	HbO
Resting state					
Hoshi <i>et al.</i> ²⁰⁶ (2006)	16 Healthy individuals (M), 38.9 ± 9.1 yrs; 14 Schizophrenia patients (M), 36.1 ± 8.7 yrs	Bilateral frontal regions	TRS-10	2/3 cm	HbO, HbT

Table 6. (Continued)

Work	Experimental population	Brain area under study	Instrument	No. of channels/ separation(s)	Analyzed parameters
Hosomi <i>et al.</i> ²⁰⁷ (2019)	53 Healthy individuals (M), 41.1 ± 1.5 yrs; 20 Schizophrenia patients (M), 50.6 ± 3.0 yrs	Prefrontal regions	WOT-100	10/3 cm	HbO, HbR
Multiple cognitive tasks					
Ikezawa <i>et al.</i> ²⁰⁸ (2009)	30 Healthy individuals (17 F and 13 M), 37.3 ± 8.7 yrs; 30 Schizophrenia patients (18 F and 12 M), 38.7 ± 11.7 yrs	PFC	NIRO-200	2/3 cm	HbO, HbR
Azechi <i>et al.</i> ²⁰⁹ (2010)	30 Healthy individuals (17 F and 13 M), 37.3 ± 8.7 yrs; 30 Schizophrenia patients (18 F and 12 M), 38.7 ± 11.7 yrs	Bilateral prefrontal and temporal regions	ETG-4000	2/3 cm	HbO
Stop-signal task					
Okada <i>et al.</i> ²¹⁰ (2016)	21 Healthy individuals (12 F and 9 M), 37.0 ± 7.0 yrs; 21 Psychosis patients (7 F and 14 M), 37.9 ± 6.0 yrs; 14 Schizophrenia patients (7 F and 7 M), 35.3 ± 9.8 yrs	Bilateral prefrontal and temporal regions	ETG-4000	52/3 cm	HbO, HbR
Tsujii <i>et al.</i> ¹⁴⁸ (2018)	18 Healthy individuals (10 F and 8 M), 36.6 ± 10.7 yrs; 21 BD patients (12 F and 9 M), 36.9 ± 10.2 yrs; 20 Schizophrenia patients (11 F and 9 M), 33.6 ± 8.7 yrs	Frontotemporal region	ETG-4000	52/3 cm	HbO
Continuous performance task					
Fallgatter and Strik ²¹¹ (2000)	10 Healthy individuals (5 F and 5 M), 30.0 ± 2.1 yrs; 9 Schizophrenia patients (3 F and 6 M), 34.7 ± 13.1 yrs	Frontal region	Critikon 2020 Cerebral Redox Monitors	2/4.5 cm	HbO, HbR
Delayed response task					
Lee <i>et al.</i> ²¹² (2008)	11 Healthy individuals (4 F and 7 M), 36.6 ± 6.4 yrs; 13 Schizophrenia patients (4 F and 9 M), 34.7 ± 8.0 yrs	PFC	ETG-100	24/3 cm	HbO, HbR, HbT

Table 6. (Continued)

Work	Experimental population	Brain area under study	Instrument	No. of channels/ separation(s)	Analyzed parameters
Tower of London task					
Zhu <i>et al.</i> ²¹³ (2010)	40 Healthy individuals (22 F and 18 M), 24.4 ± 3.63 yrs; 40 Schizophrenia patients (20 F and 20 M), 22.8 ± 4.93 yrs	Bilateral frontal regions	CW5	28/3 cm	HbO, HbR
Go/No-go task					
Nishimura <i>et al.</i> ²¹⁴ (2011)	40 Healthy individuals (20 F and 20 M), 31.4 ± 4.5 yrs; 14 Schizophrenia patients (9 F and 5 M), 36.1 ± 12.5 yrs	Bilateral prefrontal and temporal regions	ETG-4000	52/3 cm	HbO, HbR
Electroconvulsive therapy					
Fujita <i>et al.</i> ¹⁴⁵ (2011)	10 MD patients (6 F and 4 M), 64.5 ± 10.1 yrs; 11 Schizophrenia patients (9 F and 2 M), 45.8 ± 13.6 yrs	Frontal region	NIRO-200	2/3 cm	HbO, HbR
Conversation task					
Takei <i>et al.</i> ²¹⁵ (2013)	31 Healthy individuals (11 F and 20 M), 33.5 ± 10 yrs; 29 Schizophrenia patients (10 F and 19 M), 35.4 ± 11.9 yrs	Bilateral prefrontal and temporal regions	ETG-4000	52/3 cm	HbO, HbT
Reading task					
Schneider <i>et al.</i> ²¹⁶ (2015)	22 Healthy individuals (12 F and 10 M), 30 ± 12 yrs; 22 Schizophrenia patients (7 F and 15 M), 35 ± 12 yrs	Bilateral fronto-temporoparietal regions	ETG-4000	44/3 cm	HbO
Stroop task					
Holper <i>et al.</i> ²¹⁷ (2016)	27 Healthy individuals (11 F and 16 M), 29.86 ± 5.784 yrs; 62 Paranoia patients (43 F and 19 M), 30.13 ± 7.091 yrs; 34 Psychoticism patients (13 F and 21 M), 29.67 ± 6.428 yrs; 51 Paranoia-Psychoticism patients (24 F and 27 M), 29.02 ± 6.346 yrs	Bilateral prefrontal and temporal regions	ETG-4000	52/3 cm	HbT

Table 6. (Continued)

Work	Experimental population	Brain area under study	Instrument	No. of channels/ separation(s)	Analyzed parameters
Video game task Shimizu <i>et al.</i> ²¹⁸ (2017)	8 Schizophrenia patients (2 F and 6 M), 46.7 ± 13.7 yrs	Frontal lobe	LABNIRS	45	HbO
Drawing task Nakano <i>et al.</i> ²¹⁹ (2018)	28 Healthy individuals (14 F and 14 M), 30.8 ± 5.1 yrs; 28 Schizophrenia patients (14 F and 14 M), 30.8 ± 5.3 yrs	Bilateral prefrontal and temporal regions	ETG-4000	52/3 cm	HbO
Rock-paper-scissor task Sato <i>et al.</i> ²²⁰ (2018)	30 Healthy individuals (14 F and 16 M), 31.6 ± 8.5 yrs; 30 Schizophrenia patients (15 F and 15 M), 33.6 ± 8.5 yrs	Bilateral prefrontal and temporal regions	ETG-4000	52/3 cm	HbO

dorsolateral PFC and the frontopolar cortex.¹⁹⁶ A study on the association between family history and SZ found that patients with a family history of SZ exhibited an even lower hemodynamic response compared to patients without a family history of SZ, thereby revealing the effects of genetics on this condition.¹²⁹ Patients with SZ showed a posttask increase in HbO levels, revealing the impairment in their working memory.¹⁹⁷ The rehabilitation of the impairments of SZ patients did not result in any significant behavioral or neuronal activity after four weeks of therapy, emphasizing that their rehabilitation requires a longer period.¹⁹⁸ Rehabilitating SZ patients by administering transcranial direct current stimulation (tDCS) resulted in improved symptoms associated with positive and negative psychoses.¹⁹⁹

7.2. *N-back task*

The localization of activation in SZ patients was different from that in healthy individuals, and in the patient population, no changes were observed when the load of working memory tasks was increased.²⁰⁰ In a longitudinal study on SZ patients, positive effects were observed in response to the neuropsychological educational approach to cognitive remediation because the cortical activation was improved bilaterally.²⁰¹ In SZ patients, the right dorsolateral and bilateral PFCs and the right frontopolar region collectively showed a relationship with the impaired cognitive ability measured via a brief assessment on cognition in SZ.²⁰² The lateral PFC HbO response in SZ patients was directly associated with theory-of-mind scores.²⁰³

7.3. *Random number generation task*

During a random number generation task, compared to healthy individuals, SZ patients showed significantly lower activation based on the HbO, HbR, and HbT levels.²⁰⁴ Overall, the location of HbO activation in SZ patients was similar to that in healthy persons, and patients who developed SZ at a younger age showed high activation impairment in the right dorsolateral PFC.²⁰⁵

7.4. *Resting state*

The resting state HbT levels in SZ patients were lower than those in healthy persons, and they were

also associated with the age of disease onset.²⁰⁶ The spontaneous activation levels in the medial PFC during resting state were reduced in SZ patients when compared to healthy persons.²⁰⁷

7.5. *Multiple cognitive tasks*

Among several cognitive tasks, the verbal fluency and Tower of Hanoi tasks resulted in significant differences in the HbO responses, thereby facilitating good classification accuracy between healthy individuals and SZ patients.^{208,209}

7.6. *Stop-signal task*

The SZ patients differed from the patients affected by methamphetamine-associated psychosis as they exhibited better activation responses in the frontopolar area and distinct activation in the premotor region, which is related to impulsivity.²¹⁰ The impaired inferior frontal region in SZ patients was responsible for the deficiency in the inhibitory control mechanism, whereas the superior temporal region differentiated SZ patients from the BD patients.¹⁴⁸

7.7. *Continuous performance task*

The healthy persons exhibited right hemispheric lateralization while the patients with SZ did not show any lateralization during activation, which was possibly due to their left-hemispheric impairment.²¹¹

7.8. *Delayed response task*

SZ patients exhibited bilateral activation due to compensatory reorganization as activation was observed only on the right side in healthy persons.²¹²

7.9. *Tower of London task*

The HbO and HbR responses in the PFC of SZ patients during a planning task were reduced.²¹³

7.10. *Go/No-go task*

The SZ patients with excitement symptoms exhibited an impaired HbO pattern during a response inhibition task.²¹⁴

7.11. *Electroconvulsive therapy*

The patients with SZ exhibited asymmetric changes in HbO responses in the bilateral PFC after therapy, which differentiated SZ and MD patients.¹⁴⁵

7.12. *Conversation task*

During a face-to-face conversation task, the bilateral temporal regions and the right inferior frontal gyrus were responsible for disorganized thinking, owing to which SZ patients face difficulties in conversations.²¹⁵

7.13. *Language comprehension*

SZ patients exhibited a deficiency in understanding complex language as they displayed incomplete and delayed comprehension, which leads to impaired activation patterns.²¹⁶

7.14. *Stroop*

The severity of subclinical psychosis in SZ patients was inversely related to the activations in the dorsolateral PFC and middle temporal gyrus.²¹⁷

7.15. *Video game task*

Rehabilitation using interactive sports video games resulted in positive effects on SZ patients as their HbO response in the PFC was improved along with their quality of life.²¹⁸

7.16. *Drawing task*

The analysis of HbO signals showed that the activation in SZ patients during a tree-drawing task was lower than that in healthy persons.²¹⁹

7.17. *Rock-paper-scissor task*

HbO responses were impaired when a patient lost in this task, yet they were associated with scores on the Global Assessment of Functioning and the Negative Syndrome scales.²²⁰

8. Mild Cognitive Impairment

Mild cognitive impairment (MCI) is a state that causes simple/small problems associated with

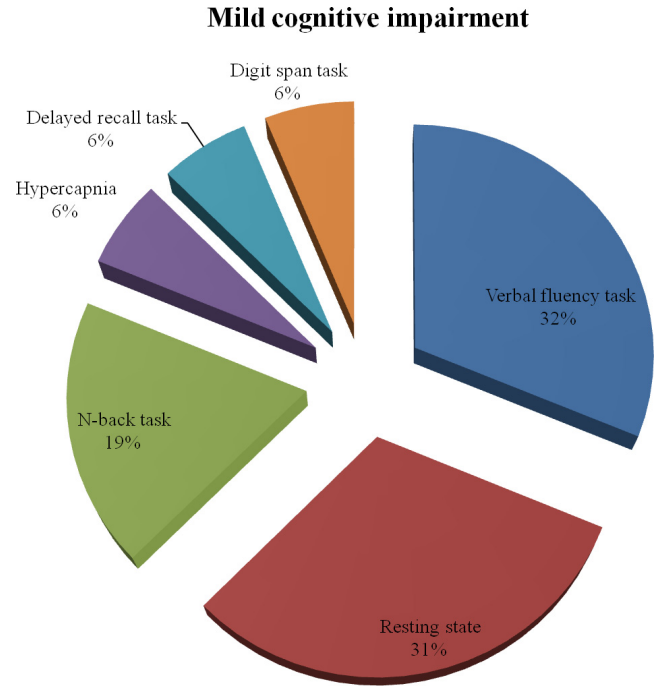


Fig. 7. Task-based distribution of studies on mild cognitive impairment (total studies: 16).

human memory or thinking. MCI patients do not normally incur any alarming situations that interfere with their routine lives; yet their cognitive standing is low based on memory or thinking when compared to that of age-matched healthy individuals. This impairment is not classified as dementia but could be a high-risk situation for developing any kind of dementia. The underlying mechanism that prevents MCI from transforming into dementia is still unclear. Therefore, detecting the condition when it is at an earlier stage is important. Several fNIRS studies have been conducted to investigate the physiology of MCI patients. The task-wise distribution is shown in Fig. 7, and the key related studies are outlined in Table 7.

8.1. *Verbal fluency task*

In an early study that examined MCI and AD patients, the overall HbO response of MCI patients was between those of healthy persons and AD patients, but the right parietal area in MCI patients exhibited the most degradation.²²¹ During a dual-task that involved walking during the VFT, the PFC activation was increased when compared to during simple walking, and this increased activation was directly associated with cognitive ability.²²²

Table 7. Studies on MCI.

Work	Experimental population	Brain area under study	Instrument	No. of channels/ separation(s)	Analyzed parameters
Verbal fluency task Arai <i>et al.</i> ²²¹ (2006)	32 Healthy individuals (16 F and 16 M), 57.3 ± 6.4 yrs; 15 MCI patients (8 F and 7 M), 63.0 ± 6.4 yrs; 15 AD patients (10 F and 5 M), 59.2 ± 3.9 yrs	Frontal, bilateral parietal, and occipital cortices	ETG-7000	60	HbO
Doi <i>et al.</i> ²²² (2013)	16 MCI patients (6 F and 10 M), 75.4 ± 7.2 yrs	Frontal cortex	OEG-16	16/3 cm	HbO
Yeung <i>et al.</i> ²²³ (2016)	26 Healthy individuals (19 F and 7 M), 68.87 ± 6.08 yrs; 26 MCI patients (6 F and 20 M), 69.07 ± 6.20 yrs	Prefrontal cortex	OEG-SpO ₂	16/3 cm	HbO
Yap <i>et al.</i> ²²⁴ (2017)	31 Healthy individuals (12 F and 19 M), 72.6 ± 8.5 yrs; 12 MCI patients (4 F and 8 M), 73.1 ± 8.2 yrs; 18 AD patients (6 F and 12 M), 74.7 ± 10.0 yrs	Prefrontal cortex	OT-R40	52/3 cm	HbO, HbR
Katzorke <i>et al.</i> ²²⁵ (2018)	55 Healthy individuals (34 F and 21 M); 55 MCI patients (25 F and 30 M),	Bilateral prefrontal and temporal regions	ETG-4000	52/3 cm	HbO, HbR
Resting state Viola <i>et al.</i> ²²⁶ (2013)	10 Healthy individuals (6 F and 4 M), 69.5 ± 6.8 yrs; 21 MCI patients (11 F and 10 M), 70.2 ± 7.3 yrs	Bilateral frontal and parietal-temporal cortices	T-NIRS EVO II	4/4 cm	TOI
Liu <i>et al.</i> ²²⁷ (2015)	21 Healthy individuals (13 F and 8 M), 67 ± 7 yrs; 32 MCI patients (19 F and 13 M), 67 ± 7 yrs	Prefrontal cortex	NIRO-200NX		TOI
Marmarelis <i>et al.</i> ²²⁸ (2017)	22 Healthy individuals (11 F and 11 M), 68.15 ± 6.24 yrs; 43 MCI patients (30 F and 13 M), 66.79 ± 6.34 yrs	Prefrontal cortex	Hamamatsu		TOI

Table 7. (Continued)

Work	Experimental population	Brain area under study	Instrument	No. of channels/ separation(s)	Analyzed parameters
Li <i>et al.</i> ²²⁹ (2018)	31 Healthy individuals (20 F and 11 M), 67.61 ± 8.86 yrs; 27 MCI patients (13 F and 14 M), 70.33 ± 8.27 yrs; 24 AD patients (15 F and 9 M), 72.25 ± 9.15 yrs	Full head	CW6	46/3.2 cm	HbO
Zeller <i>et al.</i> ²³⁰ (2019)	61 Healthy individuals (37 F and 24 M), 73.34 ± 1.7 yrs; 25 Healthy individuals (19 F and 6 M), 34.92 ± 7.4 yrs; 54 MCI patients (25 F and 29 M), 73.91 ± 1.8 yrs	Bilateral frontal and parietal cortices	ETG-4000	52/3 cm	HbO
N-back task					
Niu <i>et al.</i> ²³¹ (2013)	16 Healthy individuals, 63.1 ± 5.3 yrs; 8 MCI patients, 64.8 ± 7.2 yrs	Bilateral frontal and temporal cortices	ETG-4000	52/3 cm	HbO
Yeung <i>et al.</i> ²³² (2016)	26 Healthy individuals (19 F and 7 M), 68.87 ± 6.08 yrs; 26 MCI patients (19 F and 7 M), 69.15 ± 6.28 yrs	Bilateral prefrontal cortices	OEG-SpO2	16/3 cm	HbO
Vermeij <i>et al.</i> ²³³ (2017)	21 Healthy individuals (8 F and 13 M), 69.5 ± 5.4 yrs; 14 MCI patients (4 F and 10 M), 66.1 ± 3.9 yrs	Prefrontal cortex	Oxymon Mk III	2/5 cm	HbO HbR

Table 7. (Continued)

Work	Experimental population	Brain area under study	Instrument	No. of channels/ separation(s)	Analyzed parameters
Hypercapnia					
Babiloni <i>et al.</i> ²³⁵ (2014)	10 Healthy individuals (5 F and 5 M), 70.8 ± 2.5 yrs; 10 MCI patients (4 F and 6 M), 25.4 ± 1.02 yrs	Prefrontal cortex	ISS oximeter	2/2, 2.5, 3, and 3.5 cm	HbO HbR
Delayed recall task					
Uemura <i>et al.</i> ²³⁵ (2015)	31 Healthy individuals (20 F and 11 M), 67.61 ± 8.86 yrs; 27 MCI patients (13 F and 14 M), 70.33 ± 8.27 yrs	Prefrontal cortex	FOIRE-3000	22/3 cm	HbO
Digit span task					
Li <i>et al.</i> ²³⁶ (2018)	8 Healthy individuals (2 F and 6 M), 63.6 ± 6.5 yrs; 6 Mild AD patients (4 F and 2 M), 72.5 ± 7.3 yrs; 7 moderate/severe AD patients (4 F and 3 M), 76 ± 4.8 yrs; 9 MCI patients (3 F and 6 M), 70.3 ± 5.4 yrs	Frontal and bilateral parietal cortices	NIRScout	46/3 cm	HbO

The activation was distributed in the bilateral PFC compared to the concentrated activation in the left PFC in healthy persons, illustrating that the impairment in the left hemisphere of MCI patients was being compensated by their right hemisphere.²²³ Compared to the HbO responses of healthy persons and AD patients, MCI patients exhibited a steeper slope during activation in the right PFC owing to the hyperactivation process.²²⁴ The HbO response was reduced in the inferior frontotemporal cortex in MCI patients compared to that in healthy persons.²²⁵

8.2. Resting state

Compared to healthy persons, from the amnesic MCI patients, reduced tissue oxygen saturation was found in the bilateral temporal–parietal cortex.²²⁶ In a multimodal study that used color-coded duplex ultrasonography, fNIRS, and fMRI, the amnesic MCI patients showed neurovascular decoupling.²²⁷ The tissue oxygenation index (TOI) that was computed using HbO and HbT levels that were derived via fNIRS provided effective results that can be considered as a biomarker for amnesic MCI patients as compared to the already established biomarkers obtained via transcranial Doppler sonography.²²⁸ An entropy-based analysis revealed that the complexity of brain signals in amnesic MCI patients was higher than AD patients but was lower than healthy persons, and this reduction in complexity was associated with the clinical scores.²²⁹ During the resting state, fewer low-frequency oscillations in the PFC were observed in MCI patients compared to healthy young persons, while in the parietal cortex, the number of oscillations was low when compared to that observed in healthy older persons.²³⁰

8.3. N-back task

Compared to healthy persons, MCI patients exhibited a reduced HbO response in the left dorsolateral PFC, right supplementary motor area, and left superior temporal regions.²³¹ The working memory activations of MCI patients were comparable with those of healthy persons during low-load tasks: However, they degraded when the load was increased, thereby exhibiting an impaired working memory capability.²³² In the case of MCI patients, working memory training resulted in an improved

behavioral performance, but such corresponding improvement was not observed in the PFC activation.²³³

8.4. Hypercapnia

In amnesic MCI patients and healthy persons, no differences were found in vasomotor reactivity before, during, and after inhaling CO₂.²³⁴

8.5. Delayed recall task

The activation levels were similar in healthy individuals and MCI patients in response to the phase of memorizing words in this task, but compared to healthy persons, the MCI patients showed a reduced HbO response approximately in Brodmann area (BA) 9 during the retrieval of words phase.²³⁵

8.6. Digit span task

The mean and slope of the HbO responses were correlated with the clinical scores, and the scores of the MCI patients stayed below those of the mild and moderate-to-severe AD patients.²³⁶

9. Alzheimer's Disease

It is a form of dementia with the most rapidly increasing prevalence rate. Patients with AD can only be treated to manage their symptoms as there is still no known cure for this disease. It slowly sabotages the memory and takes away the capacity to do routine tasks. Various tasks have been utilized to get insights into the brain activity of these patients. The task-wise distribution of the studies is presented in Fig. 8, and Table 8 outlines the details of the works.

9.1. Verbal fluency task

The VFT is the most commonly used task in the studies associated with AD. The earlier findings revealed that AD patients had reduced HbO and HbT levels in the parietal areas.^{237,238} The HbO levels in the prefrontal area decreased in some patients²³⁷ while they increased in most others.²³⁸ These contradicting findings were attributed to variability caused due to subject characteristics or the location of the fNIRS channel. A better performance in the VFT is associated with the left

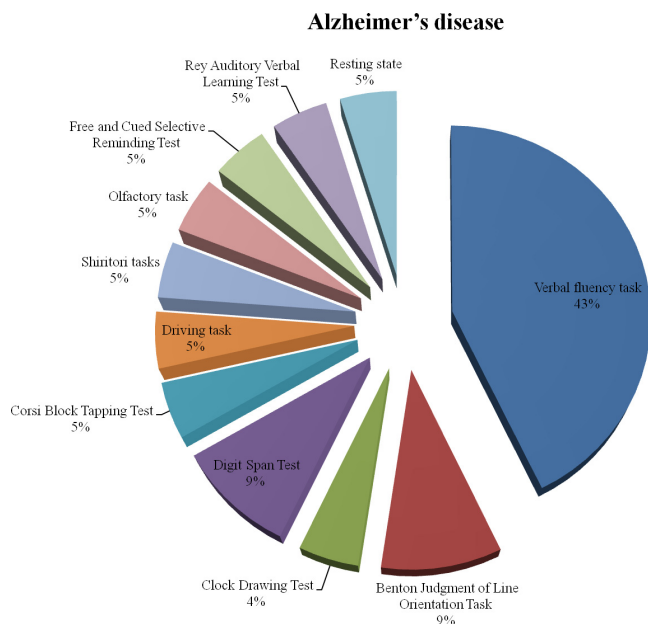


Fig. 8. Task-based distribution of studies on Alzheimer's disease (total studies: 21).

prefrontal hemisphere, but this physiological asymmetry is missing in AD patients.²³⁹ AD can be differentiated from MCI by revealing degraded global activation when measurements of most of the brain areas are taken simultaneously.²²¹ In the pursuit to enhance the quality of life of AD patients by improving their symptoms, the administration of an oral drug called memantine was beneficial when compared to not using this drug.²⁴⁰ The activation was slightly higher compared to that of patients struggling with late-life depression.¹²¹ The patients medicated with a cholinesterase inhibitor showed improved activation in the speech-related areas of the brain as a higher concentration of HbO was measured.²⁴¹ The activation region in AD patients is different compared to the patients with fronto-temporal dementia, as AD patients exhibited activation in the frontoparietal areas.²⁴² The mean activation pattern of AD patients was lower and slower than those of MCI patients.²²⁴

9.2. *Benton judgment of line orientation test*

The parietal cortex is linked with visuospatial tasks, and analyses of activation occurring in this region can be used for early detection of AD since AD patients exhibit only marginal activation when compared to the explicit activation in healthy

subjects.²⁴³ The parietal region showed considerably higher HbO activations in AD patients compared to depression patients.¹²¹

9.3. *Clock drawing test*

The clock drawing test (CDT) scores can adequately be used to differentiate between healthy individuals and AD patients; however, the entropy analysis conducted on fNIRS recordings while the subjects were performing the CDT resulted in significant differences between the results of AD patients and healthy subjects.²⁴⁴

9.4. *Digit span test*

An entropy-based fNIRS signal complexity analysis demonstrated that the digit span task (DST) could help classify AD.²⁴⁴ A time-series analysis revealed that the reduction or decline in HbO levels becomes steeper when the intensity of AD progresses.²³⁶

9.5. *Corsi block-tapping test*

Compared to the CDT and DST results, the results of the Corsi block-tapping test were the most effective in differentiating AD patients from healthy subjects via entropy analysis.²⁴⁴

9.6. *Driving task*

AD patients exhibited lower HbO values than those of healthy individuals, and the act of applying the brake during the task and HbO changes were negatively related while these were positively related in healthy persons.²⁴⁵

9.7. *Shiritori tasks*

While performing Shiritori tasks, the area and maximum value of the fNIRS signals from the dorsolateral PFC and frontal pole cortex regions of AD patients were significantly lower.²⁴⁶

9.8. *Olfactory task*

An interesting study conducted on AD patients using an active vanilla smell and a sham one revealed that brain activation occurs in the temporal region of healthy individuals while performing the olfactory task whereas the AD patients did not show any activation at all.²⁴⁷

Table 8. Alzheimer's disease (AD).

Manuscript	Experimental population	Brain area under study	Instrument	No. of channels/ separation(s)	Analyzed parameters
Verbal fluency task Hock <i>et al.</i> ²³⁷ (1996)	19 Healthy individuals (14 F and 5 M), 67 ± 10 yrs; 19 AD patients (11 F and 8 M), 71 ± 10 yrs	Frontal and parietal cortex	NIRO 500	2/4 cm	HbO HbT
Hock <i>et al.</i> ²³⁸ (1997)	27 Healthy individuals, 67 ± 10 yrs; 10 AD patients, 65 ± 13 yrs	Frontal and parietal cortex	NIRO 500	2/4 cm	HbO HbR HbT
Fallgatter <i>et al.</i> ²³⁹ (1997)	10 Healthy individuals (5 F and 5 M), 30.1 ± 2.1 yrs; 10 AD patients (6 F and 4 M), 67.3 ± 10.6 yrs	Prefrontal cortex	Critikon 2020	4/4.5 cm	HbO
Arai <i>et al.</i> ²²¹ (2006)	32 Healthy individuals (16 F and 16 M), 57.3 ± 6.4 yrs; 15 AD patients (10 F and 5 M), 59.2 ± 3.9 yrs; 15 MCI patients (8 F and 7 M), 63.0 ± 6.4 yrs	Frontal, bilateral parietal, and occipital cortices	ETG-7000	60	HbO
Araki <i>et al.</i> ²⁴⁰ (2014)	37 AD patients (19 F and 18 M), 78.8 ± 7.7 yrs	Prefrontal cortex	ETG-4000	22	HbO
Kito <i>et al.</i> ¹²¹ (2014)	33 Healthy individuals (22 F and 11 M), 69.6 ± 5.5 yrs; 28 AD patients (18 F and 10 M), 76.6 ± 6.9 yrs; 30 Depressed patients (21 F and 9 M), 71.1 ± 6.8 yrs	Frontal and parietal cortices	FOIRE-3000	44/3 cm	HbO
Metzger <i>et al.</i> ²⁴¹ (2015)	24 AD patients (16 F and 8 M), 73.44 ± 8.72 yrs	Bilateral prefrontal and temporal cortices	ETG-4000	44/3 cm	HbO HbR
Metzger <i>et al.</i> ²⁴¹ (2016)	8 Healthy individuals (3 F and 5 M), 65.5 ± 6.5 yrs; 8 AD patients (3 F and 5 M), 74.3 ± 4.5 yrs; 8 frontotemporal dementia patients (3 F and 5 M), 67.6 ± 9.8 yrs	Bilateral frontotemporal cortex	ETG-4000	44/3 cm	HbO

Table 8. (Continued)

Manuscript	Experimental population	Brain area under study	Instrument	No. of channels/ separation(s)	Analyzed parameters
Yap <i>et al.</i> ²²⁴ (2017)	31 Healthy individuals (12 F and 19 M), 72.6 ± 8.5 yrs; 18 AD patients (6 F and 12 M), 74.7 ± 10.0 yrs; 12 MCI patients (4 F and 8 M), 73.1 ± 8.2 yrs	Prefrontal cortex	OT-R40	52/3 cm	HbO HbR
Benton Judgment of Line Orientation Task					
Zeller <i>et al.</i> ²⁴³ (2010)	13 Healthy individuals (4 F and 9 M), 61.8 ± 5.5 yrs; 13 AD patients (4 F and 9 M), 61.7 ± 6.2 yrs	Parietal cortex	ETG-100	24/3 cm	HbO
Kito <i>et al.</i> ¹²¹ (2014)	33 Healthy individuals (22 F and 11 M), 69.6 ± 5.5 yrs; 28 AD patients (18 F and 10 M), 76.6 ± 6.9 yrs; 30 Depression patients (21 F and 9 M), 71.1 ± 6.8 yrs	Frontal and parietal cortices	FOIRE-3000	44/3 cm	HbO
Clock Drawing Test					
Perpetuini <i>et al.</i> ²⁴⁴ (2019)	11 AD patients (4 F and 7 M), 72.2 ± 4.5 yrs; 11 Healthy individuals (3 F and 8 M), 67.5 ± 5.0 yrs	Frontal cortex	Imagent	21/3 cm, 4 cm	HbO
Digit Span Test					
Li <i>et al.</i> ²³⁶ (2018)	8 Healthy individuals (2 F and 6 M), 63.6 ± 6.5 yrs; 6 Mild AD patients (4 F and 2 M), 72.5 ± 7.3 yrs; 7 moderate/severe AD patients (4 F and 3 M), 76 ± 4.8 yrs; 9 MCI patients (3 F and 6 M), 70.3 ± 5.4 yrs	Frontal and bilateral parietal cortices	NIRScout	46/3 cm	HbO

Table 8. (Continued)

Manuscript	Experimental population	Brain area under study	Instrument	No. of channels/ separation(s)	Analyzed parameters
Perpetuini <i>et al.</i> ²⁴⁴ (2019)	11 AD patients (4 F and 7 M), 72.2 ± 4.5 yrs; 11 Healthy individuals (3 F and 8 M), 67.5 ± 5.0 yrs	Frontal cortex	Imagent	21/3 cm, 4 cm	HbO
Corsi Block Tapping Test					
Perpetuini <i>et al.</i> ²⁴⁴ (2019)	11 AD patients (4 F and 7 M), 72.2 ± 4.5 yrs; 11 Healthy individuals (3 F and 8 M), 67.5 ± 5.0 yrs	Frontal cortex	Imagent	21/3 cm, 4 cm	HbO
Driving task					
Tomioka <i>et al.</i> ²⁴⁵ (2009)	14 Healthy individuals (M), 67.4 ± 4.4 yrs; 12 AD patients (M), 70.5 ± 8.7 yrs	Bilateral frontal and temporal cortices	ETG-4000	52	HbO
Shiritori tasks					
Kato <i>et al.</i> ²⁴⁶ (2017)	93 Healthy individuals (79 F and 14 M), 72.8 ± 6.0 yrs; 42 AD patients (26 F and 16 M), 78.9 ± 5.3 yrs; 65 LSMG (44 F and 21 M), 75.8 ± 6.2 yrs; 33 HSMG (21 F and 12 M), 78.1 ± 6.8 yrs	Bilateral prefrontal and temporal cortices	ETG-4000	44/3 cm	HbO HbR
Olfactory task					
Fladby <i>et al.</i> ²⁴⁷ (2004)	13 AD patients (7 F and 6 M), 66 (56–72) yrs; 8 Healthy individuals (3 F and 5 M), 66 (56–79) yrs	Temporal cortex	NIRO 300	2/4 cm	HbO HbR
Free and Cued Selective Reminding Test					
Perpetuini <i>et al.</i> ²⁴⁸ (2017)	11 Healthy individuals (3 F and 8 M) 67.5 ± 5.0 yrs; 11 AD patients (4 F and 7 M), 72.2 ± 4.5 yrs	Prefrontal cortex	Imagent	17/3–4 cm	TOI

Table 8. (Continued)

Manuscript	Experimental population	Brain area under study	Instrument	No. of channels/ separation(s)	Analyzed parameters
Rey Auditory Verbal Learning Test Viola <i>et al.</i> ²⁴⁹ (2013)	10 mild AD patients (3 F and 7 M), 71 ± 5.8 yrs; 10 AD patients (5 F and 5 M), 74.4 ± 7.2 yrs	Bilateral temporal- parietal and frontal cortices	T-NIRS EVO II	4/4 cm	HbO
Resting state Li <i>et al.</i> ²⁵⁹ (2018)	31 Healthy individuals (20 F and 11 M), 67.61 ± 8.86 yrs; 24 AD patients (15 F and 9 M), 72.25 ± 9.15 yrs; 27 MCI patients (13 F and 14 M), 70.33 ± 8.27 yrs	Full head	CW6	46/3.2 cm	HbO

9.9. Free and cued selective reminding test

During the delayed free recall phase of the task, higher entropy values were observed in AD patients compared to those in healthy participants in BAs 9 and 46.²⁴⁸

9.10. Rey Auditory Verbal Learning Test

AD patients exhibit higher levels of tissue oxygen saturation in the frontal cortex during the Rey Auditory Verbal Learning Test after receiving brain reperfusion rehabilitation therapy.²⁴⁹

9.11. Resting state

An entropy analysis of the fNIRS signals from all the brain areas revealed that the signal complexity in the brain networks of AD patients was reduced compared to those of healthy individuals as well as MCI patients.²²⁹

10. Parkinson's Disease

The early signs of PD are tremors in the hands that affect movement and balance. Due to a reduced sense of coordination, people with PD often drop items and are more likely to fall. Further, the posture of their bodies are slightly altered. The first problem that PD patients and their caregivers face is disorder in their gait and balance. Neuroimaging techniques are now able to provide more insights into the neural mechanisms of the pathophysiology associated with the gait disorders in PD patients that can cause freezing of gait (FOG). In this section, a few older fNIRS studies and recent investigations are reviewed. The task-wise distribution of studies on PD patients is presented in Fig. 9, while Table 9 outlines all the fNIRS studies.

10.1. Deep brain stimulation

We found two fNIRS studies conducted between 1999 and 2000 which investigated the cortical changes in the frontal area in the brain of PD patients by invasively (deep brain) stimulating the thalamic nucleus ventralis intermedius (VIM) and *globus pallidus internus* (GPi).^{250,251} At different frequency ranges, various patterns of cerebral blood

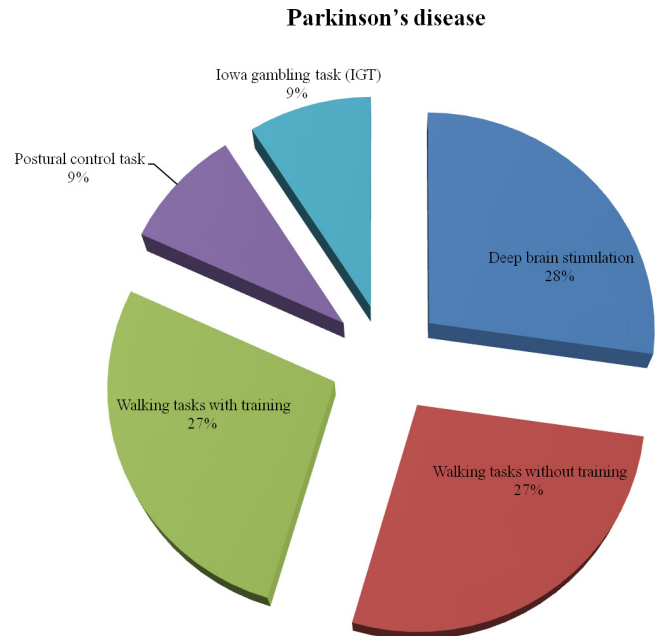


Fig. 9. Task-based distribution of studies on Parkinson's disease (total studies: 11).

oxygenation were observed. Stimulating the GPi at higher frequencies resulted in an increase in HbO and a decrease in HbR. In contrast, in the VIM, the cerebral oxygenation changes were opposite to those seen via GPi stimulation. Another pilot study on PD patients was conducted to examine the motor associated cortical activity changes in response to deep brain stimulation (DBS).²⁵² Compared to prestimulation, after DBS, the cortical activity was higher in the PFC of PD patients. This indicates the therapeutic benefits of DBS in patients with PD.

10.2. Walking tasks without training

A pilot study on PD patients who were affected by FOG demonstrated the feasibility of an fNIRS assessment of the locomotor task during real-life conditions.²⁵³ During turns, in PD patients, this study reported an increase in HbO activation in the frontal lobe before and while experiencing FOG while no changes in HbO activation were observed in healthy persons. Another comparative study on PD patients showed different activation patterns in the frontal lobe during complex walking tasks and concluded that the activation in PD patients depends on the nature of the task.²⁵⁴ During normal walking and obstacle avoidance, the PD patients showed an increase in HbO levels while in healthy persons, no activation was observed during a dual

Table 9. Parkinson's disease (PD).

Manuscript	Experimental population	Brain area under study	Instrument	No. of channels/separation(s)	Analyzed parameters
Deep brain stimulation					
Satakani <i>et al.</i> ²⁵⁰ (1999)	6 PD patients (3 F and 3 M), 46–66 yrs	Bilateral frontal lobes	NIRO-300		HbO HbR HbT
Murata <i>et al.</i> ²⁵¹ (2000)	6 PD	Bilateral frontal lobes	NIRO-300		HbO HbR
Morishita <i>et al.</i> ²⁵² (2016)	6 PD patients (4 F and 2 M), 66.8 ± 4.0 yrs	Frontal and parietal areas	FOIRE-3000	48/3 cm	HbO HbR
Walking tasks without training					
Maidan <i>et al.</i> ²⁵³ (2015)	11 Healthy individuals (3 F and 8 M), 71.2 ± 6.0 yrs; 11 PD patients (7 F and 4 M), 66.2 ± 10.0 yrs	Frontal region	OxyMon MKIII	12/3.5 cm	HbO
Maidan <i>et al.</i> ²⁵⁴ (2016)	38 Healthy individuals (18 F and 20 M), 70.4 ± 0.9 yrs; 68 PD patients (22 F and 46 M), 71.6 ± 0.9 yrs	PFC	PortaLite	2/3, 3.5, 4 cm	HbO
Maidan <i>et al.</i> ²⁵⁵ (2017)	49 PD patients (16 F and 33 M), 72.8 ± 1.0 yrs	PFC	PortaLite	2/3, 3.5, 4 cm	HbO
Walking tasks with training					
Maidan <i>et al.</i> ²⁵⁶ (2018)	All PD 34 Treadmill training (11 F and 23 M), 73.1 ± 1.1 yrs; 30 Treadmill training + virtual reality (8 F and 22 M), 70.1 ± 1.3 yrs	PFC	PortaLite	2/3, 3.5, 4 cm	HbO
Thumm <i>et al.</i> ²⁵⁷ (2018)	20 PD (10 F and 10 M), 69.81 ± 6.41 yrs	PFC	PortaLite	2/3, 3.5, 4 cm	HbO
Al-Yahya <i>et al.</i> ²⁵⁸ (2018)	22 Healthy individuals (16 F and 6 M), 59.5 ± 6.8 yrs; 29 PD patients (13 F and 16 M), 66.3 ± 5.9 yrs	PFC	OxyMon Mk III	6/3 cm	HbO HbR

Table 9. (Continued)

Manuscript	Experimental population	Brain area under study	Instrument	No. of channels/ separation(s)	Analyzed parameters
Postural control task					
Mahoney <i>et al.</i> ²⁵⁹ (2016)	126 Healthy individuals (69 F and 57 M), 74.41 ± 6.12 yrs; 26 PD patients (15 F and 11 M), 81.23 ± 5.93 yrs; 117 Mild PD patients (66 F and 51 M), 77.50 ± 6.72 yrs	PFC	fNIRs Imager 1000	16/2.5 cm	HbO
Iowa gambling task (IGT)					
Balconi <i>et al.</i> ²⁶⁰ (2018)	46 PD patients (9 F and 37 M), 62.93 ± 7.76 yrs	Prefrontal and orbitofrontal cortices	NIRScout	8/3 cm	HbO

walking task. In another recent comparative study between two groups (better and worse ambulations) of PD patients, a different role of BA 10 (involved in executive functioning) was demonstrated during normal walking and turning tasks.²⁵⁵ The decrease in the activation in BA 10 was observed while the patients were turning while an increase was observed while they were walking. Comparing groups of PD patients with worse and better ambulations revealed that a decrease in prefrontal activation was observed in the latter group during turning.

10.3. *Walking tasks with training*

In a randomized controlled trial conducted with fNIRS, the effects of treadmill training in a virtual reality environment on prefrontal activation in PD patients during normal, dual-task, and obstacle-negotiation walking were studied.²⁵⁶ Decreased prefrontal activation was observed after gait training, thereby indicating an improvement in walking. It indicates that PD patients exhibit less reliance on cognitive resources during normal walking. These findings were further supported by the researchers' recent study in which a decrease in HbO levels was observed while the patients were walking on a treadmill compared to while they were walking on the ground.²⁵⁷ Improvements in gait were also reported. Another comparative fNIRS study was conducted on the motor cortex and PFC of PD patients and healthy persons while they were walking on a treadmill at a user-defined speed and an experimenter-defined faster speed.²⁵⁸ The increase in HbO responses of the PD patients was higher in the left and right motor cortices while walking in both conditions compared to those of the healthy persons.

10.4. *Postural control task*

In an fNIRS study, compared to healthy persons, PD patients showed significantly increased prefrontal activation while maintaining postural stability.²⁵⁹ However, patients with mild PD demonstrated a similar activation pattern to healthy persons.

10.5. *Iowa gambling task*

The performances in the Iowa gambling task were assessed using fNIRS to establish the relationship between personality traits and prefrontal activity in

PD patients who were pathological gamblers and those who were not.²⁶⁰ The patients with active gambling behavior showed significantly increased activity in the dorsolateral PFC in response to high-risk and more rewarding options, which indicates a notable involvement in the frontal area in both emotional and cognitive processes.

11. *Stroke*

Stroke is a disease due to which a patient's brain does not receive sufficient blood based on its requirements. This condition occurs due to problems in the arteries that are responsible for the supply of blood to the brain. Stroke is broadly classified into two types: Ischemic stroke occurs when the blood supply is reduced or blocked due to clotting, whereas hemorrhagic stroke occurs when the blood vessels burst open. In both cases, the supply of blood is compromised in a part of the brain, which results in the death of brain cells within a short period. Every brain cell is linked with some function that our brain has to perform; therefore, the dying cells result in the loss of their associated functions. Therefore, it is best to prevent the occurrence of strokes by making changes in our lifestyles that control the cholesterol and fat levels in our body. Due to advanced treatments, the death rates due to strokes have reduced compared to those in the past. There are rehabilitation therapies and drugs that stroke patients can use to regain lost functions. Several researchers have used fNIRS to understand the impairment levels and types in stroke patients using various paradigms. The task-wise distribution of stroke papers is presented in Fig. 10, and these studies have been outlined in Table 10.

11.1. *Resting state*

Owing to the patients' conditions, most studies on stroke patients have been performed using the resting state data. In an fNIRS study, the inter-hemispheric connectivity of ischemic stroke patients was significantly different from healthy persons by examining the low-frequency cardiac and respiratory oscillations, thereby proving the efficiency of this modality.²⁶¹ In ischemic and hemorrhage stroke patients, the frontal cerebral oxygenation was directly correlated with the CBF measured via traditional CT perfusion imaging, illustrating the

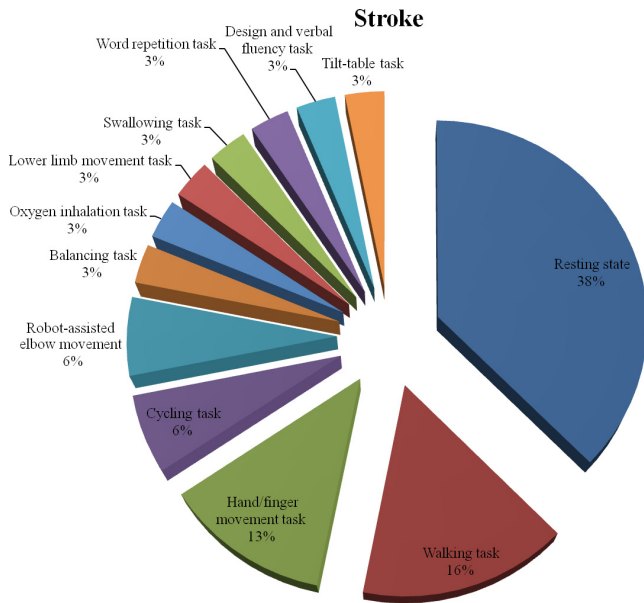


Fig. 10. Task-based distribution of studies on stroke (total studies: 32).

efficacy of the technique.²⁶² By examining the HbO signal of symptomatic carotid occlusion and hypoperfusion patients, the interhemispheric amplitude ratio was impaired when compared with that of healthy persons.²⁶³ Rehabilitation via the application of anodal tDCS induced neuronal activity by resulting in changes in the HbO and HbR values in stroke patients.²⁶⁴ The improvements in the analysis techniques conducted on interhemispheric connectivity were critical in identifying the basis of the physiological differences responsible for this condition by eliminating motion artifacts in stroke patients.²⁶⁵ The frequency-domain system allowed the calculations of the absolute values of HbT and hemoglobin oxygen saturation, which facilitated the identification of the impaired site in stroke patients.²⁶⁶ Restless leg syndrome patients with periodic limb movements (PLM) during sleep, who may be at a high risk of developing stroke, showed increased HbO and HbR levels while sleeping when compared to healthy persons.²⁶⁷ The cerebral autoregulation measured via coupling between HbO levels and average arterial pressure illustrated the impairment in poststroke patients as compared to healthy persons.²⁶⁸ The optical path length was different due to impairments in ischemic stroke patients, thereby illustrating the change in tissue characteristics.²⁶⁹ A wireless and mobile fNIRS device facilitated the early detection of stroke symptoms by revealing reduced cerebral oxygenation in

the affected hemisphere, as measured conventionally using perfusion computed tomography and perfusion-weighted magnetic resonance imaging.²⁷⁰ The effective connectivity in multiple frequency bands detected by examining HbO signals was reduced or diminished in patients with cerebral infarction as compared to healthy persons.²⁷¹ The time-domain system was able to measure significant differences in HbO and HbR values in large vessel occlusion stroke patients as compared to healthy persons, and this difference was correlated with the impairment condition.²⁷²

11.2. Walking task

Walking on a treadmill with body weight support resulted in a higher HbO response in the sensorimotor region of stroke patients.²⁷³ During the motor rehabilitation of stroke patients, instead of a simple walking task, a dual-task that involved walking while counting backward was an efficient technique as it resulted in a better HbO response.²⁷⁴ While comparing the effects of dual-task walking to those of cognitive or motor tasks, both were effective for cortical activation, but they attenuated the gait performance in poststroke patients.²⁷⁵ The poststroke patients exhibited hyperactivation in the PFC during a dual-task involving walking along with a cognitive task, and the HbO levels may become saturated while walking over obstacles demonstrating the full utilization of resources.²⁷⁶ A dual-task involving walking during calculation revealed that HbO activation in the PFC was linked with physical performance in stroke patients while it was linked with cognitive performance in healthy persons, thereby revealing a different prioritization trend between patients and healthy persons.²⁷⁷

11.3. Hand/finger movement task

Electromyography-triggered functional electrical stimulation accompanied by voluntary movements of fingers and wrists resulted in better activation as compared to that of voluntary movements or of electric stimulation individually.²⁷⁸ The cortical activation in the precuneus region in stroke patients was linked to mirror therapy, and it could be used to determine the efficacy of the therapy.²⁷⁹ In a longitudinal study, revascularization surgeries performed on stroke patients resulted in improvements as compared to the levels before surgery, the CBF

Table 10. Stroke.

Manuscript	Experimental population	Brain area under study	Instrument	No. of channels/ separation(s)	Analyzed parameters
Resting state Muehlschlegel <i>et al.</i> ²⁶¹ (2009)	9 Healthy individuals (6 F and 3 M), 63 ± 8 yrs; 9 Stroke patients (4 F and 5 M), 67 ± 12 yrs	Injured area symmetrical location of other hemisphere	NIRS2	4 cm	Optical density Cardiac Respiratory
Taussky <i>et al.</i> ²⁶² (2012)	8 Stroke (6 F and 2 M), 47–86 yrs	Frontal region	Casmed	2/4–5 cm	CBF
Phillip <i>et al.</i> ²⁶³ (2013)	16 Stroke patients (2 F and 14 M), 54–78 yrs	Frontal region	NIRS2	2/3 cm	HbO
Dutta <i>et al.</i> ²⁶⁴ (2015)	4 Stroke patients (1 F and 3 M), 31–76 yrs	Central site Cz		4/2.5 cm	HbO HbR HbT
Selb <i>et al.</i> ²⁶⁵ (2015)	46 Healthy individuals, 47 ± 13 yrs; 36 Stroke patients, 66 ± 14 yrs	Frontal region	CW6	2/3 cm	HbO
Moreau <i>et al.</i> ²⁶⁶ (2016)	11 Healthy individuals (5 F and 6 M), Median age 43 yrs; 5 Stroke patients (3 F and 2 M), Median age 64 yrs; 5 Cadaver, Median age 75 yrs	Frontal lobe, Broca's area, Rolandic sulcus, superior frontal gyrus, parietal region and Wernicke's area	OxiplexTS	1/2–3.5 cm	HbO HbR
Byun <i>et al.</i> ²⁶⁷ (2016)	4 Healthy individuals (F), 43–58 yrs; 4 Restless leg syndrome (F), 52–57 yrs	Frontal region	Lab made system	2/3 cm	HbO HbR
Su <i>et al.</i> ²⁶⁸ (2018)	17 Healthy individuals (8 F and 9 M), 51.8 ± 7.9 yrs; 8 Right hemiparesis patients (2 F and 6 M), 53.2 ± 12.6 yrs; 9 Left hemiparesis patients (1 F and 8 M), 57.2 ± 9.1 yrs	Bilateral prefrontal, parietal, and occipital lobes	NirScan	24/3 cm	HbO
Sato <i>et al.</i> ²⁶⁹ (2018)	5 Stroke patients (3 F and 2 M), 18–85 yrs	Bilateral frontal and temporal areas	TRS-20		HbO HbR HbT StO ₂

Table 10. (Continued)

Manuscript	Experimental population	Brain area under study	Instrument	No. of channels/ separation(s)	Analyzed parameters
Kwon <i>et al.</i> ²⁶⁹ (2018)	9 Stroke patients (3 F and 6 M), 51–90 yrs	Prefrontal region	NIRSIT	204	HbO HbR SO ₂
Liu <i>et al.</i> ²⁷¹ (2018)	11 Healthy individuals (6 F and 5 M), 65 ± 6.3 yrs; 11 Stroke patients (5 F and 6 M), 72 ± 7.6 yrs	Prefrontal lobe and motor sections	NirScan	10/3 cm	HbO HbR
Giacalone <i>et al.</i> ²⁷² (2019)	5 Lacunar syndrome patients, 75.4 ± 5.4 yrs; 18 Recanalized syndrome patients, 76 ± 9.6 yrs; 18 Nonrecanalized syndrome patients, 76.3 ± 13.4 yrs	Bilateral frontal, central, and parietal regions	Lab made system		HbO HbR HbT StO ₂
Walking task					
Miyai <i>et al.</i> ²⁷³ (2006)	5 Healthy individuals (2 F and 3 M), 53 ± 11 yrs; 6 Stroke patients (1 F and 5 M), 57 ± 6 yrs	Bilateral frontoparietal cortices	OMM-2001	36/3 cm	HbO
Al-Yahya <i>et al.</i> ²⁷⁴ (2016)	20 Healthy individuals (8 F and 12 M), 54.35 ± 9.38 yrs; 19 Stroke patients (2 F and 17 M), 59.61 ± 15.03 yrs	Prefrontal cortex	Oxymon Mk III	8/3 cm	HbO HbR
Liu <i>et al.</i> ²⁷⁵ (2018)	23 Stroke (2 F and 21 M), 51.5 ± 10.7 yrs	Bilateral prefrontal cortex and motor areas	NIRSport	14/3 cm	HbO HbR
Hawkins <i>et al.</i> ²⁷⁶ (2018)	15 Healthy individuals (8 F and 7 M), 77.2 ± 5.6 yrs; 9 Healthy young individuals (5 F and 4 M), 22.4 ± 3.21 yrs; 24 Stroke patients (8 F and 16 M), 58.0 ± 9.3 yrs	Left and right anterior prefrontal cortices	Niro 200NX	2/3 cm	HbO HbR
Mori <i>et al.</i> ²⁷⁷ (2018)	14 Healthy individuals (3 F and 11 M), 66.3 ± 13.3 yrs; 14 Stroke (2 F and 12 M), 61.1 ± 9.3 yrs	Prefrontal cortex	WOT™	16/3 cm	HbO

Table 10. (Continued)

Manuscript	Experimental population	Brain area under study	Instrument	No. of channels/ separation(s)	Analyzed parameters
Hand/finger movement task					
Hara <i>et al.</i> ²⁷⁸ (2013)	16 Stroke patients (3 F and 13 M), 18–73 (mean 49) yrs;	Primary sensory motor cortex	ETG-4000	24/3 cm	HbO
Brunetti <i>et al.</i> ²⁷⁹ (2015)	11 Stroke patients (4 F and 7 M), 49–74 (mean 66) yrs	Bilateral occipito- parietal and precentral areas	NIRScout	24/2.5, 3 cm	HbO HbR
Shidoh <i>et al.</i> ²⁸⁰ (2015)	3 Healthy individuals (1 F and 2 M), (mean 33) yrs; 8 Stroke patients (1 F and 7 M), (mean 64.25) yrs;	Primary motor cortex	OMM3000	3 cm	HbO HbR HbT
Tamashiro <i>et al.</i> ²⁸¹ (2019)	59 Stroke patients (20 F and 39 M), (mean 61.1) yrs	Frontal, sensory-motor and motor areas	FOIRE-3000	49/3 cm	HbO
Cycling task					
Lin <i>et al.</i> ²⁸² (2013)	17 Stroke patients (1 F and 16 M), 55.53 ± 12.06 yrs	Sensory-motor and motor areas	Imagent	20/3 cm	HbO
Lo <i>et al.</i> ²⁸³ (2018)	9 Stroke patients (4 F and 5 M), 53–75 yrs	Sensory and motor areas	NIRScout	28	HbO
Robot-assisted elbow movement					
Saita <i>et al.</i> ²⁸⁴ (2017)	7 Stroke patients (4 F and 3 M), 60.6 ± 8.4 yrs;	Bilateral frontal and parietal areas	FOIRE-3000	48	HbO HbR
Saita <i>et al.</i> ²⁸⁵ (2018)	10 Stroke patients (2 F and 8 M), 66.8 ± 12.0 yrs	Bilateral frontal and parietal areas	FOIRE-3000	48	HbO HbR
Balancing task					
Mihara <i>et al.</i> ²⁸⁶ (2012)	20 Stroke patients (5 F and 15 M), 61.6 ± 11.9 yrs	Frontoparietal region	OMM-3000	50/3 cm	HbO HbR
Oxygen inhalation task					
Ebihara <i>et al.</i> ²⁸⁷ (2012)	30 Healthy individuals (5 F and 25 M), 22–56 yrs 33 Stroke patients (4 F and 29 M), 58–78 yrs	Bilateral fronto- temporal areas	ETG-4000	48/3 cm	HbO HbR
Lower limb movement task					
Rea <i>et al.</i> ²⁸⁸ (2014)	7 Stroke patients (3 F and 4 M), 54.7 ± 14.10 yrs	Bilateral frontal, motor, and sensory areas	ETG-4000	48/3 cm	HbO HbR HbT

Table 10. (Continued)

Manuscript	Experimental population	Brain area under study	Instrument	No. of channels/ separation(s)	Analyzed parameters
Swallowing task Kober <i>et al.</i> ²⁸⁹ (2015)	7 Stroke patients (3 F and 4 M), 68–80 yrs	Bilateral inferior frontal gyrus	NIRSport 88	20/3 cm	HbO HbR
Word repetition task Hara <i>et al.</i> ²⁹⁰ (2017)	8 Stroke patients (2 F and 6 M), 42–75 yrs	Bilateral inferior frontal gyrus	SMARTNIRS	48	HbO
Design and verbal fluency task Saita <i>et al.</i> ²⁹¹ (2017)	58 yrs M vertigo and ataxia, 74 yrs F stroke	Prefrontal region	FOIRE	48	HbO
Tilt-table task Moriya <i>et al.</i> ²⁹² (2018)	8 Stroke patients (6 F and 2 M), 70.8 ± 11.8 yrs	Bilateral prefrontal cortex	Pocket NIRS Duo	2/3 cm	HbO

increased when measured after two weeks and again three months after surgery.²⁸⁰ The right-handed stroke patients with an impairment in the right hemisphere and vice versa exhibited better motor recovery owing to a combination therapy of low-frequency repetitive transcranial magnetic stimulation and intensive occupational therapy in the left (unaffected) hemisphere.²⁸¹

11.4. *Cycling task*

The rehabilitation of stroke patients via cycling resulted in better cortical activation in the premotor cortex and in better physical performance in response to providing them feedback on their speed.²⁸² Comparing the electrical stimulation intensity during the rehabilitation of stroke patients while they were performing the cycling task, an intensity of 10 mA resulted in better cortical excitations compared to a higher intensity of 30 mA.²⁸³

11.5. *Robot-assisted elbow movement*

In poststroke patients, the combination of robot-assisted rehabilitation therapy and botulinum toxin A injections was effective as the HbO response in the primary sensorimotor region was improved when examined after two weeks and again after four months.²⁸⁴ The task-related cortical activity was significantly improved on providing biofeedback to the subjects as the robot changed the color of light based on the patient's performance.²⁸⁵

11.6. *Balancing task*

During a balancing task, stroke patients exhibited cortical activation in the bilateral prefrontal, premotor, and parietal regions similar to that of healthy persons, thereby illustrating no functional reorganization in the brain, yet the activation was smaller in the affected areas of the brain.²⁸⁶

11.7. *Oxygen inhalation task*

The patients with cerebral ischemia showed reduced weights via PCA of the HbO responses in impaired regions as compared to those in normal regions.²⁸⁷

11.8. *Lower limb movement task*

The HbT responses utilized in a linear discriminant analysis (LDA) revealed a significant discrimination

in the movements between the paretic and non-paretic limbs of stroke patients.²⁸⁸

11.9. *Swallowing task*

Compared to the observed responses in healthy persons, the stroke patients showed prolonged HbO and HbR responses while actively swallowing saliva or imagining swallow.²⁸⁹

11.10. *Word repetition task*

During a language task, stroke patients received repetitive transcranial magnetic stimulations on the opposite hemisphere from the activated hemisphere, and poststroke patients received intensive speech therapy to improve the cortical excitations and language function.²⁹⁰

11.11. *Design and verbal fluency task*

During two case studies on stroke patients, due to visuospatial and language functions, marginal cortical activations were exhibited only in the unaffected hemisphere.²⁹¹

11.12. *Tilt-table task*

The poststroke patients with right-lateralized PFC activation at rest exhibited increased HbO levels in the PFC during a tilting task whereas the patients with left-lateralized HbO responses exhibited a decrease in HbO levels during this task.²⁹²

12. *Traumatic Brain Injury*

Traumatic brain injury (TBI) results from accidents that subject the brain to sudden damage due to an injury to the head. The most common causes of TBI are traffic accidents, falls, and sports injuries. A TBI patient can suffer from a wide range of physiological and psychological symptoms based on the affected location of the brain, and the impairments can last for short, long, or even life-long periods. The symptoms can appear immediately, or in some cases, they may appear after some days or weeks. The treatments for TBI involve rest, medication, and/or surgery in some cases. The fNIRS has been used to study the hemodynamic responses associated with the various types of symptoms caused by

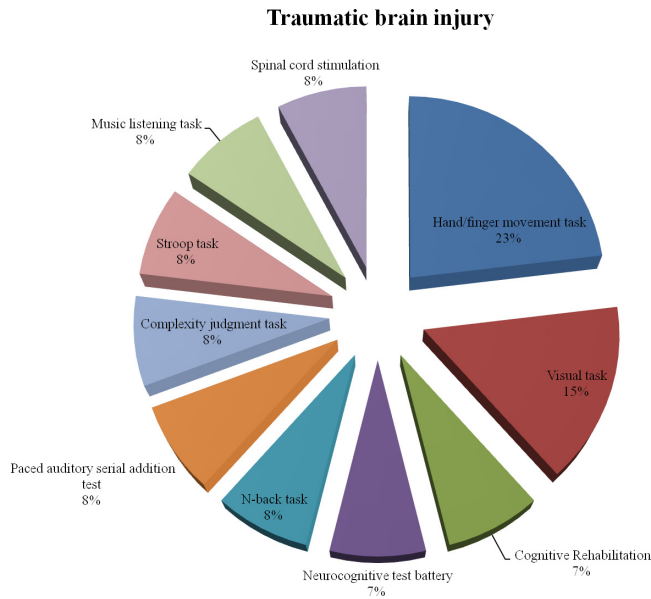


Fig. 11. Task-based distribution of studies on traumatic brain injury (total studies: 13).

TBI. Figure 11 presents the task-wise distribution of the works, and Table 11 outlines them.

12.1. Hand/finger movement task

The patients with TBI showed lower cerebral oxygenation, but a similar blood volume in the left PFC during a right-hand gripping task when compared to healthy persons.²⁹³ Children with concussion exhibited a reduced HbT and HbO coherence exhibiting impaired interhemispheric connectivity when compared to healthy children during a finger-tapping task.²⁹⁴ Compared to healthy persons, the patients with mild TBI also showed lower functional connectivity that was inversely linked with impairment intensity, and the difference in connectivity was more pronounced during the task period as compared to the resting state.²⁹⁵

12.2. Visual task

The TBI patients exhibited a reduced HbO response in the bilateral dorsolateral PFC during an attention task when compared to healthy persons, thereby revealing the impaired intentional networks.²⁹⁶ The patients with sports-related concussions showed a higher hemodynamic response in the frontal regions and a strong interhemispheric correlation in the occipital cortex when compared to healthy persons.²⁹⁷

12.3. Cognitive rehabilitation

While undergoing training involving nine cognitive tasks, the TBI patients showed similar HbO responses in the lateral frontal regions and a higher HbO response in the medial frontal regions when compared to healthy persons.²⁹⁸

12.4. Neurocognitive test battery

The patients with sport-related concussions showed reduced cortical activations in the affected areas during a computerized test involving various working memory tasks compared to healthy persons.²⁹⁹

12.5. N-back task

During a working memory task, the analysis of HbO, HbR, and HbT responses in TBI patients revealed significant differences compared to those of healthy persons even though the behavioral performance was similar.³⁰⁰

12.6. Paced auditory serial addition test

The cortical activation regions were different in TBI patients compared to healthy persons during the task with or without distraction, thereby revealing poor inhibitory control.³⁰¹

12.7. Complexity judgment task

The oxygenation variability index measured via the HbO and HbR values resulted in high sensitivity in differentiating TBI patients from healthy persons during various levels of complexity judgment.³⁰²

12.8. Stroop task

An increase in neural activation was observed in healthy persons by increasing the cognitive demand while the TBI patients achieved higher activations while performing more straightforward tasks, thereby revealing the impaired frontal lobe efficiency.³⁰³

12.9. Music listening task

A vector phase analysis conducted during music identification with or without distraction revealed

Table 11. Traumatic brain injury.

Manuscript	Experimental population	Brain area under study	Instrument	No. of channels/ separation(s)	Analyzed parameters
Hand/finger movement task Bhambhani <i>et al.</i> ²⁹³ (2006)	13 Healthy individuals (5 F and 8 M), 31.5 ± 4.5 yrs; 25 TBI patients (21 F and 4 M), 31.6 ± 9.8 yrs	Left prefrontal lobe	MRM91	2/4 cm	HbO HbR HbT
Urban <i>et al.</i> ²⁹⁴ (2015)	8 Healthy individuals (3 F and 5 M), 14.0 ± 2.2 yrs; 12 TBI patients (6 F and 6 M), 15.3 ± 1.9 yrs	Motor cortex	CW5	14/2 cm	HbO HbT
Hoeke <i>et al.</i> ²⁹⁵ (2018)	12 Healthy individuals (9 F and 3 M), 30 ± 11 yrs; 12 TBI patients (7 F and 5 M), 29 ± 10 yrs	Dorsolateral PFC and primary motor cortex	CW7	24/3 cm	HbO
Visual task					
Merzagora <i>et al.</i> ²⁹⁶ (2011)	11 Healthy individuals, 32 ± 15 yrs; 5 TBI patients, 41 ± 10 yrs	Frontal cortex	Lab developed system	16/2.5 cm	HbO HbR
Wu <i>et al.</i> ²⁹⁷ (2018)	27 Healthy individuals (11 F and 16 M), 21.5 ± 2.50 yrs; 27 TBI patients (11 F and 16 M), 20.5 ± 2.28 yrs	Bilateral middle frontal gyri, calcarine gyri, and inferior occipital cortices	CW6	24/1,3 cm	HbO
Cognitive Rehabilitation					
Hibino <i>et al.</i> ²⁹⁸ (2013)	47 Healthy individuals (32 F and 15 M), 20.5 ± 2.2 yrs; 9 TBI patients (3 F and 6 M), 28.1 ± 7.4 yrs	Bilateral and mid frontal regions	FOIRE-3000	47/3 cm	HbO
Neurocognitive test battery					
Kontos <i>et al.</i> ²⁹⁹ (2014)	5 Healthy individuals (4 F and 1 M), 22.00 ± 0.28 yrs; 9 TBI (4 F and 5 M), 22.73 ± 1.32 yrs	Bilateral frontal and temporal regions	CW6	32/3.2 cm	HbO HbR
N-back task					
Merzagora <i>et al.</i> ³⁰⁰ (2014)	11 Healthy individuals, 31 ± 13 yrs; 6 TBI patients, 42 ± 10 yrs	PFC	Lab developed system	16/2.5 cm	HbO HbR HbT

Table 11. (Continued)

Manuscript	Experimental population	Brain area under study	Instrument	No. of channels/ separation(s)	Analyzed parameters
Paced auditory serial addition test					
Sawamura <i>et al.</i> ³⁰¹ (2014)	10 Healthy individuals (3 F and 7 M), 31.6 ± 3.9 yrs; 10 TBI patients (3 F and 7 M), 34.9 ± 6.9 yrs	PFC and primary auditory cortex	LABNIRS	52/3 cm	HbO
Complexity judgment task					
Chernomordik <i>et al.</i> ³⁰² (2016)	14 Healthy individuals (4 F and 10 M), 35 ± 3 yrs; 29 TBI patients (6 F and 23 M), 37 ± 2 yrs	PFC	fNIR Devices	16/3 cm	HbO HbR
Stroop task					
Plenger <i>et al.</i> ³⁰³ (2016)	13 Healthy individuals (6 F and 7 M), 38.8 ± 10.9 yrs; 14 TBI patients (1 F and 13 M), 39.8 ± 15.1 yrs	Bilateral frontal, temporal, and mid to inferior parietal areas	ETG-4000	52/3 cm	HbO
Music listening task					
Jeong <i>et al.</i> ³⁰⁴ (2018)	22 Healthy individuals, 55.7 ± 5.98 yrs; 15 TBI patients, 53.60 ± 8.88 yrs	Frontopolar region	OEG-16	16	HbO HbR
Spinal cord stimulation					
Zhang <i>et al.</i> ³⁰⁵ (2018)	9 Consciousness disorder patients (4 F and 5 M), 17–64 yrs	Prefrontal and occipital areas	Lab developed system	8/3 cm	HbO HbR

that frequent oxygen exchanges in the left dorso-lateral PFC of TBI patients were responsible for auditory attention deficits.³⁰⁴

12.10. Spinal cord stimulation

The patients with disorders in consciousness due to TBI exhibited that a shorter interstimulus interval of spinal cord stimulation resulted in higher HbT levels in the PFC, implying a higher level of awareness of the patients.³⁰⁵

13. Discussion and Future Implications

In this paper, we summarized the studies conducted on notable diseases using fNIRS as a neuroimaging tool. Such notable diseases were examined/included only when we could find more than 10 studies involving a patient population.

13.1. Preprocessing of fNIRS signals

Compared to fMRI, a well-established modality, fNIRS, is still a growing modality for understanding neuronal activities. The methods adopted to examine hemodynamic changes via fNIRS are diverse, and it has been eagerly proposed that a standard procedure should be followed.³⁰⁶ If studies follow a standard data processing pipeline, they can be compared, and a verifiable knowledge database can be established. The acquired raw fNIRS data are affected by various noise sources like physiological (respiratory, cardiac, Mayer waves, etc.), environmental (ambient light, subject movement, source/detector attached to the scalp, etc.), and instrumental ones (sensor noise, communication noise, line noise, etc.). The details of the noises and their properties can be found in the literature.³⁰⁷ These noises reduce the signal-to-noise ratio of the desired signal, and they can override the neuronal activation for the task performed following an experimental paradigm not carefully designed.^{306,308} Therefore, the removal of these noises to obtain a clean fNIRS signal is a pivotal step. Various techniques are employed to remove them as they are identified by their approximate frequencies like cardiac (1 Hz), respiratory (0.3 Hz), and Mayer waves (0.1 Hz). Mostly digital filters are used to remove these frequency bands from the raw signals. Two types of filtering are commonly used: A band-pass filter (used to retain a frequency range from the

signal while discarding the remaining part) and a low-pass filter (used to remove the high-frequency part beyond a certain frequency). Some researchers prefer to use a filter on the light-intensity signals while others use on the hemodynamic signals.³⁰⁶ In the recent past, the use of short-separation channels to remove the extracerebral effects is gaining attention. The short-separation channels are configured by making the source–detector separation lower than 10 mm.³⁰⁹ The NIR light in these channels does not penetrate deep enough and is considered to carry information only from the superficial layer.³¹⁰ The maximal source–detector separation was found to be 8.4 mm for a typical adult brain, and 2.15 mm was most suitable for an infant brain.³¹¹ If the distance for short-separation channels is not carefully configured, the information from the gray matter is also included.³¹² In some research, the information from short-separation channels were included in a regressor to clean the fNIRS signal. But, its utilization globally across the surface of a head is critically argued due to the heterogeneous response of scalp.^{313,314} One notable idea is to use two short-separation channels in the regression equation; one at the source side and the other at the detector side.³¹⁵

The experiments conducted on patient populations are more critical and yet are more prone to motion artifacts due to patient conditions.^{90,265} The removal of motion artifacts from the raw signals is necessary along with physiological noises for further processing.³¹⁶ The signal is largely affected by motion artifacts in the case of newborns as they are more prone to movement during the experiment resulting in data loss.^{317,318} Threshold levels were defined for signal changes to discard motion artifacts due to infant head movements.^{319,320} Many research works are being carried out on infants to understand the developing brain. The hemodynamic response of infants has been reported to alter from adults, which can be due to the effect of various variables like stimulus complexity and experimental designs.³²¹ If the duration of an experimental study is long, the patients are more likely to move during the test. The experimental design should also be planned critically to hold the patient's attention while performing the tasks without burdening or boring them, which result in mind wandering-based activations.³²² The duration of the initial baseline, task duration, and the rest period between multiple tasks should be considered

carefully as the hemodynamic response is a slow process that takes time to revert to the baseline after activation.³²³ The positioning of patients is also an important aspect during the experiment and ensuring that the patients are in similar postures improves the fNIRS data.^{229,264,324}

13.2. Processing of fNIRS signals

There have been different analyses performed on hemodynamic variables. The fNIRS systems have the capability to provide HbO, HbR, and HbT values instead of only HbR values that are acquired via fMRI. Many researchers employ HbO values to conduct their analyses with the justification that these values have a more direct relationship with cortical activations and can facilitate understanding them better.^{18–22,25,121,169,170,263} The fNIRS variables have multiple data embedded in them that can be extracted by various signal processing techniques, which range from various filtering adaptive filtering methods to signal complexity analyses, such as entropy analyses.^{228,229,325,326} Researchers have utilized fNIRS variables to extract several biomarkers for the classification and identification of diseases, such as low-frequency oscillations, heart rate, CBV, CBF, TOI, Cytos, and cerebral oxygen exchange.^{75,230,261–263,267,302} The features of fNIRS variables that consist of, but are not limited to, peak, mean, skewness, variance, slope, kurtosis, standard deviation, number of peaks, sum of peaks, root mean square, and median are frequently utilized in classification algorithms like LDA, SVM, extreme machine learning, Bayes classifiers, and neural networks.^{13,327,328}

The processing of fNIRS signals is usually done by the user's choice by mostly utilizing the software provided by the device manufacturer without having a deep understanding of the underlying methods.³²⁹ The results are largely affected by the choice of procedure employed. The recommended procedure is to use a standardized preprocessing pipeline and do personalized processing to get the required information. In most studies, the authors write their codes/routines for their own purposes. Instead, to facilitate the processing of fNIRS signals, various tools have been developed. HomER and NIRS-SPM are the most commonly utilized software packages in the fNIRS community that allow device-independent analyses of the signals.^{330,331} Other important tools

being used are fOSA, NAP, FC-NIRS, NinPy, NIRS brain AnalyzIR, ICNNA, and GRETNA, which have allowed fNIRS practitioners to explore many aspects of brain development, behavior, and pathologies.^{332–338} The utilization of advanced signal processing and adaptive control algorithms in the future can be helpful to achieve earlier detection of the hemodynamic response not to mention the accuracy.^{11,339–343}

13.3. Channel localization

Patients are usually classified based on the impaired hemodynamic responses caused due to some disease.^{128–133} The localization of an impairment in the brain is a vital step to evaluate the intensity and type of the disease. Therefore, the placement of fNIRS sources, detectors, or optodes on a patient's head based on the task involved is important as most tasks are associated with known brain regions.^{8,344} Unlike fMRI, fNIRS does not allow for structural imaging, which makes it difficult to compare studies using different channel configurations and placements. Therefore, a standardized placement system should be followed like the EEG electrode placement such as the 10–20, 10–10, or 10–5 systems so that the findings are comparable and reproducible among studies and subjects.^{9,345,346} Another method for standardized locations is to involve the brain's structural information by utilizing an fMRI scanner to select the locations for fNIRS channels initially.³⁴⁷ The involvement of an fMRI scanner diminishes the advantages of utilizing fNIRS for neuroimaging and adds extra burden to the subject under study.³⁴⁸ A useful approach for identifying the channel locations that are similar to fMRI using the Montreal Neurological Institute coordinate system is the utilization of a 3D digitizer to cast the fNIRS channels to a brain atlas.³⁴⁹ A recently developed toolbox recommends the placement of optodes based on the desired location of the brain.³⁵⁰ Most studies reviewed in this paper utilized an EEG location system, while the utilization of fMRI and a digitizer together was rare.^{98,103,107,212} The most probable reason for this is the involvement of the extra cost of equipment and the extra time consumption for the subject as well as for the experiment conductor. Forming a channel for fNIRS is also associated with the distance between the

light source and photodetector. The achieved depth of an fNIRS channel can vary with variations in the source–detector separation. While most of the studies measured the fNIRS signal with a 3-cm separation, variations of 2–5 cm were observed.^{96,97,109} The headgears/caps are also provided by the system manufacturers, therefore, in most cases, these headgears/caps are used to place and hold the optodes at a fixed distance of 3 cm.^{28–34,121,194–199,224,241,242} It is recommended to use a channel separation of 2 cm for children and infants due to smaller head size and the resulting reduced width between superficial layers.^{23,42,167,294}

13.4. Channel resolution and limitation

The limited number of optodes available on fNIRS machines and the resulting number of channels are still not sufficient to study the changes in the brain. Few studies could examine most of the brain regions.^{85,91,104,108,229} Neuronal activations occurring in response to a single task are not linked to a single brain location.³⁵¹ Therefore, the outcomes of the studies that focus on a specific narrow location in the brain might not be sufficient for understanding the brain functions. Brain functional reorganization happens when a certain portion of the brain is impaired.^{98,286} Therefore, studying multiple brain areas is important to understand the underlying changes occurring in patients' brains.^{30–34,79,121,236,266,272} Functional and effective connectivity analyses are useful to understand the processing that takes place in the human brain, and covering more brain areas will allow for better understanding based on the experimental conditions.^{4,271,295–297,352} The bundled optode approach that creates hundreds of channels at different brain depths with high spatial resolution can assuredly assist in the creation of 3D images via fNIRS, which can be compared with those created via fMRI.⁷ This technique involves spatially resolved spectroscopy that utilizes multidistance channel formation among groups of sources and detectors placed as close to each other as possible.³⁵³ The resultant number of channels will be in the thousands compared to the maximum of a few hundred that is possible using the present state-of-the-art systems. This technique will open the gates to machine learning-based signal processing algorithms that are commonly used for large datasets like neural

networks and many others.^{354,355} It will facilitate the quick expansion of the research scope via fNIRS, which will help in further revealing the currently hidden patterns and properties of hemodynamics. Although physical constraints do not allow fNIRS to penetrate beyond a specific depth, however, it can be used as an alternative technology for limited brain depth imaging. Therefore, new fNIRS systems with an extensive number of optodes should be developed to assist in examining the full brain with high spatial and temporal resolutions. Most of the available commercial device manufacturers do not allow the configuration of short-separation channels in their fixed optode holders.³²⁹ The integration of short-separation channels by manufacturers is recommended as it is one of the important methods for getting a clean fNIRS signal.

13.5. The fNIRS-based brain–computer interface

The utilization of fNIRS in diagnosing and classification of various diseases has been established and covered in this paper. The importance of BCI in the healthcare industry is critical, especially for aggravated conditioned patients with physical disabilities. fNIRS has been used as a neuroimaging modality in developing BCIs due to its various benefits.³⁵⁶ As the hemodynamics signal has inherently slow nature, the light intensity signals of fNIRS known as fast optical signals were explored in comparison to the event-related potentials of EEG.³⁵⁷ The quality and reliability of fast optical signals are still very low, and further research with stable results is required for practical applications. The classification of fNIRS signals has been a challenging task and normally averaged samples are used for classification, yet researchers have showed promising results for single-trial as well as online classification of VFT, Stroop task, and resting state.^{358–361} Promising research has been done to reduce the time delay in fNIRS activity detection.^{12,362} The BCI usually involves imagining of tasks to generate brain activity, which can be utilized for command generation. Imagining “yes” or “no” can be a very basic imagining task that could be suitable for a wide range of patients and the classification accuracy for this task was reported to be significant for most users.³⁶³ Motor imagery is popularly used in BCIs as imagination of movement

of limbs produces reliable hemodynamic response, which is comparable to the hemodynamic response of actual limb movement.³⁶⁴ The neuronal activity generation due to motor imagery was found to be enhanced with visual feedback during a robot movement control using motor imagery.³⁶⁵ The acquisition of data from a realistic environment and its processing are vital for the development of BCI.^{366,367} Research on the mental states and neuroergonomics of pilots during actual as well as simulated environment was conducted using fNIRS.^{368,369} Satisfactory results from these studies strengthened the use of fNIRS in BCI applications. The understanding of encoding and decoding of neuronal activation is important in developing BCI applications to complement the neural encoding and decoding being used in medical robotics research which use nerve-machine interfaces.³⁷⁰⁻³⁷⁴

13.6. Tasks for fNIRS signals

Various tasks have been used to understand the deficits related to the PFC. The covered studies in this paper reveal that the VFT was the most widely used task in understanding the impaired activation of the diseased population. The VFT has demonstrated efficient performance levels in distinguishing healthy participants from a mixed population of patients and healthy persons.^{96,191,208,209} The cortical activations in response to VFTs in a hybrid population comprising of patients affected by multiple diseases were used to differentiate patients of one disease from another as well as to generate information of the disease severity.^{28,113,116,118,125,179,181-183} Different working memory tasks have been used to perceive the neuronal activations associated with various diseases using multiple task loads.^{52,200,232} Various studies involving electric and magnetic stimulations have been conducted and have described the effects of stimulation during rehabilitation therapy on hemodynamic responses, thereby demonstrating the beneficial nature of fNIRS.^{9,105,199,250-252,264,290,375,376} The fNIRS captures optical intensity signals via photodetectors, which are unaltered by electric and magnetic fields. Therefore, fNIRS is a more suitable neuroimaging modality for evaluating the effects of rehabilitation in the brain compared to fMRI and EEG. This paper presents widely utilized tasks associated with each disease that can serve as a guideline for future classification studies. Also, it

suggests new possible directions for research on a specific disease that may have been followed for another disease.

14. Conclusions

In this paper, we reviewed studies involving patient populations that used fNIRS to examine mental/physical impairments. The fNIRS is a portable neuroimaging modality that has been extensively employed to evaluate and classify various diseases. By the broad utilization of fNIRS, it is evident that this technology is appropriate to examine neuronal behavior of healthy subjects as well as patients.

This paper described briefly the significant findings associated with impaired neuronal activations that were specific to tasks and mental disorders. We indicated the tasks that could be used to show significant cortical activations in diseased populations. Distinct patterns of activation or low-frequency oscillations were associated with specific diseases and were used for classification. Although the intensity and disease classifications were achieved, yet haphazardness in pre- and post-processing schemes and parameter reporting exists in the literature, which needs to be standardized.

We described the studies that used various channel configurations and significant variations in the resultant number of channels. Most studies restricted their scope to a single brain area while a few studies covered multiple lobes and rarely examined the full head. The constraint on the available number of optodes in currently available commercial fNIRS systems restricts the number of channels with an intermediate spatial resolution. The dense placement of optodes covering the entire surface of the head will allow for superior spatial resolution up to a limited brain depth. The resulting massive number of channels will require new methodologies for processing big fNIRS data. The frequent application of machine learning algorithms on fNIRS data, which is currently not possible due to limited datasets, will be interesting to observe in the future.

Acknowledgments

This work was supported by the National Research Foundation (NRF) of Korea under the auspices of the Ministry of Science and ICT, Republic of Korea (Grant No. NRF-2017R1A2A1A17069430).

References

1. C. Patterson, "World Alzheimer Report 2018: The state of the art of dementia research: New frontiers," Alzheimer's Disease International (ADI), London, UK (2018).
2. S. M. Jyoti, W. G. Besio, K. Mankodiya, "Wearlight: Toward a wearable, configurable functional NIR spectroscopy system for noninvasive neuroimaging," *IEEE Trans. Biomed. Circuits Syst.* **13**, 91–102 (2019).
3. A. Gamma *et al.*, "Comparison of simultaneously recorded [H215O]-PET and LORETA during cognitive and pharmacological activation," *Hum. Brain Mapp.* **22**, 83–96 (2004).
4. M. A. Yaqub, S.-W. Woo, K.-S. Hong, "Effects of HD-tDCS on resting-state functional connectivity in the prefrontal cortex: An fNIRS study," *Complexity* **2018**, 1613402 (2018).
5. B. Chance, Z. Zhuang, C. UnAh, C. Alter, L. Lipton, "Cognition-activated low-frequency modulation of light absorption in human brain," *Proc. Natl. Acad. Sci. U. S. A.* **90**, 3770–3774 (1993).
6. M. R. Bhutta *et al.*, "Note: Three wavelengths near-infrared spectroscopy system for compensating the light absorbance by water," *Rev. Sci. Instrum.* **85**, 026111 (2014).
7. H. D. Nguyen, K.-S. Hong, "Bundled-optode implementation for 3D imaging in functional near-infrared spectroscopy," *Biomed. Opt. Express* **7**, 3491–3507 (2016).
8. K.-S. Hong, M. R. Bhutta, X. Liu, Y. I. Shin, "Classification of somatosensory cortex activities using fNIRS," *Behav. Brain Res.* **333**, 225–234 (2017).
9. X. S. Hu, K.-S. Hong, S. S. Ge, "Reduction of trial-to-trial variability in functional near-infrared spectroscopy signals by accounting for resting-state functional connectivity," *J. Biomed. Opt.* **18**, 017003 (2013).
10. A. Zafar, K.-S. Hong, "Detection and classification of three-class initial dips from prefrontal cortex," *Biomed. Opt. Express* **8**, 367–383 (2016).
11. M. J. Khan, U. Ghafoor, K.-S. Hong, "Early detection of hemodynamic responses using EEG: A hybrid EEG-fNIRS study," *Front. Hum. Neurosci.* **12**, 479 (2018).
12. A. Zafar, K.-S. Hong, "Neuronal activation detection using vector phase analysis with dual threshold circles: A functional near-infrared spectroscopy study," *Int. J. Neural Syst.* **28**, 1850031 (2018).
13. K.-S. Hong, M. J. Khan, M. J. Hong, "Feature extraction and classification methods for hybrid fNIRS-EEG brain-computer interfaces," *Front. Hum. Neurosci.* **12**, 246 (2018).
14. X. Liu, K.-S. Hong, "Detection of primary RGB colors projected on a screen using fNIRS," *J. Innov. Opt. Health Sci.* **10**, 1750006 (2017).
15. M. J. Khan, K.-S. Hong, "Passive BCI based on drowsiness detection: An fNIRS study," *Biomed. Opt. Express* **6**, 4063–4078 (2015).
16. Y. Kita *et al.*, "Self-face recognition in children with autism spectrum disorders: A near-infrared spectroscopy study," *Brain Dev.* **33**, 494–503 (2011).
17. Y. Nakadoi *et al.*, "Multi-channel near-infrared spectroscopy shows reduced activation in the prefrontal cortex during facial expression processing in pervasive developmental disorder," *Psychiatry Clin. Neurosci.* **66**, 26–33 (2012).
18. A. Kajiume, S. Aoyama-Setoyama, Y. Saito-Hori, N. Ishikawa, M. Kobayashi, "Reduced brain activation during imitation and observation of others in children with pervasive developmental disorder: A pilot study," *Behav. Brain Funct.* **9**, 21 (2013).
19. H. Ichikawa *et al.*, "Novel method to classify hemodynamic response obtained using multi-channel fNIRS measurements into two groups: Exploring the combinations of channels," *Front. Hum. Neurosci.* **8**, 480 (2014a).
20. H. Zhu *et al.*, "Atypical prefrontal cortical responses to joint/non-joint attention in children with autism spectrum disorder (ASD): A functional near-infrared spectroscopy study," *Biomed. Opt. Express* **6**, 690–701 (2015).
21. C. E. Jung, L. Strother, D. J. Feil-Seifer, J. J. Hutsler, "Atypical asymmetry for processing human and robot faces in autism revealed by fNIRS," *PLoS One* **11**, e0158804 (2016).
22. N. Liu *et al.*, "Optical-imaging-based neurofeedback to enhance therapeutic intervention in adolescents with autism: Methodology and initial data," *Neurophotonics* **4**, 011003 (2016).
23. S. Lloyd-Fox *et al.*, "Cortical responses before 6 months of life associate with later autism," *Eur. J. Neurosci.* **47**, 736–749 (2018).
24. H. Kuwabara *et al.*, "Decreased prefrontal activation during letter fluency task in adults with pervasive developmental disorders: A near-infrared spectroscopy study," *Behav. Brain Res.* **172**, 272–277 (2006).
25. Y. Kawakubo *et al.*, "Impaired prefrontal hemodynamic maturation in autism and unaffected siblings," *PLoS One* **4**, e6881 (2009).
26. A. Iwanami *et al.*, "Task dependent prefrontal dysfunction in persons with Asperger's disorder investigated with multi-channel near-infrared

- spectroscopy," *Res. Autism Spectr. Disord.* **5**, 1187–1193 (2011).
27. A. Ishii-Takahashi *et al.*, "Prefrontal activation during inhibitory control measured by near-infrared spectroscopy for differentiating between autism spectrum disorders and attention deficit hyperactivity disorder in adults," *NeuroImage-Clin.* **4**, 53–63 (2014).
 28. K. Hirata *et al.*, "Differences in frontotemporal dysfunction during social and non-social cognition tasks between patients with autism spectrum disorder and schizophrenia," *Sci. Rep.* **8**, 3014 (2018).
 29. M. K. Yeung, T. L. Lee, A. S. Chan, "Frontal lobe dysfunction underlies the differential word retrieval impairment in adolescents with high-functioning autism," *Autism Res.* **12**, 600–613 (2019).
 30. Y. Li, D. Yu, "Weak network efficiency in young children with autism spectrum disorder: Evidence from a functional near-infrared spectroscopy study," *Brain Cogn.* **108**, 47–55 (2016).
 31. Y. Li, D. Yu, "Variations of the functional brain network efficiency in a young clinical sample within the autism spectrum: A fNIRS investigation," *Front. Physiol.* **9**, 67 (2018).
 32. Y. Li, H. Jia, D. Yu, "Novel analysis of fNIRS acquired dynamic hemoglobin concentrations: Application in young children with autism spectrum disorder," *Biomed. Opt. Express* **9**, 3694 (2018).
 33. H. Jia, Y. Li, D. Yu, "Attenuation of long-range temporal correlations of neuronal oscillations in young children with autism spectrum disorder," *NeuroImage-Clin.* **20**, 424–432 (2018).
 34. H. Jia, Y. Li, D. Yu, "Normalized spatial complexity analysis of neural signals," *Sci. Rep.* **8**, 7912 (2018).
 35. T. Xiao *et al.*, "Response inhibition impairment in high functioning autism and attention deficit hyperactivity disorder: Evidence from near-infrared spectroscopy data," *PLoS One* **7**, e46569 (2012).
 36. T. Ikeda *et al.*, "Hypoactivation of the right prefrontal cortex underlying motor-related inhibitory deficits in children with autism spectrum disorder: A functional near-infrared spectroscopy study," *Jpn. Psychol. Res.* **60**, 251–264 (2018).
 37. S. Sutoko *et al.*, "Distinct methylphenidate-evoked response measured using functional near-infrared spectroscopy during go/no-go task as a supporting differential diagnostic tool between attention-deficit/hyperactivity disorder and autism spectrum disorder comorbid children," *Front. Hum. Neurosci.* **13**, 7 (2019).
 38. M. Kikuchi *et al.*, "Anterior prefrontal hemodynamic connectivity in conscious 3- to 7-year-old children with typical development and autism spectrum disorder," *PLoS One* **8**, e5608 (2013).
 39. H. Zhu, Y. Fan, H. Guo, D. Huang, S. He, "Reduced interhemispheric functional connectivity of children with autism spectrum disorder: Evidence from functional near infrared spectroscopy studies," *Biomed. Opt. Express* **5**, 1262 (2014).
 40. J. Li *et al.*, "Characterization of autism spectrum disorder with spontaneous hemodynamic activity," *Biomed. Opt. Express* **7**, 3871 (2016).
 41. Y. Minagawa-Kawai *et al.*, "Cerebral laterality for phonemic and prosodic cue decoding in children with autism," *Neuroreport* **20**, 1219–1224 (2009).
 42. Y. Funabiki, T. Murai, M. Toichi, "Cortical activation during attention to sound in autism spectrum disorders," *Res. Dev. Disabil.* **33**, 518–524 (2012).
 43. R. Iwanaga *et al.*, "Usefulness of near-infrared spectroscopy to detect brain dysfunction in children with autism spectrum disorder when inferring the mental state of others," *Psychiatry Clin. Neurosci.* **67**, 203–209 (2013).
 44. K. Mori *et al.*, "Neuroimaging in autism spectrum disorders: 1H-MRS and NIRS study," *J. Med. Invest.* **62**, 29–36 (2015).
 45. K. Yanagisawa, N. Nakamura, H. Tsunashima, N. Narita, "Proposal of auxiliary diagnosis index for autism spectrum disorder using near-infrared spectroscopy," *Neurophotonics* **3**, 031413 (2016).
 46. Y. Inoue *et al.*, "Reduced prefrontal hemodynamic response in children with ADHD during the Go/NoGo task: A NIRS study," *Neuroreport* **23**, 55–60 (2012).
 47. Y. Monden *et al.*, "Clinically-oriented monitoring of acute effects of methylphenidate on cerebral hemodynamics in ADHD children using fNIRS," *Clin. Neurophysiol.* **123**, 1147–1157 (2012).
 48. Y. Monden *et al.*, "Right prefrontal activation as a neuro-functional biomarker for monitoring acute effects of methylphenidate in ADHD children: An fNIRS study," *NeuroImage-Clin.* **1**, 131–140 (2012).
 49. M. Nagashima *et al.*, "Acute neuropharmacological effects of atomoxetine on inhibitory control in ADHD children: A fNIRS study," *NeuroImage-Clin.* **6**, 192–201 (2014).
 50. Y. Monden *et al.*, "Individual classification of ADHD children by right prefrontal hemodynamic responses during a go/no-go task as assessed by fNIRS," *NeuroImage-Clin.* **9**, 1–12 (2015).
 51. S. Miao *et al.*, "Reduced prefrontal cortex activation in children with attention-deficit/hyperactivity disorder during go/no-go task: A functional near-infrared spectroscopy study," *Front. Neurosci.* **11**, 367 (2017).

52. A. C. Ehlis, C. G. Bähne, C. P. Jacob, M. J. Herrmann, A. J. Fallgatter, "Reduced lateral prefrontal activation in adult patients with attention-deficit/hyperactivity disorder (ADHD) during a working memory task: A functional near-infrared spectroscopy (fNIRS) study," *J. Psychiatr. Res.* **42**, 1060–1067 (2008).
53. M. Schecklmann *et al.*, "Working memory and response inhibition as one integral phenotype of adult ADHD? A behavioral and imaging correlational investigation," *J. Atten. Disord.* **17**, 470–482 (2013).
54. Y. Gu *et al.*, "Complexity analysis of fNIRS signals in ADHD children during working memory task," *Sci. Rep.* **7**, 829 (2017).
55. A. Crippa *et al.*, "The utility of a computerized algorithm based on a multi-domain profile of measures for the diagnosis of attention deficit/hyperactivity disorder," *Front. Psychiatry* **8**, 189 (2017).
56. Y. Gu *et al.*, "Identifying ADHD children using hemodynamic responses during a working memory task measured by functional near-infrared spectroscopy," *J. Neural Eng.* **15**, 035005 (2018).
57. S. J. Moser, S. Cutini, P. Weber, M. L. Schroeter, "Right prefrontal brain activation due to Stroop interference is altered in attention-deficit hyperactivity disorder—a functional near-infrared spectroscopy study," *Psychiatry Res. Neuroimaging* **173**, 190–195 (2009).
58. H. Negoro *et al.*, "Prefrontal dysfunction in attention-deficit/hyperactivity disorder as measured by near-infrared spectroscopy," *Child Psychiat. Hum. Dev.* **41**, 193–203 (2010).
59. O. Oner *et al.*, "Association among SNAP-25 Gene Dde I and Mnl I polymorphisms and hemodynamic changes during methylphenidate use: A functional near-infrared spectroscopy study," *J. Atten. Disord.* **15**, 628–637 (2011).
60. A. Yasumura *et al.*, "Neurobehavioral and hemodynamic evaluation of Stroop and reverse Stroop interference in children with attention-deficit/hyperactivity disorder," *Brain Dev.* **36**, 97–106 (2014).
61. A. Ishii-Takahashi *et al.*, "Neuroimaging-aided prediction of the effect of methylphenidate in children with attention-deficit hyperactivity disorder: A randomized controlled trial," *Neuropsychopharmacology* **40**, 2676 (2015).
62. H. Ichikawa *et al.*, "Hemodynamic response of children with attention-deficit and hyperactive disorder (ADHD) to emotional facial expressions," *Neuropsychologia* **63**, 51–58 (2014b).
63. A. M. Marx *et al.*, "Near-infrared spectroscopy (NIRS) neurofeedback as a treatment for children with attention deficit hyperactivity disorder (ADHD): A pilot study," *Front. Hum. Neurosci.* **8**, 1038 (2015).
64. M. Nagashima *et al.*, "Neuropharmacological effect of atomoxetine on attention network in children with attention deficit hyperactivity disorder during oddball paradigms as assessed using functional near-infrared spectroscopy," *Neurophotonics* **1**, 025007 (2014).
65. M. Nagashima *et al.*, "Neuropharmacological effect of methylphenidate on attention network in children with attention deficit hyperactivity disorder during oddball paradigms as assessed using functional near-infrared spectroscopy," *Neurophotonics* **1**, 015001 (2014).
66. M. Schecklmann *et al.*, "Diminished prefrontal oxygenation with normal and above-average verbal fluency performance in adult ADHD," *J. Psychiatr. Res.* **43**, 98–106 (2008).
67. M. Schecklmann *et al.*, "Altered frontal and temporal brain function during olfactory stimulation in adult attention-deficit/hyperactivity disorder," *Neuropsychobiology* **63**, 66–76 (2011).
68. M. Schecklmann *et al.*, "Effects of methylphenidate on olfaction and frontal and temporal brain oxygenation in children with ADHD," *J. Psychiatr. Res.* **45**, 1463–1470 (2011).
69. P. Weber, J. Lutschg, H. Fahnenstich, "Cerebral hemodynamic changes in response to an executive function task in children with attention-deficit hyperactivity disorder measured by near-infrared spectroscopy," *J. Dev. Behav. Pediatr.* **26**, 105–111 (2005).
70. M. Schecklmann *et al.*, "Prefrontal oxygenation during working memory in ADHD," *J. Psychiatr. Res.* **44**, 621–628 (2010).
71. S. Tsujimoto *et al.*, "Increased prefrontal oxygenation related to distractor-resistant working memory in children with attention-deficit/hyperactivity disorder (ADHD)," *Child Psychiat. Hum. Dev.* **44**, 678–688 (2013).
72. A. Araki *et al.*, "Improved prefrontal activity in AD/HD children treated with atomoxetine: A NIRS study," *Brain Dev.* **37**, 76–87 (2015).
73. A. Kochel, F. Schongabner, S. Feierl-Gsodam, A. Schienle, "Processing of affective prosody in boys suffering from attention deficit hyperactivity disorder: A near-infrared spectroscopy study," *Soc. Neurosci.* **10**, 583–591 (2015).
74. A. Villringer *et al.*, "Noninvasive assessment of cerebral hemodynamics and tissue oxygenation during activation of brain cell function in human adults using near infrared spectroscopy," *Adv. Exp. Med. Biol.* **345**, 559–565 (1994).

75. B. J. Steinhoff, G. Herrendorf, C. Kurth, "Ictal near infrared spectroscopy in temporal lobe epilepsy: A pilot study," *Seizure* **5**, 97–101 (1996).
76. P. D. Adelson *et al.*, "Noninvasive continuous monitoring of cerebral oxygenation periictally using near-infrared spectroscopy: A preliminary report," *Epilepsia* **40**, 1484–1489 (1999).
77. D. K. Sokol, O. N. Markand, E. C. Daly, T. G. Luerssen, M. D. Malkoff, "Near infrared spectroscopy (NIRS) distinguishes seizure types," *Seizure* **9**, 323–327 (2000).
78. E. Watanabe *et al.*, "Non-invasive cerebral blood volume measurement during seizures using multi-channel near infrared spectroscopic topography," *J. Biomed. Opt.* **5**, 287–291 (2000).
79. E. Watanabe, Y. Nagahori, Y. Mayanagi, "Focus diagnosis of epilepsy using near-infrared spectroscopy," *Epilepsia* **43**, 50–55 (2002).
80. K. Haginoya *et al.*, "Ictal cerebral haemodynamics of childhood epilepsy measured with near-infrared spectrophotometry," *Brain* **125**, 1960–1971 (2002).
81. K. Buchheim *et al.*, "Decrease in haemoglobin oxygenation during absence seizures in adult humans," *Neurosci. Lett.* **354**, 119–122 (2004).
82. G. A. Diaz, E. Cesaron, I. Alfonso, C. Dunoyer, I. Yaylali, "Near infrared spectroscopy in the management of status epilepticus in a young infant," *Eur. J. Paediatr. Neurol.* **10**, 19–21 (2006).
83. N. Roche-Labarbe *et al.*, "NIRS-measured oxy- and deoxyhemoglobin changes associated with EEG spike-and-wave discharges in children," *Epilepsia* **49**, 1871–1880 (2008).
84. A. Gallagher *et al.*, "Non-invasive pre-surgical investigation of a 10 year-old epileptic boy using simultaneous EEG–NIRS," *Seizure* **17**, 576–582 (2008).
85. D. K. Nguyen *et al.*, "Non-invasive continuous EEG–fNIRS recording of temporal lobe seizures," *Epilepsy Res.* **99**, 112–126 (2012).
86. Y. Sato, M. Fukuda, M. Oishi, A. Shirasawa, Y. Fujii, "Ictal near-infrared spectroscopy and electrocorticography study of supplementary motor area seizures," *J. Biomed. Opt.* **18**, 076022 (2013).
87. D. K. Nguyen *et al.*, "Noninvasive continuous functional near-infrared spectroscopy combined with electroencephalography recording of frontal lobe seizures," *Epilepsia* **54**, 331–340 (2013).
88. K. Peng *et al.*, "fNIRS-EEG study of focal interictal epileptiform discharges," *Epilepsy Res.* **108**, 491–505 (2014).
89. M. Seyal, "Frontal hemodynamic changes precede EEG onset of temporal lobe seizures," *Clin. Neurophysiol.* **125**, 442–448 (2014).
90. M. A. Yucel, J. Selb, D. A. Boas, S. S. Cash, R. J. Cooper, "Reducing motion artifacts for long-term clinical NIRS monitoring using collodion-fixed prism-based optical fibers," *Neuroimage* **85**, 192–201 (2014).
91. P. Pouliot *et al.*, "Hemodynamic changes during posterior epilepsies: An EEG–fNIRS study," *Epilepsy Res.* **108**, 883–890 (2014).
92. P. Monrad *et al.*, "Haemodynamic response associated with both ictal and interictal epileptiform activity using simultaneous video electroencephalography/near infrared spectroscopy in a within-subject study," *J. Near Infrared Spectrosc.* **23**, 209–218 (2015).
93. E. E. Rizki *et al.*, "Determination of epileptic focus side in mesial temporal lobe epilepsy using long-term noninvasive fNIRS/EEG monitoring for pre-surgical evaluation," *Neurophotonics* **2**, 025003 (2015).
94. J. Jeppesen, S. Beniczky, P. Johansen, P. Sidenius, A. Fuglsang-Frederiksen, "Exploring the capability of wireless near infrared spectroscopy as a portable seizure detection device for epilepsy patients," *Seizure* **26**, 43–48 (2015).
95. G. Pellegrino *et al.*, "Hemodynamic response to interictal epileptiform discharges addressed by personalized EEG–fNIRS recordings," *Front. Neurosci.* **10**, 102 (2016).
96. A. Gallagher *et al.*, "Near-infrared spectroscopy as an alternative to the Wada test for language mapping in children, adults and special populations," *Epileptic Disord.* **9**, 241–255 (2007).
97. A. Gallagher *et al.*, "A noninvasive, presurgical expressive and receptive language investigation in a 9-year-old epileptic boy using near-infrared spectroscopy," *Epilepsy Behav.* **12**, 340–346 (2008).
98. P. Vannasing *et al.*, "Potential brain language reorganization in a boy with refractory epilepsy; an fNIRS–EEG and fMRI comparison," *Epilepsy Behav. Case Rep.* **5**, 34–37 (2016).
99. E. Watanabe *et al.*, "Non-invasive assessment of language dominance with near-infrared spectroscopic mapping," *Neurosci. Lett.* **256**, 49–52 (1998).
100. N. F. Watson, C. Dodrill, D. Farrell, M. D. Holmes, J. W. Miller, "Determination of language dominance with near-infrared spectroscopy: Comparison with the intracarotid amobarbital procedure," *Seizure* **13**, 399–402 (2004).
101. T. Ota *et al.*, "Refined analysis of complex language representations by non-invasive neuroimaging techniques," *Br. J. Neurosurg.* **25**, 197–202 (2010).

102. A. Machado *et al.*, "Detection of hemodynamic responses to epileptic activity using simultaneous electro-encephalography (EEG)/near infra-red spectroscopy (NIRS) acquisitions," *Neuroimage* **56**, 114–125 (2011).
103. P. Pouliot *et al.*, "Nonlinear hemodynamic responses in human epilepsy: A multimodal analysis with fNIRS-EEG and fMRI-EEG," *J. Neurosci. Methods* **204**, 326–340 (2012).
104. P. Sirpal, A. Kassab, P. Pouliot, D. K. Nguyen, F. Lesage, "fNIRS improves seizure detection in multimodal EEG-fNIRS recordings," *J. Biomed. Opt.* **24**, 051408 (2019).
105. N. Honda *et al.*, "Reorganization of sensorimotor function after functional hemispherectomy studied using near-infrared spectroscopy," *Pediatr. Neurosurg.* **46**, 313–317 (2009).
106. Y. Sato, M. Oishi, M. Fukuda, Y. Fujii, "Hemodynamic and electrophysiological connectivity in the language system: Simultaneous near-infrared spectroscopy and electrocorticography recordings during cortical stimulation," *Brain Lang.* **123**, 64–67 (2012).
107. E. Visani *et al.*, "Hemodynamic and EEG time-courses during unilateral hand movement in patients with cortical myoclonus. An EEG-fMRI and EEG-TD-fNIRS study," *Brain Topogr.* **28**, 915–925 (2014).
108. D. Safi *et al.*, "Recruitment of the left precentral gyrus in reading epilepsy: A multimodal neuroimaging study," *Epilepsy Behav. Case Rep.* **5**, 19–22 (2016).
109. K. Matsuo, N. Kato, T. Kato, "Decreased cerebral haemodynamic response to cognitive and physiological tasks in mood disorders as shown by near-infrared spectroscopy," *Psychol. Med.* **32**, 1029–37 (2002).
110. K. Matsuo, A. Watanabe, Y. Onodera, N. Kato, T. Kato, "Prefrontal hemodynamic response to verbal-fluency task and hyperventilation in bipolar disorder measured by multi-channel near-infrared spectroscopy," *J. Affect. Disord.* **82**, 85–92 (2004).
111. K. Matsuo *et al.*, "Hypofrontality and microvascular dysregulation in remitted late-onset depression assessed by functional near-infrared spectroscopy," *Neuroimage* **26**, 234–42 (2005).
112. S. Pu *et al.*, "Reduced frontopolar activation during verbal fluency task associated with poor social functioning in late-onset major depression: Multi-channel near-infrared spectroscopy study," *Psychiatry Clin. Neurosci.* **62**, 728–37 (2008).
113. T. Suto, M. Fukuda, M. Ito, T. Uehara, M. Mikuni, "Multichannel near-infrared spectroscopy in depression and schizophrenia: Cognitive brain activation study," *Biol. Psychiatry* **55**, 501–511 (2004).
114. S. Pu *et al.*, "The relationship between the prefrontal activation during a verbal fluency task and stress-coping style in major depressive disorder: A near-infrared spectroscopy study," *J. Psychiatr. Res.* **46**, 1427–1434 (2012).
115. S. Shimodera *et al.*, "Near-infrared spectroscopy of bipolar disorder may be distinct from that of unipolar depression and of healthy controls," *Asia-Pacific Psychiatry* **4**, 258–265 (2012).
116. T. Noda *et al.*, "Frontal and right temporal activations correlate negatively with depression severity during verbal fluency task: A multi-channel near-infrared spectroscopy study," *J. Psychiatr. Res.* **46**, 905–912 (2012).
117. J. Aoki *et al.*, "Evaluation of cerebral activity in the prefrontal cortex in mood [affective] disorders during animal-assisted therapy (AAT) by near-infrared spectroscopy (NIRS): A pilot study," *Int. J. Psychiat. Clin.* **16**, 205–213 (2012).
118. M. Kinou *et al.*, "Differential spatiotemporal characteristics of the prefrontal hemodynamic response and their association with functional impairment in schizophrenia and major depression," *Schizophr. Res.* **150**, 459–267 (2013).
119. S. Koseki *et al.*, "The relationship between positive and negative automatic thought and activity in the prefrontal and temporal cortices: A multi-channel near-infrared spectroscopy (NIRS) study," *J. Affect. Disord.* **151**, 352–359 (2013).
120. M. Usami, Y. Iwadare, M. Kodaira, K. Watanabe, K. Saito, "Near infrared spectroscopy study of the frontopolar hemodynamic response and depressive mood in children with major depressive disorder: A pilot study," *PLoS One* **9**, e86290 (2014).
121. H. Kito *et al.*, "Comparison of alterations in cerebral hemoglobin oxygenation in late life depression and Alzheimer's disease as assessed by near-infrared spectroscopy," *Behav. Brain Funct.* **10**, 8 (2014).
122. X. Liu *et al.*, "Relationship between the prefrontal function and the severity of the emotional symptoms during a verbal fluency task in patients with major depressive disorder: A multi-channel NIRS study," *Prog. Neuro-Psychopharmacol. Biol. Psychiatry* **54**, 114–121 (2014).
123. Y. Nishimura *et al.*, "Social function and frontopolar activation during a cognitive task in patients with bipolar disorder," *Neuropsychobiology*, **72**, 81–90 (2015).
124. Y. Nishimura *et al.*, "Dorsolateral prefrontal hemodynamic responses during a verbal fluency

- task in hypomanic bipolar disorder,” *Bipolar Disord.* **17**, 172–183 (2015).
125. W. Mikawa *et al.*, “Left temporal activation associated with depression severity during a verbal fluency task in patients with bipolar disorder: A multichannel near-infrared spectroscopy study,” *J. Affect. Disord.* **173**, 193–200 (2015).
 126. S. Pu *et al.*, “Prefrontal activation predicts social functioning improvement after initial treatment in late-onset depression,” *J. Psychiatr. Res.* **62**, 62–70 (2015).
 127. N. Tsujii *et al.*, “Relationship between prefrontal hemodynamic responses and quality of life differs between melancholia and non-melancholic depression,” *Psychiatr. Res. Neuroimaging* **253**, 26–35 (2016).
 128. S. Kinoshita, T. Kanazawa, H. Kikuyama, H. Yoneda, “Clinical application of DEX/CRH test and multi-channel NIRS in patients with depression,” *Behav. Brain Funct.* **12**, 25 (2016).
 129. K. Ohi *et al.*, “Impact of familial loading on prefrontal activation in major psychiatric disorders: A near-infrared spectroscopy (NIRS) study,” *Sci. Rep.* **7**, 44268 (2017).
 130. K. Masuda *et al.*, “Different functioning of prefrontal cortex predicts treatment response after a selective serotonin reuptake inhibitor treatment in patients with major depression,” *J. Affect. Disord.* **214**, 44–52 (2017).
 131. X. Y. Ma *et al.*, “Near-infrared spectroscopy reveals abnormal hemodynamics in the left dorsolateral prefrontal cortex of menopausal depression patients,” *Dis. Markers* **2017**, 1695930 (2017).
 132. N. Tsujii *et al.*, “Reduced left precentral regional responses in patients with major depressive disorder and history of suicide attempts,” *PLoS One* **12**, e0175249 (2017).
 133. K. Yamamuro *et al.*, “Distinct patterns of blood oxygenation in the prefrontal cortex in clinical phenotypes of schizophrenia and bipolar disorder,” *J. Affect. Disord.* **234**, 45–53 (2018).
 134. J. J. Sun, X. M. Liu, C. Y. Shen, K. Feng, P. Z. Liu, “Abnormal prefrontal brain activation during a verbal fluency task in bipolar disorder patients with psychotic symptoms using multichannel NIRS,” *Neuropsychiatr. Dis. Treat.* **14**, 3081 (2018).
 135. T. Akiyama, M. Koeda, Y. Okubo, M. Kimura, “Hypofunction of left dorsolateral prefrontal cortex in depression during verbal fluency task: A multi-channel near-infrared spectroscopy study,” *J. Affect. Disord.* **231**, 83–90 (2018).
 136. T. Fujiwara *et al.*, “Evaluation of brain activity using near-infrared spectroscopy in inflammatory bowel disease patients,” *Sci. Rep.* **8**, 402 (2018).
 137. F. L. Yan, H. Wang, Z. Liu, “Reduced prefrontal activation during the Tower of London and verbal fluency task in patients with bipolar depression: A multi-channel NIRS study,” *Front. Psychiatry* **9**, 214 (2018).
 138. Y. Satomura *et al.*, “Severity-dependent and-independent brain regions of major depressive disorder: A long-term longitudinal near-infrared spectroscopy study,” *J. Affect. Disord.* **243**, 249–254 (2019).
 139. S. Pu *et al.*, “A multi-channel near-infrared spectroscopy study of prefrontal cortex activation during working memory task in major depressive disorder,” *Neurosci. Res.* **70**, 91–97 (2011).
 140. S. Pu *et al.*, “Reduced prefrontal cortex activation during the working memory task associated with poor social functioning in late-onset depression: Multi-channel near-infrared spectroscopy study,” *Psychiatr. Res. Neuroimaging* **203**, 222–228 (2012).
 141. Y. Zhu *et al.*, “Prefrontal activation during a working memory task differs between patients with unipolar and bipolar depression: A preliminary exploratory study,” *J. Affect. Disord.* **225**, 64–70 (2018).
 142. T. Matsubara *et al.*, “Prefrontal activation in response to emotional words in patients with bipolar disorder and major depressive disorder,” *Neuroimage* **85**, 489–97 (2014).
 143. H. Zhu *et al.*, “Decreased functional connectivity and disrupted neural network in the prefrontal cortex of affective disorders: A resting-state fNIRS study,” *J. Affect. Disord.* **221**, 132–44 (2017).
 144. S. Wu, L. Gao, C. Chen, J. Li, S. He, “Resting-state functional connectivity in prefrontal cortex investigated by functional near-infrared spectroscopy: A longitudinal and cross-sectional study,” *Neurosci. Lett.* **683**, 94–99 (2018).
 145. Y. Fujita *et al.*, “Asymmetric alternation of the hemodynamic response at the prefrontal cortex in patients with schizophrenia during electroconvulsive therapy: A near-infrared spectroscopy study,” *Brain Res.* **1410**, 132–140 (2011).
 146. Y. Takei *et al.*, “Near-infrared spectroscopic study of frontopolar activation during face-to-face conversation in major depressive disorder and bipolar disorder,” *J. Psychiatr. Res.* **57**, 74–83 (2014).
 147. F. Tian *et al.*, “Prefrontal responses to digit span memory phases in patients with post-traumatic stress disorder (PTSD): A functional near infrared spectroscopy study,” *NeuroImage-Clin.* **4**, 808–819 (2014).
 148. N. Tsujii, W. Mikawa, T. Adachi, T. Hirose, O. Shirakawa, “Shared and differential cortical functional abnormalities associated with inhibitory

- control in patients with schizophrenia and bipolar disorder," *Sci. Rep.* **8**, 4686 (2018).
149. A. Kondo *et al.*, "Characteristics of oxygenated hemoglobin concentration change during pleasant and unpleasant image-recall tasks in patients with depression: Comparison with healthy subjects," *Psychiatr. Clin. Neurosci.* **72**, 611–622 (2018).
 150. N. Zaproudina *et al.*, "Tooth clenching induces abnormal cerebrovascular responses in migraineurs," *Front. Neurol.* **9**, 1112 (2018).
 151. Y. Nishimura *et al.*, "Frontal dysfunction during a cognitive task in drug-naive patients with panic disorder as investigated by multi-channel near-infrared spectroscopy imaging," *Neurosci. Res.* **59**, 107–112 (2007).
 152. T. Dresler *et al.*, "Revise the revised? New dimensions of the neuroanatomical hypothesis of panic disorder," *J. Neural Transm.* **120**, 3–29 (2013).
 153. Y. Nishimura *et al.*, "Relationship between the prefrontal function during a cognitive task and the severity of the symptoms in patients with panic disorder: A multi-channel NIRS study," *Psychiatr. Res. Neuroimaging* **172**, 168–172 (2009).
 154. H. Tanii *et al.*, "Asymmetry of prefrontal cortex activities and catechol-O-methyltransferase Val158Met genotype in patients with panic disorder during a verbal fluency task: Near-infrared spectroscopy study," *Neurosci. Lett.* **452**, 63–67 (2009).
 155. S. Deppermann *et al.*, "Does rTMS alter neuro-cognitive functioning in patients with panic disorder/agoraphobia? An fNIRS-based investigation of prefrontal activation during a cognitive task and its modulation via sham-controlled rTMS," *Biomed. Res. Int.* **2014**, 542526 (2014).
 156. S. Deppermann *et al.*, "Neurobiological and clinical effects of fNIRS-controlled rTMS in patients with panic disorder/agoraphobia during cognitive-behavioural therapy," *NeuroImage-Clin.* **16**, 668–677 (2017).
 157. C. Yokoyama *et al.*, "Dysfunction of ventrolateral prefrontal cortex underlying social anxiety disorder: A multi-channel NIRS study," *NeuroImage-Clin.* **8**, 455–461 (2015).
 158. C. Kawashima *et al.*, "Hyperfunction of left lateral prefrontal cortex and automatic thoughts in social anxiety disorder: A near-infrared spectroscopy study," *J. Affect. Disord.* **206**, 256–260 (2016).
 159. K. Marumo, R. Takizawa, Y. Kawakubo, T. Onitsuka, K. Kasai, "Gender difference in right lateral prefrontal hemodynamic response while viewing fearful faces: A multi-channel near-infrared spectroscopy study," *Neurosci. Res.* **63**, 89–94 (2009).
 160. A. Roos, F. Robertson, C. Lochner, B. Vythilingum, D. J. Stein, "Altered prefrontal cortical function during processing of fear-relevant stimuli in pregnancy," *Behav. Brain Res.* **222**, 200–205 (2011).
 161. A. Kochel *et al.*, "Auditory symptom provocation in dental phobia: A near-infrared spectroscopy study," *Neurosci. Lett.* **503**, 48–51 (2011).
 162. S. V. Tupak *et al.*, "Neuropeptide S receptor gene: Fear-specific modulations of prefrontal activation," *Neuroimage* **66**, 353–360 (2013).
 163. R. Holtzer, R. Kraut, M. Izzetoglu, K. Ye, "The effect of fear of falling on prefrontal cortex activation and efficiency during walking in older adults," *GeroScience* **41**, 89–100 (2019).
 164. A. C. Ruocco *et al.*, "Medial prefrontal cortex hyperactivation during social exclusion in borderline personality disorder," *Psychiatr. Res. Neuroimaging* **181**, 233–236 (2010).
 165. L. H. Glassman *et al.*, "The effects of a brief acceptance-based behavioral treatment versus traditional cognitive-behavioral treatment for public speaking anxiety: An exploratory trial examining differential effects on performance and neurophysiology," *Behav. Modificat.* **40**, 748–776 (2016).
 166. H. F. H. Jeong, Z. Yuan, "Abnormal resting-state functional connectivity in the orbitofrontal cortex of heroin users and its relationship with anxiety: A pilot fNIRS study," *Sci. Rep.* **7**, 46522 (2017).
 167. T. Fekete, F. D. Beacher, J. Cha, D. Rubin, L. R. Mujica-Parodi, "Small-world network properties in prefrontal cortex correlate with predictors of psychopathology risk in young children: A NIRS study," *Neuroimage* **85**, 345–353 (2014).
 168. A. Landowska, D. Roberts, P. Eachus, A. Barrett, "Within-and between-session prefrontal cortex response to virtual reality exposure therapy for acrophobia," *Front. Hum. Neurosci.* **12**, 362 (2018).
 169. K. Sakatani, M. Fujii, N. Takemura, T. Hirayama, "Effects of acupuncture on anxiety levels and prefrontal cortex activity measured by near-infrared spectroscopy: A pilot study," *Adv. Exp. Med. Biol.* **876**, 297–302 (2016).
 170. A. Brugnera, C. Zarbo, R. Adorni, A. Compare, K. Sakatani, "Cortical and autonomic stress responses in adults with high versus low levels of trait anxiety: A pilot study," *Adv. Exp. Med. Biol.* **977**, 127–132 (2017).
 171. A. Watanabe, T. Kato, "Cerebrovascular response to cognitive tasks in patients with schizophrenia measured by near-infrared spectroscopy," *Schizophr. Bull.* **30**, 435–444 (2004).
 172. Y. Kubota *et al.*, "Prefrontal activation during verbal fluency tests in schizophrenia — A

- near-infrared spectroscopy (NIRS) study,” *Schizophr. Res.* **77**, 65–73 (2005).
173. R. Takizawa *et al.*, “Reduced frontopolar activation during verbal fluency task in schizophrenia: A multi-channel near-infrared spectroscopy study,” *Schizophr. Res.* **99**, 250–262 (2008).
 174. R. Takizawa *et al.*, “Association between catechol-O-methyltransferase Val108/158Met genotype and prefrontal hemodynamic response in schizophrenia,” *PLoS One* **4**, e5495 (2009).
 175. R. Takizawa *et al.*, “Association between sigma-1 receptor gene polymorphism and prefrontal hemodynamic response induced by cognitive activation in schizophrenia,” *Prog. Neuro-Psychopharmacol. Biol. Psychiatr.* **33**, 491–498 (2009).
 176. K. Ohi *et al.*, “The SIGMAR1 gene is associated with a risk of schizophrenia and activation of the prefrontal cortex,” *Prog. Neuro-Psychopharmacol. Biol. Psychiatr.* **35**, 1309–1315 (2011).
 177. Y. Nishimura *et al.*, “Association of decreased prefrontal hemodynamic response during a verbal fluency task with EGR3 gene polymorphism in patients with schizophrenia and in healthy individuals,” *Neuroimage* **85**, 527–534 (2014).
 178. K. Takeshi, T. Nemoto, M. Fumoto, H. Arita, M. Mizuno, “Reduced prefrontal cortex activation during divergent thinking in schizophrenia: A multi-channel NIRS study,” *Prog. Neuro-Psychopharmacol. Biol. Psychiatr.* **34**, 1327–1332 (2010).
 179. S. Koike *et al.*, “Different hemodynamic response patterns in the prefrontal cortical sub-regions according to the clinical stages of psychosis,” *Schizophr. Res.* **132**, 54–61 (2011).
 180. S. Shimodera *et al.*, “Mapping hypofrontality during letter fluency task in schizophrenia: A multi-channel near-infrared spectroscopy study,” *Schizophr. Res.* **136**, 63–69 (2012).
 181. R. Takizawa *et al.*, “Joint project for psychiatric application of near-infrared spectroscopy (JPSY-NIRS) group: Neuroimaging-aided differential diagnosis of the depressive state,” *Neuroimage* **85**, 498–507 (2014).
 182. K. Yamamuro *et al.*, “Differential patterns of blood oxygenation in the prefrontal cortex between patients with methamphetamine-induced psychosis and schizophrenia,” *Sci. Rep.* **5**, 12107 (2015).
 183. M. Kawano *et al.*, “Correlation between frontal lobe oxy-hemoglobin and severity of depression assessed using near-infrared spectroscopy,” *J. Affect. Disord.* **205**, 154–158 (2016).
 184. S. Pu *et al.*, “Association between cognitive insight and prefrontal function during a cognitive task in schizophrenia: A multichannel near-infrared spectroscopy study,” *Schizophr. Res.* **150**, 81–87 (2013).
 185. S. Pu *et al.*, “Association between subjective well-being and prefrontal function during a cognitive task in schizophrenia: A multi-channel near-infrared spectroscopy study,” *Schizophr. Res.* **149**, 180–185 (2013).
 186. K. Marumo *et al.*, “Functional abnormalities in the left ventrolateral prefrontal cortex during a semantic fluency task, and their association with thought disorder in patients with schizophrenia,” *Neuroimage* **85**, 518–526 (2014).
 187. P. H. Chou *et al.*, “Distinct effects of duration of untreated psychosis on brain cortical activities in different treatment phases of schizophrenia: A multi-channel near-infrared spectroscopy study,” *Prog. Neuro-Psychopharmacol. Biol. Psychiatr.* **49**, 63–69 (2014).
 188. P. H. Chou *et al.*, “Duration of untreated psychosis and brain function during verbal fluency testing in first-episode schizophrenia: A near-infrared spectroscopy study,” *Sci. Rep.* **5**, 18069 (2015).
 189. W. Quan *et al.*, “Reduced prefrontal activation during a verbal fluency task in Chinese-speaking patients with schizophrenia as measured by near-infrared spectroscopy,” *Prog. Neuro-Psychopharmacol. Biol. Psychiatr.* **58**, 51–58 (2015).
 190. L. Holper *et al.*, “Brain correlates of verbal fluency in subthreshold psychosis assessed by functional near-infrared spectroscopy,” *Schizophr. Res.* **168**, 23–29 (2015).
 191. Z. Li, Y. Wang, W. Quan, T. Wu, B. Lv, “Evaluation of different classification methods for the diagnosis of schizophrenia based on functional near-infrared spectroscopy,” *J. Neurosci. Methods* **241**, 101–110 (2015).
 192. P. H. Chou *et al.*, “Similar age-related decline in cortical activity over frontotemporal regions in schizophrenia: A multichannel near-infrared spectroscopy study,” *Schizophr. Bull.* **41**, 268–279 (2014).
 193. S. Pu *et al.*, “Self-reported social functioning and prefrontal hemodynamic responses during a cognitive task in schizophrenia,” *Psychiatr. Res. Neuroimaging* **234**, 121–129 (2015).
 194. N. Iwashiro *et al.*, “Association between impaired brain activity and volume at the sub-region of Broca’s area in ultra-high risk and first-episode schizophrenia: A multi-modal neuroimaging study,” *Schizophr. Res.* **172**, 9–15 (2016).
 195. S. Pu *et al.*, “Associations between depressive symptoms and fronto-temporal activities during a verbal fluency task in patients with schizophrenia,” *Sci. Rep.* **6**, 30685 (2016).
 196. M. Itakura *et al.*, “Association between social functioning and prefrontal cortex function during a verbal fluency task in schizophrenia: A near-infrared

- spectroscopic study," *Psychiatr. Clin. Neurosci.* **71**, 769–779 (2017).
197. T. Noda, K. Nakagome, S. Setoyama, E. Matsushima, "Working memory and prefrontal/temporal hemodynamic responses during post-task period in patients with schizophrenia: A multi-channel near-infrared spectroscopy study," *J. Psychiatr. Res.* **95**, 288–298 (2017).
 198. X. Luo *et al.*, "Prefrontal cortex dysfunction during verbal fluency task after atypical antipsychotic treatment in schizophrenia: A near-infrared spectroscopy imaging study," *Neurosci. Lett.* **686**, 101–105 (2018).
 199. Z. Narita *et al.*, "The effect of transcranial direct current stimulation on psychotic symptoms of schizophrenia is associated with oxy-hemoglobin concentrations in the brain as measured by near-infrared spectroscopy: A pilot study," *J. Psychiatr. Res.* **103**, 5–9 (2018).
 200. S. Koike *et al.*, "Reduced but broader prefrontal activity in patients with schizophrenia during n-back working memory tasks: A multi-channel near-infrared spectroscopy study," *J. Psychiatr. Res.* **47**, 1240–1246 (2013).
 201. S. Pu *et al.*, "A pilot study on the effects of cognitive remediation on hemodynamic responses in the prefrontal cortices of patients with schizophrenia: A multi-channel near-infrared spectroscopy study," *Schizophr. Res.* **153**, 87–95 (2014).
 202. S. Pu *et al.*, "The association between cognitive deficits and prefrontal hemodynamic responses during performance of working memory task in patients with schizophrenia," *Schizophr. Res.* **172**, 114–122 (2016).
 203. S. Pu *et al.*, "Social cognition and prefrontal hemodynamic responses during a working memory task in schizophrenia," *Sci. Rep.* **6**, 22500 (2016).
 204. T. Shinba *et al.*, "Near-infrared spectroscopy analysis of frontal lobe dysfunction in schizophrenia," *Biol. Psychiatr.* **55**, 154–164 (2004).
 205. S. Koike *et al.*, "Association between severe dorsolateral prefrontal dysfunction during random number generation and earlier onset in schizophrenia," *Clin. Neurophysiol.* **122**, 1533–1540 (2011).
 206. Y. Hoshi, T. Shinba, C. Sato, N. Doi, "Resting hypofrontality in schizophrenia: A study using near-infrared time-resolved spectroscopy," *Schizophr. Res.* **84**, 411–420 (2006).
 207. F. Hosomi *et al.*, "Capturing spontaneous activity in the medial prefrontal cortex using near-infrared spectroscopy and its application to schizophrenia," *Sci. Rep.* **9**, 5283 (2019).
 208. K. Ikezawa *et al.*, "Impaired regional hemodynamic response in schizophrenia during multiple prefrontal activation tasks: A two-channel near-infrared spectroscopy study," *Schizophr. Res.* **108**, 93–103 (2009).
 209. M. Azechi *et al.*, "Discriminant analysis in schizophrenia and healthy subjects using prefrontal activation during frontal lobe tasks: A near-infrared spectroscopy," *Schizophr. Res.* **117**, 52–60 (2010).
 210. N. Okada *et al.*, "Characterizing prefrontal cortical activity during inhibition task in methamphetamine-associated psychosis versus schizophrenia: A multi-channel near-infrared spectroscopy study," *Addict. Biol.* **21**, 489–503 (2016).
 211. A. J. Fallgatter, W. K. Strik, "Reduced frontal functional asymmetry in schizophrenia during a cued performance test assessed with near-infrared spectroscopy," *Schizophr. Bull.* **26**, 913–919 (2000).
 212. J. Lee, B. S. Folley, J. Gore, S. Park, "Origins of spatial working memory deficits in schizophrenia: An event-related fMRI and near-infrared spectroscopy study," *PLoS One* **3**, e1760 (2008).
 213. Y. Zhu *et al.*, "Reduced prefrontal activation during Tower of London in first-episode schizophrenia: A multi-channel near-infrared spectroscopy study," *Neurosci. Lett.* **478**, 136–140 (2010).
 214. Y. Nishimura *et al.*, "Prefrontal cortex activity during response inhibition associated with excitement symptoms in schizophrenia," *Brain Res.* **1370**, 194–203 (2011).
 215. Y. Takei *et al.*, "Temporal lobe and inferior frontal gyrus dysfunction in patients with schizophrenia during face-to-face conversation: A near-infrared spectroscopy study," *J. Psychiatr. Res.* **47**, 1581–1589 (2013).
 216. S. Schneider *et al.*, "Haemodynamic and electrophysiological markers of pragmatic language comprehension in schizophrenia," *World J. Biol. Psychiatr.* **16**, 398–410 (2015).
 217. L. K. Holper *et al.*, "Distribution of response time, cortical, and cardiac correlates during emotional interference in persons with subclinical psychotic symptoms," *Front. Behav. Neurosci.* **10**, 172 (2016).
 218. N. Shimizu, T. Umemura, M. Matsunaga, T. Hirai, "An interactive sports video game as an intervention for rehabilitation of community-living patients with schizophrenia: A controlled, single-blind, crossover study," *PLoS One* **12**, e0187480 (2017).
 219. S. Nakano *et al.*, "Comparison of changes in oxygenated hemoglobin during the tree-drawing task between patients with schizophrenia and healthy controls," *Neuropsychiatr. Dis. Treat.* **14**, 1071 (2018).
 220. M. Sato *et al.*, "Comparison of changes in the oxygenated hemoglobin level during a 'modified

- rock-paper-scissors task' between healthy subjects and patients with schizophrenia," *Psychiatr. Clin. Neurosci.* **72**, 490–501 (2018).
221. H. Arai *et al.*, "A quantitative near-infrared spectroscopy study: A decrease in cerebral hemoglobin oxygenation in Alzheimer's disease and mild cognitive impairment," *Brain Cogn.* **61**, 189–194 (2006).
 222. T. Doi *et al.*, "Brain activation during dual-task walking and executive function among older adults with mild cognitive impairment: A fNIRS study," *Aging Clin. Exp. Res.* **25**, 539–544 (2013).
 223. M. K. Yeung *et al.*, "Altered frontal lateralization underlies the category fluency deficits in older adults with mild cognitive impairment: A near-infrared spectroscopy study," *Front. Aging Neurosci.* **8**, 59 (2016).
 224. K. H. Yap *et al.*, "Visualizing hyperactivation in neurodegeneration based on prefrontal oxygenation: A comparative study of mild Alzheimer's disease, mild cognitive impairment, and healthy controls," *Front. Aging Neurosci.* **9**, 287 (2017).
 225. A. Katzorke *et al.*, "Decreased hemodynamic response in inferior frontotemporal regions in elderly with mild cognitive impairment," *Psychiatr. Res. Neuroimaging* **274**, 11–18 (2018).
 226. S. Viola, P. Viola, M. P. Buongarzone, L. Fiorelli, P. Litterio, "Tissue oxygen saturation and pulsatility index as markers for amnesic mild cognitive impairment: NIRS and TCD study," *Clin. Neurophysiol.* **124**, 851–856 (2013).
 227. J. Liu *et al.*, "Global brain hypoperfusion and oxygenation in amnesic mild cognitive impairment," *Alzheimer's Dement.* **10**, 162–170 (2015).
 228. V. Z. Marmarelis, D. C. Shin, T. Tarumi, R. Zhang, "Comparison of model-based indices of cerebral autoregulation and vasomotor reactivity using transcranial doppler versus near-infrared spectroscopy in patients with amnesic mild cognitive impairment," *J. Alzheimer's Dis.* **56**, 89–105 (2017).
 229. X. Li *et al.*, "Decreased resting-state brain signal complexity in patients with mild cognitive impairment and Alzheimer's disease: A multi-scale entropy analysis," *Biomed. Opt. Express* **9**, 1916–1929 (2018).
 230. J. B. Zeller *et al.*, "Reduced spontaneous low frequency oscillations as measured with functional near-infrared spectroscopy in mild cognitive impairment," *Brain Imaging Behav.* **13**, 283–292 (2019).
 231. H. J. Niu *et al.*, "Reduced frontal activation during a working memory task in mild cognitive impairment: A non-invasive near-infrared spectroscopy study," *CNS Neurosci. Ther.* **19**, 125–131 (2013).
 232. M. K. Yeung *et al.*, "Reduced frontal activations at high working memory load in mild cognitive impairment: Near-infrared spectroscopy," *Dement. Geriatr. Cogn. Disord.* **42**, 278–296 (2016).
 233. A. Vermeij *et al.*, "Prefrontal activation may predict working-memory training gain in normal aging and mild cognitive impairment," *Brain Imaging Behav.* **11**, 141–154 (2017).
 234. C. Babiloni *et al.*, "Hypercapnia affects the functional coupling of resting state electroencephalographic rhythms and cerebral haemodynamics in healthy elderly subjects and in patients with amnesic mild cognitive impairment," *Clin. Neurophysiol.* **125**, 685–693 (2014).
 235. K. Uemura *et al.*, "Reduced prefrontal oxygenation in mild cognitive impairment during memory retrieval," *Int. J. Geriatr. Psychiatr.* **31**, 583–591 (2015).
 236. R. Li *et al.*, "Early detection of Alzheimer's disease using noninvasive near-infrared spectroscopy," *Front. Aging Neurosci.* **10**, 366 (2018).
 237. C. Hock *et al.*, "Near infrared spectroscopy in the diagnosis of Alzheimer's diseases," *Ann. N. Y. Acad. Sci.* **777**, 22–29 (1996).
 238. C. Hock *et al.*, "Decrease in parietal cerebral hemoglobin oxygenation during performance of a verbal fluency task in patients with Alzheimer's disease monitored by means of near-infrared spectroscopy (NIRS) — correlation with simultaneous rCBF-PET measurements," *Brain Res.* **755**, 293–303 (1997).
 239. Fallgatter *et al.*, "Loss of functional hemispheric asymmetry in Alzheimer's dementia assessed with near-infrared spectroscopy," *Cognit. Brain Res.* **6**, 67–72 (1997).
 240. T. Araki *et al.*, "The effects of combine treatment of memantine and donepezil on Alzheimer's disease patients and its relationship with cerebral blood flow in the prefrontal area," *Int. J. Geriatr. Psychiatr.* **29**, 881–889 (2014).
 241. F. G. Metzger, A. C. Ehli, F. B. Haeussinger, A. J. Fallgatter, K. Hagen, "Effects of cholinesterase inhibitor on brain activation in Alzheimer's patients measured with functional near-infrared spectroscopy," *Psychopharmacology* **232**, 4383–4391 (2015).
 242. F. G. Metzger *et al.*, "Brain activation in fronto-temporal and Alzheimer's dementia: A functional near-infrared spectroscopy study," *Alzheimer's Res. Ther.* **8**, 56 (2016).
 243. J. B. Zeller, M. J. Herrmann, A. C. Ehli, T. Polak, A. J. Fallgatter, "Altered parietal brain oxygenation in Alzheimer's disease as assessed with near-infrared spectroscopy," *Am. J. Geriatr. Psychiatr.* **18**, 433–441 (2010).

244. D. Perpetuini *et al.*, "Complexity of frontal cortex fNIRS can support Alzheimer disease diagnosis in memory and visuo-spatial tests," *Entropy* **21**, 26 (2019).
245. H. Tomioka *et al.*, "Detection of hypofrontality in drivers with Alzheimer's disease by near-infrared spectroscopy," *Neurosci. Lett.* **451**, 252–256 (2009).
246. Y. Kato *et al.*, "Evaluation of changes in oxyhemoglobin during Shiritori task in elderly subjects including those with Alzheimer's disease," *Psychogeriatrics* **17**, 238–246 (2017).
247. T. Fladby *et al.*, "Olfactory response in the temporal cortex of the elderly measured with near-infrared spectroscopy: A preliminary feasibility study," *J. Cereb. Blood Flow Metab.* **24**, 677–680 (2004).
248. D. Perpetuini, R. Bucco, M. Zito, A. Merla, "Study of memory deficit in Alzheimer's disease by means of complexity analysis of fNIRS signal," *Neurophotonics* **5**, 011010 (2017).
249. S. Viola *et al.*, "New brain reperfusion rehabilitation therapy improves cognitive impairment in mild Alzheimer's disease: A prospective, controlled, open-label 12-month study with NIRS correlates," *Aging Clin. Exp. Res.* **26**, 417–425 (2014).
250. K. Sakatani, Y. Katayama, T. Yamamoto, S. Suzuki, "Changes in cerebral blood oxygenation of the frontal lobe induced by direct electrical stimulation of thalamus and globus pallidus: A near infrared spectroscopy study," *J. Neurol. Neurosurg. Psychiatr.* **67**, 769–773 (1999).
251. Y. Murata *et al.*, "Changes in cerebral blood oxygenation induced by deep brain stimulation: Study by near-infrared spectroscopy (NIRS)," *Keio J. Med.* **49**, A61–A63 (2000).
252. T. Morishita *et al.*, "Changes in motor-related cortical activity following deep brain stimulation for Parkinson's disease detected by functional near infrared spectroscopy: A pilot study," *Front. Hum. Neurosci.* **10**, 629 (2016).
253. I. Maidan *et al.*, "Changes in oxygenated hemoglobin link freezing of gait to frontal activation in patients with Parkinson disease: An fNIRS study of transient motor-cognitive failures," *J. Neurol.* **262**, 899–908 (2015).
254. I. Maidan *et al.*, "The role of the frontal lobe in complex walking among patients with Parkinson's disease and healthy older adults: An fNIRS study," *Neurorehabil. Neural Repair* **30**, 963–971 (2016).
255. I. Maidan, H. Bernad-Elazari, N. Giladi, J. M. Hausdorff, A. Mirelman, "When is higher level cognitive control needed for locomotor tasks among patients with Parkinson's disease?" *Brain Topogr.* **30**, 531–538 (2017).
256. I. Maidan *et al.*, "Evidence for differential effects of 2 forms of exercise on prefrontal plasticity during walking in Parkinson's disease," *Neurorehabil. Neural Rep.* **32**, 200–208 (2018).
257. P. C. Thumm *et al.*, "Treadmill walking reduces pre-frontal activation in patients with Parkinson's disease," *Gait Posture* **62**, 384–387 (2018).
258. E. Al-Yahya, W. Mahmoud, D. Meester, P. Esser, H. Dawes, "Neural substrates of cognitive motor interference during walking; peripheral and central mechanisms," *Front. Hum. Neurosci.* **12**, 536 (2018).
259. J. R. Mahoney *et al.*, "The role of prefrontal cortex during postural control in Parkinsonian syndromes a functional near-infrared spectroscopy study," *Brain Res.* **1633**, 126–138 (2016).
260. M. Balconi, C. Siri, N. Meucci, G. Pezzoli, L. Angioletti, "Personality Traits and Cortical Activity Affect Gambling Behavior in Parkinson's Disease," *J. Parkinson's Dis.* **8**, 341–352 (2018).
261. S. Muehlschlegel *et al.*, "Feasibility of NIRS in the neurointensive care unit: A pilot study in stroke using physiological oscillations," *Neurocrit. Care* **11**, 288 (2009).
262. P. Taussky *et al.*, "Validation of frontal near-infrared spectroscopy as noninvasive bedside monitoring for regional cerebral blood flow in brain-injured patients," *Neurosurg. Focus* **32**, E2 (2012).
263. D. Phillip *et al.*, "Altered low frequency oscillations of cortical vessels in patients with cerebrovascular occlusive disease — a NIRS study," *Front. Neurol.* **4**, 204 (2013).
264. A. Dutta, A. Jacob, S. R. Chowdhury, A. Das, M. A. Nitsche, "EEG-NIRS based assessment of neurovascular coupling during anodal transcranial direct current stimulation—a stroke case series," *J. Med. Syst.* **39**, 36 (2015).
265. J. J. Selb *et al.*, "Effect of motion artifacts and their correction on near-infrared spectroscopy oscillation data: A study in healthy subjects and stroke patients," *J. Biomed. Opt.* **20**, 056011 (2015).
266. F. Moreau, R. Yang, V. Nambiar, A. M. Demchuk, J. F. Dunn, "Near-infrared measurements of brain oxygenation in stroke," *Neurophotonics* **3**, 031403 (2016).
267. J. I. Byun, K. Y. Jung, G. T. Lee, C. K. Kim, B. M. Kim, "Spontaneous low-frequency cerebral hemodynamics oscillations in restless legs syndrome with periodic limb movements during sleep: A near-infrared spectroscopy study," *J. Clin. Neurol.* **1**, 107–114 (2016).
268. H. Su *et al.*, "Alterations in the coupling functions between cerebral oxyhaemoglobin and arterial

- blood pressure signals in post-stroke subjects,” *PLoS One* **13**, e0195936 (2018).
269. Y. Sato *et al.*, “Differences in tissue oxygenation, perfusion and optical properties in brain areas affected by stroke: A time-resolved NIRS study,” *Adv. Exp. Med. Biol.* **1072**, 63–67 (2018).
 270. H. Kwon *et al.*, “Early detection of cerebral infarction with middle cerebral artery occlusion with functional near-infrared spectroscopy: A pilot study,” *Front. Neurol.* **9**, 898 (2018).
 271. Q. Liu *et al.*, “Frequency-specific effective connectivity in subjects with cerebral infarction as revealed by NIRS method,” *Neuroscience* **373**, 169–181 (2018).
 272. G. Giacalone *et al.*, “Time-domain near-infrared spectroscopy in acute ischemic stroke patients,” *Neurophotonics* **6**, 015003 (2019).
 273. I. Miyai, M. Suzuki, M. Hatakenaka, K. Kubota, “Effect of body weight support on cortical activation during gait in patients with stroke,” *Exp. Brain Res.* **169**, 85–91 (2006).
 274. E. Al-Yahya *et al.*, “Prefrontal cortex activation while walking under dual-task conditions in stroke: A multimodal imaging study,” *Neurorehabil. Neural Rep.* **30**, 591–599 (2016).
 275. Y. C. Liu, Y. R. Yang, Y. A. Tsai, R. Y. Wang, C. F. Lu, “Brain activation and gait alteration during cognitive and motor dual task walking in stroke: A functional near-infrared spectroscopy study,” *IEEE Trans. Neural Syst. Rehabil. Eng.* **26**, 2416–2423 (2018).
 276. K. A. Hawkins *et al.*, “Prefrontal over-activation during walking in people with mobility deficits: Interpretation and functional implications,” *Hum. Mov. Sci.* **59**, 46–55 (2018).
 277. T. Mori, N. Takeuchi, S. I. Izumi, “Prefrontal cortex activation during a dual task in patients with stroke,” *Gait Posture*, **59**, 193–198 (2018).
 278. Y. Hara, S. Obayashi, K. Tsujiuchi, Y. Muraoka, “The effects of electromyography-controlled functional electrical stimulation on upper extremity function and cortical perfusion in stroke patients,” *Clin. Neurophysiol.* **124**, 2008–2015 (2013).
 279. M. Brunetti *et al.*, “Potential determinants of efficacy of mirror therapy in stroke patients: A pilot study,” *Restor. Neurol. Neurosci.* **33**, 421–434 (2015).
 280. S. Shidoh, T. Akiyama, T. Horiguchi, T. Ohira, K. Yoshida, “The process of change in hemodynamics after revascularization in the ischemic brain,” *Neuroreport* **26**, 629–633 (2015).
 281. H. Tamashiro, S. Kinoshita, T. Okamoto, N. Urushidani, M. Abo, “Effect of baseline brain activity on response to low-frequency rTMS/intensive occupational therapy in poststroke patients with upper limb hemiparesis: A near-infrared spectroscopy study,” *Int. J. Neurosci.* **129**, 337–343 (2019).
 282. P. Y. Lin, J. J. Chen, S. I. Lin, “The cortical control of cycling exercise in stroke patients: An fNIRS study,” *Hum. Brain Mapp.* **34**, 2381–2390 (2013).
 283. C. C. Lo, P. Y. Lin, Z. Y. Hoe, J. J. Chen, “Near infrared spectroscopy study of cortical excitability during electrical stimulation-assisted cycling for neurorehabilitation of stroke patients,” *IEEE Trans. Neural Syst. Rehabil. Eng.* **26**, 1292–1300 (2018).
 284. K. Saita *et al.*, “Combined therapy using botulinum toxin A and single-joint hybrid assistive limb for upper-limb disability due to spastic hemiplegia,” *J. Neurol. Sci.* **373**, 182–187 (2017).
 285. K. Saita *et al.*, “Biofeedback effect of hybrid assistive limb in stroke rehabilitation: A proof of concept study using functional near infrared spectroscopy,” *PLoS One* **13**, e0191361 (2018).
 286. M. Mihara *et al.*, “Cortical control of postural balance in patients with hemiplegic stroke,” *Neuroreport* **23**, 314–319 (2012).
 287. A. Ebihara *et al.*, “Evaluation of cerebral ischemia using near-infrared spectroscopy with oxygen inhalation,” *J. Biomed. Opt.* **17**, 096002 (2012).
 288. M. Rea *et al.*, “Lower limb movement preparation in chronic stroke: A pilot study toward an fNIRS-BCI for gait rehabilitation,” *Neurorehabil. Neural Rep.* **28**, 564–575 (2014).
 289. S. E. Kober *et al.*, “Hemodynamic signal changes accompanying execution and imagery of swallowing in patients with dysphagia: A multiple single-case near-infrared spectroscopy study,” *Front. Neurol.* **6**, 151 (2015).
 290. T. Hara *et al.*, “The effect of selective transcranial magnetic stimulation with functional near-infrared spectroscopy and intensive speech therapy on individuals with post-stroke aphasia,” *Eur. Neurol.* **77**, 186–194 (2017).
 291. K. Saita *et al.*, “Contralateral cerebral hypometabolism after cerebellar stroke: A functional near-infrared spectroscopy study,” *J. Stroke Cerebrovasc. Dis.* **26**, e69–71 (2017).
 292. M. Moriya, K. Sakatani, “Relation Between Asymmetry of Prefrontal Activity and Autonomic Nervous System in Post-Stroke Patients with a Disorder of Consciousness,” *Adv. Exp. Med. Biol.* **1072**, 53–58 (2018).
 293. Y. Bhamhani, R. Maikala, M. Farag, G. Rowland, “Reliability of near-infrared spectroscopy measures of cerebral oxygenation and blood volume during handgrip exercise in nondisabled and traumatic brain-injured subjects,” *J. Rehabil. Res. Dev.* **43**, 845 (2006).

294. K. J. Urban, K. M. Barlow, J. J. Jimenez, B. G. Goodyear, J. F. Dunn, "Functional near-infrared spectroscopy reveals reduced interhemispheric cortical communication after pediatric concussion," *J. Neurotrauma* **32**, 833–840 (2015).
295. L. M. Hocke, C. C. Duszynski, C. T. Debert, D. Dleikan, J. F. Dunn, "Reduced functional connectivity in adults with persistent post-concussion symptoms: A functional near-infrared spectroscopy study," *J. Neurotrauma* **35**, 1224–1232 (2018).
296. A. C. Merzagora, M. T. Schultheis, B. Onaral, M. Izzetoglu, "Functional near-infrared spectroscopy-based assessment of attention impairments after traumatic brain injury," *J. Innov. Opt. Health Sci.* **4**, 251–260 (2011).
297. Z. Wu *et al.*, "Altered cortical activation and connectivity patterns for visual attention processing in young adults post-traumatic brain injury: A functional near infrared spectroscopy study," *CNS Neurosci. Ther.* **24**, 539–548 (2018).
298. S. Hibino *et al.*, "Oxyhemoglobin changes during cognitive rehabilitation after traumatic brain injury using near infrared spectroscopy," *Neurol. Med.-Chir.* **53**, 299–303 (2013).
299. A. P. Kontos *et al.*, "Brain activation during neurocognitive testing using functional near-infrared spectroscopy in patients following concussion compared to healthy controls," *Brain Imaging Behav.* **8**, 621–634 (2014).
300. A. C. R. Merzagora, M. Izzetoglu, B. Onaral, M. T. Schultheis, "Verbal working memory impairments following traumatic brain injury: An fNIRS investigation," *Brain Imaging Behav.* **8**, 446–459 (2014).
301. D. Sawamura *et al.*, "Active inhibition of task-irrelevant sounds and its neural basis in patients with attention deficits after traumatic brain injury," *Brain Inj.* **28**, 1455–1460 (2014).
302. V. Chernomordik *et al.*, "Abnormality of low frequency cerebral hemodynamics oscillations in TBI population," *Brain Res.* **1639**, 194–199 (2016).
303. P. Plenger *et al.*, "fNIRS-based investigation of the Stroop task after TBI," *Brain Imaging Behav.* **10**, 357–366 (2016).
304. E. Jeong *et al.*, "High oxygen exchange to music indicates auditory distractibility in acquired brain injury: An fNIRS study with a vector-based phase analysis," *Sci. Rep.* **8**, 16737 (2018).
305. Y. Zhang *et al.*, "Influence of inter-stimulus interval of spinal cord stimulation in patients with disorders of consciousness: A preliminary functional near-infrared spectroscopy study," *NeuroImage-Clin.* **17**, 1–9 (2018).
306. P. Pinti, F. Scholkmann, A. Hamilton, P. Burgess, I. Tachtsidis, "Current status and issues regarding pre-processing of fNIRS neuroimaging data: An investigation of diverse signal filtering methods within a general linear model framework," *Front. Hum. Neurosci.* **12**, 505 (2018).
307. T. J. Huppert, "Commentary on the statistical properties of noise and its implication on general linear models in functional near-infrared spectroscopy," *Neurophotonics* **3**, 010401 (2016).
308. I. Tachtsidis, F. Scholkmann, "False positives and false negatives in functional near-infrared spectroscopy: Issues, challenges, and the way forward," *Neurophotonics* **3**, 031405 (2016).
309. D. G. Wyser, O. Lamercy, F. Scholkmann, M. Wolf, R. Gassert, "Wearable and modular functional near-infrared spectroscopy instrument with multidistance measurements at four wavelengths," *Neurophotonics* **4**, 041413 (2017).
310. F. Scholkmann *et al.*, "A review on continuous wave functional near-infrared spectroscopy and imaging instrumentation and methodology," *Neuroimage* **85**, 6–27 (2014).
311. S. Brigadoi, R. J. Cooper, "How short is short? Optimum source — detector distance for short-separation channels in functional near-infrared spectroscopy," *Neurophotonics* **2**, 025005 (2015).
312. F. Scholkmann, A. J. Metz, M. Wolf, "Measuring tissue hemodynamics and oxygenation by continuous-wave functional near-infrared spectroscopy: How robust are the different calculation methods against movement artifacts?" *Physiol. Meas.* **35**, 717 (2014).
313. M. Caldwell *et al.*, "Modelling confounding effects from extracerebral contamination and systemic factors on functional near-infrared spectroscopy," *Neuroimage* **143**, 91–105 (2016).
314. L. Gagnon *et al.*, "Short separation channel location impacts the performance of short channel regression in NIRS," *Neuroimage* **59**, 2518–2528 (2012).
315. L. Gagnon, M. A. Yücel, D. A. Boas, R. J. Cooper, "Further improvement in reducing superficial contamination in NIRS using double short separation measurements," *Neuroimage* **85**, 127–135 (2014).
316. K. T. Sweeney *et al.*, "A methodology for validating artifact removal techniques for physiological signals," *IEEE T. Inf. Technol. Biomed.* **16**, 918–926 (2012).
317. C. Issard, J. Gervain, "Adult-like processing of time-compressed speech by newborns: A NIRS study," *Dev. Cogn. Neurosci.* **25**, 176–184 (2017).
318. B. Molavi *et al.*, "Analyzing the resting state functional connectivity in the human language system using near infrared spectroscopy," *Front. Hum. Neurosci.* **7**, 921 (2014).

319. A. Cristia *et al.*, “Neural correlates of infant accent discrimination: An fNIRS study,” *Dev. Sci.* **17**, 628–635 (2014).
320. L. May, J. Gervain, M. Carreiras, J. F. Werker, “The specificity of the neural response to speech at birth,” *Dev. Sci.* **21**, e12564 (2018).
321. C. Issard, J. Gervain, “Variability of the hemodynamic response in infants: Influence of experimental design and stimulus complexity,” *Dev. Cogn. Neurosci.* **33**, 182–193 (2018).
322. G. Durantin, F. Dehais, A. Delorme, “Characterization of mind wandering using fNIRS,” *Front. Syst. Neurosci.* **9**, 98 (2015).
323. P.-H. Chou, T.-H. Lan, “The role of near-infrared spectroscopy in Alzheimer’s disease,” *J. Clin. Gerontol. Geriatr.* **4**, 33–36 (2013).
324. I. Tachtsidis *et al.*, “Investigation of cerebral haemodynamics by near-infrared spectroscopy in young healthy volunteers reveals posture-dependent spontaneous oscillations,” *Physiol. Meas.* **25**, 437–445 (2004).
325. X.-S. Hu, K.-S. Hong, S. S. Ge, M.-Y. Jeong, “Kalman estimator- and general liner model-based on-line brain activation mapping by near-infrared spectroscopy,” *Biomed. Eng. Online* **9**, 82 (2010).
326. P. Pinti *et al.*, “The present and future use of functional near-infrared spectroscopy (fNIRS) for cognitive neuroscience,” *Ann. NY. Acad. Sci.* (2018), doi: 10.1111/nyas.13948.
327. K.-S. Hong, A. Zafar, “Existence of initial dip for BCI: An illusion or reality,” *Front. Neurorobotics* **12**, 69 (2018).
328. T. T. Q. Bui, T. T. Vu, K.-S. Hong, “Extraction of sparse features of color images in recognizing objects,” *Int. J. Control Autom. Syst.* **14**, 616–627 (2016).
329. M. D. Pfeifer, F. Scholkmann, R. Labruyère, “Signal processing in functional near-infrared spectroscopy (fNIRS): Methodological differences lead to different statistical results,” *Front. Hum. Neurosci.* **11**, 641 (2018).
330. T. J. Huppert, S. G. Diamond, M. A. Franceschini, D. A. Boas, “HomER: A review of time-series analysis methods for near-infrared spectroscopy of the brain,” *Appl. Optics* **48**, D280–D298 (2009).
331. J. C. Ye, S. Tak, K. E. Jang, J. Jung, J. Jang, “NIRS-SPM: Statistical parametric mapping for near-infrared spectroscopy,” *Neuroimage* **44**, 428–447 (2009).
332. P. H. Koh *et al.*, “Functional optical signal analysis: A software tool for near-infrared spectroscopy data processing incorporating statistical parametric mapping,” *J. Biomed. Opt.* **12**, 064010 (2007).
333. T. Fekete, D. Rubin, J. M. Carlson, L. R. Mujica-Parodi, “The NIRS analysis package: Noise reduction and statistical inference,” *PLoS One* **6**, e24322 (2011).
334. J. Xu *et al.*, “FC-NIRS: A functional connectivity analysis tool for near-infrared spectroscopy data,” *Biomed Res. Int.* **2015**, 248724 (2015).
335. G. E. Strangman, Q. Zhang, T. Zeffiro, “Near-infrared neuroimaging with NimPy,” *Front. Neuroinformatics* **3**, 12 (2009).
336. H. Santosa, X. Zhai, F. Fishburn, T. Huppert, “The NIRS brain AnalyzIR toolbox,” *Algorithms* **11**, 73 (2018).
337. J. Wang *et al.*, “GRETNA: A graph theoretical network analysis toolbox for imaging connectomics,” *Front. Hum. Neurosci.* **9**, 386 (2015).
338. F. Orihuela-Espina, D. R. Leff, D. R. C. James, A. W. Darzi, G.-Z. Yang, “Imperial College near infrared spectroscopy neuroimaging analysis framework,” *Neurophotonics* **5**, 011011 (2017).
339. M. Hamadache, D. Lee, “Principal component analysis based signal-to-noise ratio improvement for inchoate faulty signals: Application to ball bearing fault detection,” *Int. J. Control Autom. Syst.* **15**, 506–517 (2017).
340. H. Chen, B. Jiang, N. Lu, “A multi-mode incipient sensor fault detection and diagnosis method for electrical traction systems,” *Int. J. Control Autom. Syst.* **16**, 1783–1793 (2018).
341. Q. C. Nguyen, M. Piao, K.-S. Hong, “Multivariable adaptive control of the rewinding process of a roll-to-roll system governed by hyperbolic partial differential equations,” *Int. J. Control Autom. Syst.* **16**, 2177–2186 (2018).
342. G. Yi, J. Mao, Y. Wang, S. Guo, Z. Miao, “Adaptive tracking control of nonholonomic mobile manipulators using recurrent neural networks,” *Int. J. Control Autom. Syst.* **16**, 1390–1403 (2018).
343. M. Yazdani, H. Salarieh, M. S. Foumani, “Bio-inspired decentralized architecture for walking of a 5-link biped robot with compliant knee joints,” *Int. J. Control Autom. Syst.* **16**, 2935–2947 (2018).
344. M. Brett, I. S. Johnsrude, A. M. Owen, “The problem of functional localization in the human brain,” *Nat. Rev. Neurosci.* **3**, 243–249 (2002).
345. H. Zhang *et al.*, “Test-retest assessment of independent component analysis-derived resting-state functional connectivity based on functional near-infrared spectroscopy,” *Neuroimage* **55**, 607–615 (2011).
346. I. M. Wiggins, C. A. Anderson, P. T. Kitterick, D. E. H. Hartley, “Speech-evoked activation in adult temporal cortex measured using functional near-infrared spectroscopy (fNIRS): Are the measurements reliable?” *Hear. Res.* **339**, 142–154 (2016).

347. F. Orihuela-Espina, D. R. Leff, D. R. C. James, A. W. Darzi, G. Z. Yang, "Quality control and assurance in functional near infrared spectroscopy (fNIRS) experimentation," *Phys. Med. Biol.* **55**, 3701–3724 (2010).
348. F. Herold, P. Wiegel, F. Scholkmann, N. G. Müller, "Applications of functional near-infrared spectroscopy (fNIRS) neuroimaging in exercise-cognition science: A systematic, methodology-focused review," *J. Clin. Med.* **7**, 466 (2018).
349. D. Tsuchi, I. Dan, "Spatial registration for functional near-infrared spectroscopy: From channel position on the scalp to cortical location in individual and group analyses," *Neuroimage* **85**, 92–103 (2014).
350. G. A. Zimeo Morais, J. B. Balardin, J. R. Sato, "fNIRS optodes' location decider (fOLD): A toolbox for probe arrangement guided by brain regions-of-interest," *Sci. Rep.* **8**, 3341 (2018).
351. J. M. Jonas, H. Jörntell, "Somatosensory cortical neurons decode tactile input patterns and location from both dominant and non-dominant digits," *Cell Reports* **26**, 13 (2019).
352. S. Tak, A. M. Kempny, K. J. Friston, A. P. Leff, W. D. Penny, "Dynamic causal modelling for functional near-infrared spectroscopy," *Neuroimage* **111**, 338–349 (2015).
353. D. A. Boas, C. E. Elwell, M. Ferrari, G. Taga, "Twenty years of functional near-infrared spectroscopy: Introduction for the special issue," *Neuroimage* **85**, 1–5 (2014).
354. X. Li, J.-A. Fang, H. Li, "Exponential synchronization of stochastic memristive recurrent neural networks under alternate state feedback control," *Int. J. Control Autom. Syst.* **16**, 2859–2869 (2018).
355. J. Moon, H. Kim, B. Lee, "View-point invariant 3d classification for mobile robots using a convolutional neural network," *Int. J. Control Autom. Syst.* **16**, 2888–2895 (2018).
356. N. Naseer, K.-S. Hong, "fNIRS-based brain-computer interfaces: A review," *Front. Hum. Neurosci.* **9**, 3 (2015).
357. P. Nicole, A.-A. Samadani, T. Chau, "Quantifying fast optical signal and event-related potential relationships during a visual oddball task," *Neuroimage* **178**, 119–128 (2018).
358. L. C. Schudlo, T. Chau, "Towards a ternary NIRS-BCI: Single-trial classification of verbal fluency task, Stroop task and unconstrained rest," *J. Neural Eng.* **12**, 066008 (2015).
359. L. C. Schudlo, T. Chau, "Development of a ternary near-infrared spectroscopy brain-computer interface: Online classification of verbal fluency task, Stroop task and rest," *Int. J. Neural Syst.* **28**, 1750052 (2018).
360. S. Weyand, L. Schudlo, K. Takehara-Nishiuchi, T. Chau, "Usability and performance-informed selection of personalized mental tasks for an online near-infrared spectroscopy brain-computer interface," *Neurophotonics* **2**, 025001 (2015).
361. K.-S. Hong, N. Naseer, Y.-H. Kim, "Classification of prefrontal and motor cortex signals for three-class fNIRS-BCI," *Neurosci. Lett.* **587**, 87–92 (2015).
362. K.-S. Hong, N. Naseer, "Reduction of delay in detecting initial dips from functional near-infrared spectroscopy signals using vector-based phase analysis," *Int. J. Neural Syst.* **26**, 1650012 (2016).
363. A. R. Sereshkeh, R. Yousefi, A. T. Wong, T. Chau, "Online classification of imagined speech using functional near-infrared spectroscopy signals," *J. Neural Eng.* **16**, 016005 (2018).
364. A. M. Batula, J. A. Mark, Y. E. Kim, H. Ayaz, "Comparison of brain activation during motor imagery and motor movement using fNIRS," *Comput. Intell. Neurosci.* **2017**, 5491296 (2017).
365. A. M. Batula, Y. E. Kim, H. Ayaz, "Virtual and actual humanoid robot control with four-class motor-imagery-based optical brain-computer interface," *Biomed Res. Int.* **2017**, 1463512 (2017).
366. T. Gateau, H. Ayaz, F. Dehais, "In silico versus over the clouds: On-the-fly mental state estimation of aircraft pilots, using a functional near infrared spectroscopy based passive-BCI," *Front. Hum. Neurosci.* **12**, 187 (2018).
367. K. J. Verdière, R. N. Roy, F. Dehais, "Detecting pilot's engagement using fNIRS connectivity features in an automated vs. manual landing scenario," *Front. Hum. Neurosci.* **12**, 6 (2018).
368. T. Gateau, G. Durantin, F. Lancelot, S. Scannella, F. Dehais, "Real-time state estimation in a flight simulator using fNIRS," *PLoS One* **10**, e0121279 (2015).
369. G. Durantin, S. Scannella, T. Gateau, A. Delorme, F. Dehais, "Processing functional near infrared spectroscopy signal with a Kalman filter to assess working memory during simulated flight," *Front. Hum. Neurosci.* **9**, 707 (2016).
370. U. Ghafoor, S. Kim, K.-S. Hong, "Selectivity and longevity of peripheral-nerve and machine interfaces: A review," *Front. Neurorobotics* **11**, 59 (2017).
371. K.-S. Hong, N. Aziz, U. Ghafoor, "Motor-commands decoding using peripheral nerve signals: A review," *J. Neural Eng.* **15**, 031004 (2018).
372. H. W. Gomma, J. Thomas, "Neurogenic bladder dysfunction: A novel treatment using robust model predictive control supported by noise attenuation technique," *Int. J. Control Autom. Syst.* **15**, 2669–2680 (2017).

373. B. Xu, C. Zhou, S. Y. Ko, "Closed-loop planar fuzzy control system for a curvature-controllable steerable bevel-tip needle," *Int. J. Control Autom. Syst.* **16**, 2421–2431 (2018).
374. Q. C. Nguyen, Y. Kim, H. Kwon, "Optimization of layout and path planning of surgical robotic system," *Int. J. Control Autom. Syst.* **15**, 375–384 (2017).
375. A. Curtin *et al.*, "Enhancing neural efficiency of cognitive processing speed via training and neurostimulation: An fNIRS and TMS study," *Neuroimage* **198**, 73–82 (2019).
376. U. Ghafoor *et al.*, "Effects of acupuncture therapy on MCI patients using functional near-infrared spectroscopy," *Front. Aging Neurosci.* **11**, 237 (2019).